NREL/TP-411-5457 • UC Category: 271 • DE93010021

RECEIVED
MAY 13 1993
OSTI

Structural and Electronic Studies of a-SiGe:H Alloys

Final Subcontract Report
1 January 1991 – 28 February 1993

W. Paul
Harvard University
Cambridge, Massachusetts

NREL technical monitor: B. Stafford

National Renewable Energy Laboratory
1617 Cole Boulevard
Golden, Colorado 80401-3393
Operated by Midwest Research Institute
for the U.S. Department of Energy
under Contract No. DE-AC02-83CH10093

Prepared under Subcontract No. XX-8-18131-1-1

April 1993

MASTER

DISTRIBUTION OF THIS DOCUMENT IS UNLIMITED

This publication was reproduced from the best available camera-ready copy
submitted by the subcontractor and received no editorial review at NREL.

NOTICE

This report was prepared as an account of work sponsored by an agency of the United States government. Neither the United States government nor any agency thereof, nor any of their employees, makes any warranty, express or implied, or assumes any legal liability or responsibility for the accuracy, completeness, or usefulness of any information, apparatus, product, or process disclosed, or represents that its use would not infringe privately owned rights. Reference herein to any specific commercial product, process, or service by trade name, trademark, manufacturer, or otherwise does not necessarily constitute or imply its endorsement, recommendation, or favoring by the United States government or any agency thereof. The views and opinions of authors expressed herein do not necessarily state or reflect those of the United States government or any agency thereof.

Printed in the United States of America
Available from:
National Technical Information Service
U.S. Department of Commerce
5285 Port Royal Road
Springfield, VA 22161

Price: Microfiche A01
Printed Copy A04

Codes are used for pricing all publications. The code is determined by the number of pages in the publication. Information pertaining to the pricing codes can be found in the current issue of the following publications which are generally available in most libraries: *Energy Research Abstracts (ERA); Government Reports Announcements* and Index (*GRA* and I); *Scientific and Technical Abstract Reports (STAR)*; and publication NTIS-PR-360 available from NTIS at the above address.

DISCLAIMER

Portions of this document may be illegible electronic image products. Images are produced from the best available original document.

Preface

This final report includes and updates the results, discussion and conclusions put forward in our annual subcontract report dated December 1991. That report covered work carried out up to December 1990, when major funding for this study was terminated. The subsequent period has been funded at a much reduced level primarily to complete the research being done in December 1990 by three graduate students, two of whom have now received the Ph.D. degree. During that period twenty papers have been published or accepted for publication, by this group, some of them with collaborators.

The work performed in the latter period was a collaborative effort of the following group members:

Professor William Paul

Professor Joseph H. Chen (Boston College Visiting Professor)

Mr. Bruce Bateman — technical associate

Ms. Dawen Pang — technical associate

Dr. Warren A. Turner — postdoctoral fellow

Dr. Erzhuang Liu — postdoctoral fellow

Mr. (now Dr.) Paul Wickboldt — graduate student

Mr. (now Dr.) Scott J. Jones — graduate student

Ms. Anna Wetsel — graduate student

Since this final phase of the Harvard program on amorphous semiconductors was started in 1988, three other students (Y.-M. Li, W.A. Turner and S.M. Lee) have graduated with the Ph.D. degree, and two postdoctoral fellows (Dr. F.C. Marques and Dr. K.D. Mackenzie) have also participated.

Collaborations with the research groups of Professor Richard Norberg (Washington University, St. Louis), of Dr. M.L. Theye (Laboratoire d'Optique, Paris), of Professor J. Tauc (Brown University, Providence), of Dr. Y.-M. Li (Solarex), and of Professor C. Lee (KAIST, Korea) have continued into the present period, and are reflected in the Publication List reported later, and in short verbal communications (unlisted) at meetings of the American Physical Society.

Summary

Introduction

The use of low bandgap alloys in multi-junction photovoltaic cells is required to achieve the efficiencies required for the DOE National Photovoltaic Program's long-term technical goals. The most suitable low bandgap alloy for amorphous silicon technology is amorphous silicon-germanium. However, it has been established by world-wide research that the properties of these alloys deteriorate continuously as the germanium content increases. Various hypotheses have been put forward, including preferential hydrogen bonding, inhomogeneity and voids. The Harvard group proposed that it would be instructive to conduct an in-depth study of the end-member, a-Ge:H, to find a way to optimize its properties, and to determine whether the optimizing deposition parameters were similar or otherwise to those appropriate for a-Si:H.

During the major part of this program, extensive studies were carried out on the structural, electrical and optical properties of films of a-Ge:H made while varying systematically the temperature of deposition, the gas pressures and flow rates, the power levels, the apparatus geometry and the bias on the electrodes. The characterizational measurements included hydrogen evolution *versus* temperature (GE), transmission electron microscopy (TEM), scanning electron microscopy (SEM), differential scanning calorimetry (DSC), infrared (IR) and visible optical absorption, photothermal deflection spectroscopy (PDS), electrical conductivity, photoluminescence, steady-state photoconductivity, transient photoconductivity, ambipolar diffusion length, and electron spin resonance (ESR).

A very important empirical result of these studies was the demonstration that films of a-Ge:H placed on a substrate which was subjected to a certain amount of ion bombardment has improved structural properties: instead of low density, porous material with easily visible island-tissue entities produced without bombardment, one obtained high density, compact material with no microstructure revealed by electron microscopy. An obvious inference was that the absence of microstructure was linked to the superior $\eta\mu\tau$ (efficiency-mobility-lifetime product) of the compact material, and a clear extension was that poor microstructure was at least one cause of the observed universal poor performance of amorphous SiGe alloys. In brief, the poor microstructure could be linked both to a higher density of point defects, and to variations in band gap (i.e., potential fluctuations), both of which would cause deterioration of photoresponse. We now set out in systematic detail the general *modus operandi* of this research and its conclusions.

Objectives

The principal objectives of this research have been (1) to carry out a comprehensive study of the structural, electrical and optical properties of a-Ge:H, the end-component of the a-$Si_{1-x}Ge_x$:H alloy series, prepared systematically under a wide range of deposition conditions, in order to improve the photoelectronic properties to the point where these alloys could be more useful components of photovoltaic devices, (2) to extend this study to a-$Si_{1-x}Ge_x$:H alloys of large x, so as to produce alloys with better photoelectronic properties than have hitherto been available, (3) to continue a collaboration with Professor Richard Norberg of Washington University to prepare films of a-Si and a-Ge containing deuterium, so that the Norberg laboratory could study deuteron magnetic resonances (DMR), which have been used to give information on the microstructure of films on a 100 Å scale, (4) to continue a collaboration with the group of Dr. M. L. Theye of the Laboratoire d'Optique, Paris, France, to compare and contrast the information about the density-of-states obtained from steady-state photoconductivity (PC), and from low photon energy absorption spectra determined by photothermal deflection spectroscopy (PDS), and (5) to renew a collaboration with Professor J. Tauc of Brown University to examine photon modulation spectroscopy of amorphous semiconductors, including experiments on femtosecond time scales.

Discussion

All of these projects have been successfully pursued and their results either published or accepted for publication.[1-20] The central thrust on a-Ge:H has been very successful, so that we are now able to produce films with overall properties relevant to photovoltaics much superior to those previously available. The systematic variation of deposition parameters has shed light on which conditions at the growing surface of the film will result in high quality material, on the importance of ion bombardment resulting from self-bias of the substrate platform, and on the extent to which alterations in the plasma itself control the deposition process.

Extension of this work to a-$Si_{1-x}Ge_x$:H alloys of large x has been carried out, and it has been demonstrated that improved $\eta\mu\tau$'s are possible compared with the values extrapolated from our (and others) earlier work on alloys of small x.

The several collaborative efforts have all been successful, as will be discussed below.

Conclusions

Our principal conclusions may be summarized as follows:

(1) A-Ge:H produced by PECVD under conditions of temperature, gas pressures and flows, r.f. power and substrate bias similar to those employed for the fabrication of films of a-Si:H yield material of poor photoelectronic quality ($\eta\mu\tau$ product). This material has low density, large small angle X-ray scattering consistent with the presence of voids, visible microstructure revealed by TEM and SEM, low-temperature evolution of hydrogen, and unstable optical and electrical characteristics easily modified by atmospheric gaseous contamination.

(2) Modified PECVD conditions are possible which yield material of opposite properties: high density, on small angle X-ray scattering no larger than that in device-grade a-Si:H, no microstructure visible in TEM and SEM, and stable optical and electrical characteristics which include $\eta\mu\tau$ values two to three orders of magnitude larger than have hitherto been reported. The modified PECVD conditions involve a substantial change in the intrinsic d.c. bias developed on one of two parallel electrodes, so that there is more ion bombardment. However, this is only part of the change, and we have established that changes in the constitution of the plasma, which depend sensitively on the mix of gases (GeH_4 and H_2), on r.f. power and on apparatus geometry, are also important.

(3) The assertions in item (2) have been confirmed by very detailed examination of the structural and photoelectronic properties, which have been published (see below). The structural studies include infrared absorption, gas evolution, differential scanning calorimetry, TEM, SEM and small angle X-ray scattering. The difference between the porous heterostructure consisting of two differentiable phases, attributable to films produced at the larger of our two parallel electrodes (where conditions approximate those used to produce device-grade a-Si:H) and the more homogeneous material produced under the "modified" conditions at the smaller (bombarded) electrode has been confirmed in numerous studies. The material with porous heterostructure has islands on the order of 100 Å diameter which have relatively few defects, and surrounding tissue which is rich in GeH_x groups, has lower atomic density, many defects, and is plausibly associated with the pick-up over time of atmospheric gases which alter the overall properties of the film. The structural studies include the above-mentioned ones, but there has also been spectacular confirmation in the DMR studies of the Norberg group.

(4) A model for the deteriorated properties of a-Ge:H with respect to a-Si:H, and by implication of a-$Si_{1-x}Ge_x$:H alloys produced under PECVD conditions approximating those used for a-Si:H, has been suggested. The poorly made a-Ge:H and a-$Si_{1-x}Ge_x$:H alloys have a higher density of point and other defects, which lead to a higher density of states in the bandgap and to more rapid

recombination of photocarriers. More importantly, the heterostructure leads to fluctuations in electrostatic potential and to the creation of charged defects which amplify the potential fluctuations: the result is a dramatic reduction in carrier drift mobility, which is the principal cause of $\eta\mu\tau$ values in the 10^{-9}–10^{-10} cm^2/V range.

(5) In contrast, the a-Ge:H and a-$Si_{1-x}Ge_x$:H alloys where deposition conditions have been used which have been chosen to minimize the microstructure established by TEM, SEM, IR and SAXS have consistently lower subband gap absorption and ESR density, consistently higher $\eta\mu\tau$ and μ (drift) and stable photoelectronic parameters unaffected by atmospheric contamination. The $\eta\mu\tau$ for electrons in a-Ge:H is consistently and reproducibly in the range of $2 - 5 \times 10^{-7}$ cm^2/V when measured using 8×10^{15} photons/cm^2s of 1.25 eV photon energy.

(6) Two series of alloys, corresponding to E_{04} gaps of $\sim$ 1.4 eV and $\sim$ 1.55 eV (Tauc gaps of approximately 1.25 eV and 1.38 eV) have been made, using deposition conditions modified somewhat from those used for a-Ge:H. The 1.4 eV alloys have subbandgap absorption coefficients at 0.8 eV photon energy averaging 1.6 cm^{-1}, Urbach tail energies averaging 52 meV, and give $\eta\mu\tau$'s from steady-state photoconductivity averaging 7.3×10^{-8} cm^2V^{-1}. See Tables 1 and 3. These $\eta\mu\tau$ values are about two orders of magnitude larger than those for similar bandgaps in a recently published NREL study,[21] and two orders of magnitude larger than we found in an earlier study where the samples were made under conditions resembling those for a-Si:H.[22] The 1.55 eV alloys (also see Table 3) have been less studied. They have $\eta\mu\tau$ values averaging 2.7×10^{-8} cm^2V^{-1}, which are only slightly better than those for samples made following a-Si:H conditions.[20,21] We regard these results as confirming beyond doubt the necessity for altered deposition conditions in order to produce improved alloys of high Ge-content, and of the efficacy of using as a best vehicle the elimination, or at least reduction, of microstructure on the 30–100 Å scale. We note also that in our present films, the $\eta\mu\tau$'s decrease as Si is added to Ge, whereas in earlier studies the $\eta\mu\tau$'s decreased as Ge was added to Si. In contrast to the variation of $\eta\mu\tau$, the ambipolar L_0's remain virtually constant near 600 Å, only a factor of two below that for a-Si:H. Based on the $\eta\mu\tau$, L_0 changes, we postulate a model for the alloys which includes compositional fluctuations. Since the valence band offset between a-Si:H and a-Ge:H is very small,[23] it would be expected that composition fluctuations would not affect L_0. We suggest that a significant extension of our studies would be direct compositional studies on a 10 nm scale in optimized material.

(7) Our study concluded with attempts to identify the conditions in the plasma which controlled the eventual film properties. We have been able to establish empirical correlations between the $\eta\mu\tau$, the basic structural and optical parameters, and certain parameters describing the plasma chemistry. Nevertheless, understanding of the plasma chemistry itself will require more extensive investigations than we have been able to carry out.

Report

Since the studies establishing the above conclusions have, for the most part, been reported in the open literature, we shall refer only briefly to those publications. The work on a-$Si_{1-x}Ge_x$:H alloys has not yet reached the literature, so that a more extensive summary of it will be included in this document.

Table of Contents

Notice . . . . *i*

Preface . . . . *ii*

Summary *Introduction* . . . . *iii*
Objectives . . . . *iii*
Discussion . . . . *iv*
Conclusions . . . . *iv*
Report . . . . *v*

Table of Contents . . . . *vi*

List of Figures . . . . *xii*

List of Tables . . . . *xv*

List of Appendices . . . . *xvii*

I. Introduction 1

II. Optimization of Amorphous Hydrogenated Germanium and its Alloys Prepared by R.F. Glow-Discharge 1

Published Works 1

Studies of a-$Si_{1-x}Ge_x$:H Alloys of large x, having E_{04} optical gaps near 1.4 eV and 1.55 eV 1

III. Collaborative Research 34

Professor Richard Norberg, Washington University: Deuteron Magnetic Resonance Studies 34

Dr. M.L. Theye, Laboratoire d'Optique, Paris: Comparative Studies of Subbandgap Optical Absorption by Photothermal Deflection Spectroscopy and by Photoconductivity using the Constant Photocurrent Method 36

Professor J. Tauc, Brown University: Photomodulation Spectroscopy and Femtosecond Dynamics 38

IV. Theses Completed 38

Dr. S.M. Lee: Structural and Optical Properties of Variable Bandgap Crystalline and Amorphous Semiconductors of Tetrahedral Coordination 38

Dr. Y.-M. Li: Optical and Phototransport Properties of Hydrogenated Amorphous Semiconductors 39

Dr. W.A. Turner: An Optimization of the Photoelectronic Properties of Glow Discharge Prepared a-Ge:H 40

Dr. S.J. Jones: Structural Studies of a-Ge:H and a-$Si_{1-x}Ge_x$:H Alloys 40

Dr. P. Wickboldt: Deposition and Examination of Glow Discharge Produced a-Ge:H 41

V. Publication List 1988–92 42

VI. Abstracts of Papers Published Since 1991 45

Studies on the Structure of a-Ge:H using Differential Scanning Calorimetry, Gas Evolution on Heating and Transmission Electron Microscopy 45

Femtosecond Studies of Photoinduced Bleaching and Hot Carrier Dynamics in a-Si:H and a-Ge:H 45

Studies of Surface Effects in Hydrogenated Amorphous Silicon by Photothermal Deflection Experiments 45

An Electron Microscopy Study of the Effects of Deposition Conditions on the Growth of Glow Discharge Prepared a-Ge:H Films 46

Structural, Optical, and Electrical Studies of Amorphous Hydrogenated Germanium 46

States in the Gap of Improved a-Ge:H Studied by Photomodulation Spectroscopy . 46

Comments on the Determination of Defect Density in a-Si:H Alloys by Integrating the Subbandgap Optical Absorption Coefficient 46

Influence of Deposition Conditions on the Optical and Electronic Properties of a-Ge:H 47

Correlation of Structure and Structural Changes with Photovoltaic Quality of a-Si:D,H and a-Ge:D,H Films 47

Structural Properties of Amorphous Hydrogenated Germanium 47

A Study of the Properties of Hydrogenated Amorphous Germanium Produced by r.f. Glow-Discharge as the Electrode Gap is Varied: The Link Between Microstructure and Optoelectronic Properties 48

Structural, Optical and Photoelectronic Properties of Improved PECVD a-Ge:H . . 48

Stress Measurement of Glow-Discharge Produced a-Ge:H Thin Films and its Relation to Electronic and Structural Properties 48

Connections Between Photovoltaic Quality and the Structure of Deuterated Amorphous Si and Ge Films 48

True Position of Dangling Bonds in the Gap of Undoped Hydrogenated Amorphous Silicon 49

Deuteron Magnetic Resonance Studies of Structure and Photo-induced Metastable Rearrangements in Deuterated Amorphous Si, Ge and SiGe Films 49

Time-of-Flight Measurement on a-Ge:H and a-SiGe:H Alloys 49

Direct Evidence of Geminate Recombination in Hydrogenated Amorphous Silicon at Low Temperature 49

Effects of Gas Dilution on the Growth and Properties of Glow Discharge a-Ge:H . . 49

Hydrogenated Amorphous Semiconductors 50

VII. References 51

List of Figures

Figure 1. Empirical correlation between the magnitude of the compressive stress in films of a-Ge:H and their $\eta\mu\tau$ product. 2

Figure 2. Variation of physical parameters of films produced at deposition temperatures T_s between 150°C and 250°C. 8

Figure 3. Variation of physical parameters of films produced at different powers, when T_s = 225°C, total pressure = 0.95 Torr, D-spacing = 1.4 cm, and the H_2:GeH_4:SiH_4 flow rates are in the ratio of 40 sccm:1.00 sccm:0.6 sccm. 10

Figure 4. Variation of physical parameters of films produced at different powers, when T_s = 225°C, total pressure = 0.95 Torr, D-spacing = 1.0 cm, and the H_2:GeH_4:SiH_4 flow rates are in the ratio of 40 sccm:1.00 sccm:1.50 sccm. 12

Figure 5. Variation of physical parameters of films produced at different powers, when T_s = 225°C, total pressure = 1.20 Torr, D-spacing = 1.0 cm, and the H_2:GeH_4:SiH_4 flow rates are in the ratio of 80 sccm:1.00 sccm:0.60 sccm. 14

Figure 6. Variation of physical parameters of films produced at different electrode spacings, when T_s = 225°C, power = 30 W, total pressure = 0.95 Torr, and the H_2:GeH_4:SiH_4 flow rates are in the ratio of 40 sccm:1.00 sccm:0.6 sccm. 17

Figure 7. Variation of physical parameters of films produced at different electrode spacings, when T_s = 225°C, power = 30 W, total pressure = 0.95 Torr, and the H_2:GeH_4:SiH_4 flow rates are in the ratio of 40 sccm:1.00 sccm:2.00 sccm. . . . 20

Figure 8. Variation of physical parameters of films produced at different SiH_4 flow rates, when T_s = 225°C, power = 30 W, total pressure = 0.95 Torr, D-spacing = 1.0 cm and the H_2:GeH_4 flow rates are in the ratio of 40 sccm:1.00 sccm. . . . 22

Figure 9. Variation of physical parameters of films produced at different SiH_4 flow rates, when T_s = 225°C, power = 30 W, total pressure = 0.95 Torr, D-spacing = 1.0 cm and the H_2:GeH_4 flow rates are in the ratio of 40 sccm:0.50 sccm. . . . 25

Figure 10. Variation of physical parameters of films produced at different H_2 dilution, when T_s = 225°C, power = 30 W, total pressure = 0.95 Torr, D-spacing = 1.0 cm and the GeH_4:SiH_4 flow ratio is 1.00 sccm:1.00 sccm. 27

Figure 11. Variation of the physical parameters of films produced at different total pressure, when T_s = 225°C, power = 30 W, D-spacing = 1.0 cm and the H_2:GeH_4:SiH_4 flow rates are in the ratio of 40 sccm:1.00 sccm:0.60 sccm. 29

Figure 12. Variation of the physical parameters of films produced at different total pressure, when T_s = 225°C, power = 30 W, D-spacing = 1.0 cm and the H_2:GeH_4:SiH_4

flow rates are in the ratio of 80 sccm:1.00 sccm:2.00 sccm. 32

Figure 13. Variation of $\eta\mu\tau$ and L_0 with E_{04} gap and with composition x when material is prepared under conditions resembling those for optimized a-Ge:H. 35

Figure 14. A comparison of the relative proportion of tightly-bonded Ge-D with $\eta\mu\tau$ products of different films of a-Ge:H:D. 36

Figure 15. Demonstration that the inverse rate constants for M_z recoveries in DMR correlate with the photovoltaic quality factor $\eta\mu\tau$ in films of a-Ge:D:H and a-Si:D:H. 37

List of Tables

Table 1. Preparation conditions and physical properties of 76 films reported in this document. 4

Table 2. Preparation conditions for selected alloys of a-$Si_{1-x}Ge_x$:H of different E_{04}. 34

Table 3. Photoelectronic properties of a-Ge:H of E_{04} gap 1.25 ev, a-$Si_{1-x}Ge_x$:H of E_{04} gap 1.4 ev, and a-$Si_{1-x}Ge_x$:H of E_{04} gap 1.55 ev. 34

I. Introduction

In Section II, we discuss the optimization of amorphous hydrogenated germanium and silicon-germanium alloys prepared by R.F. glow discharge, in Section III report on our three major collaborative efforts, in Section IV give abstracts of five Ph.D. theses completed since 1988, in Section V list the publications during the term of the present contract, and in Section VI give abstracts of the papers published since our earlier report.

II. Optimization of Amorphous Hydrogenated Germanium and its Alloys Prepared by R.F. Glow Discharge

In our last report,[24] we covered much material which we now summarize briefly. We started by offering a rationalization for concentrating on the end-component, a-Ge:H, of the a-$Si_{1-x}Ge_x$:H alloy series, after noting the pitfalls involved in extrapolating the preparation parameters from SiH_4 to SiH_4—GeH_4 mixed plasma conditions. There followed a report of the properties of a-Ge:H deposited under conditions that were very close to those used to produce a-Si:H, and the conclusion—which agreed with similar conclusions worldwide—that these properties were badly deteriorated compared to those of a-Si:H. These properties were in sharp contrast to those found when the deposition conditions were changed so as to involve some bombardment of the substrates. The changed conditions and resultant properties were discussed in detail. We then described, in detail also, studies of the dependence on substrate material of the structural properties of films produced under the first set (a-Si:H-like) of conditions, and followed with an account of the dependence of the *improved* properties on systematically-varied parameters such as R.F. power, H_2 gas dilution and substrate temperature.

A second reactor was designed to study better the films produced under the altered conditions. This reactor, also described in the report, was used to study the change in properties with variation of the usual deposition parameters, but also including the variation of the separation between the reactor electrodes. It turned out that this was a crucial variable which permitted us to replicate systematically a wide variety of material properties found in other combinations of deposition parameters.[11]

Published Works

Publications on this contract since its inception in 1988 to the end of 1990 are listed in Section V, items 1 through 19. We shall concentrate here on papers 20 through 39, which have been published since that time.

Studies on the Structure of a-Ge:H Using IR, DSC, GE, DMR, TEM, X-ray, Raman and SAXS Techniques

Extensive studies were carried out on a-Ge:H deposited under conditions optimizing the photoelectronic properties of a-Si:H (these were samples deposited at an electrode with only a small plasma-produced d.c. bias, referred to in the published work as the "unpowered" electrode), and also under conditions optimizing the photoelectronic properties of a-Ge:H (samples deposited at an electrode carrying a larger plasma-produced d.c. bias, the "powered" electrode). The structural results were very different: the former samples showed major structural reconstruction and gas evolution, on heating, long before the crystallization temperature, and they demonstrated clearly visible heterostructure in TEM and considerable small angle X-ray scattering (SAXS), while the latter were of higher density, showed minimal TEM heterostructure and SAXS intensities comparable to those found for device-grade a-Si:H. These results were reported in several publications (Section V, numbers 20, 23, 24, 28, 29–33, 39), whose abstracts are given in Section VI.

Photoelectronic Properties of a-Ge:H

Just as the structural studies fall into two clearly-differentiated groups with internally self-consistent properties, so too do the measurements of electronic band structure and photoelectronic properties.[25] Thus, the defect density from ESR and the midgap density of states inferred from sub-bandgap optical absorption spectra derived from photoconductivity spectra or photothermal deflection spectroscopy,[26] are at least an order of magnitude larger in the "unpowered" electrode samples. The Urbach edge is sharper in the "powered" electrode samples,[26] and the steady-state photoconductivity and time-of-flight electron mobility are several orders of magnitude larger.

Such results establish beyond reasonable doubt that a *sine qua non* for good photoelectronic performance is a homogeneous, although non-crystalline, microstructure. The details of the measurements are given in the papers of Section V, numbers 24, 27, 30, 31 and 39, whose abstracts are given in Section VI.

Stress Measurement of Glow-discharge Produced Films and Its Relation to Electronic and Structural Properties

In the study of thin films of amorphous semiconductors, stress has been a topic repeatedly visited. Most of the studies have concentrated on a-Si:H. Stresses may plausibly be associated with effects at the film/substrate interface, impurity gases, and thermal or post-deposition processes. However, even after accounting for these effects, many films still demonstrate a very high stress that cannot be satisfactorily explained. This stress will be referred to as the "intrinsic" stress. We have measured the stress in all of the films from both the "unpowered" and "powered" electrodes and find very consistent behavior as a function of the structural quality (qualitatively defined, of course) and the photoresponse: (i) all of the films produced at the unpowered electrode, which have inhomogeneous microstructure, have tensile stresses, while all of the films produced at the powered electrode possess large compressive stresses (ii) there is a strong correlation between the $\eta\mu\tau$ and the magnitude of the compressive stress. Figure 1 illustrates this relationship.

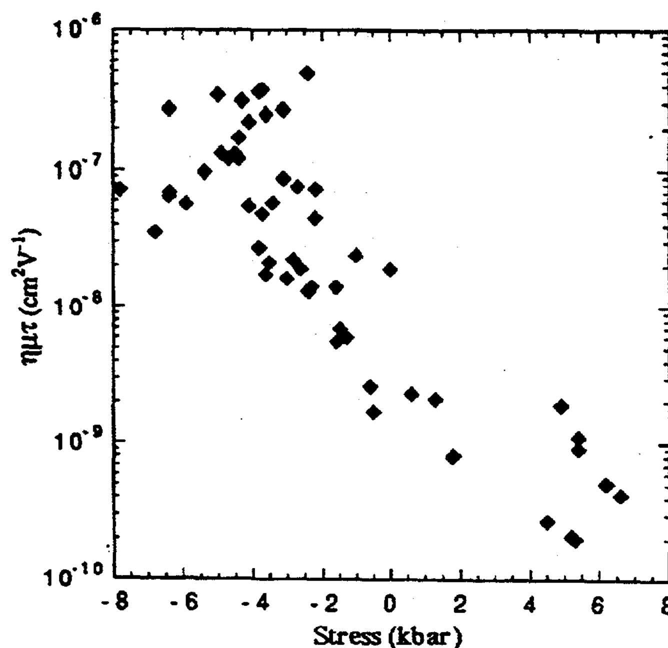

Figure 1. Empirical correlation between the magnitude of the compressive stress in films of a-Ge:H and their $\eta\mu\tau$ product.

The correlations found for a-Ge:H are the same as those found for a-Si:H, but neither is understood. There appears to be an empirical relationship between the total hydrogen content (bound and unbound) and the stress, but the reason for this can only be speculated. We postulate that microstructure plays the dominant role in determining the as-deposited intrinsic stress, and that the relation with total hydrogen content is primarily a consequence of microstructures which provide a more compressive stress being more favorable for the incorporation of large amounts of hydrogen. The details of the measurements of stress are given in paper 32 of Section V, whose abstract is included in Section VI.

Studies of a-$Si_{1-x}Ge_x$:H Alloys of Large x, Having E_{04} Optical Gaps Near 1.4 eV and 1.55 eV

The Effect of Variation of Deposition Temperature, T_s

Four samples were prepared at T_s between 150°C and 250°C. See Table 1 (136–138, 141) for preparation parameters. The energy gaps E_{04} and E_{03}, monotonically decrease, while the refractive index, N_0, monotonically increases. Both effects are probably the result of smaller H-incorporation, but this was not checked, therefore one cannot exclude higher density and homogeneity. The Fermi level stays near gap center, within 10–20 meV, and the $\eta\mu\tau$ seem to vary inversely as the activation energy. Thus, although T_s alters the properties, there is no definitive evidence for an optimum T_s in the range of T_s examined.

Corresponding numbers are, for T_s = 250°C: $\eta\mu\tau = 8.4\times10^{-8}$ cm^2/V; L_0 = 560 Å; E_{act} = 0.67 eV.

The variations of the different parameters are displayed in Figure 2.

The Effect of Variation of Power

Three power studies were done (137, 143, 144, 145, 161; 195–199; and 216, 217, 219, 223, 225, 226), at different combinations of H_2 flow, SiH_4 flow and D-spacing. See Table 1 for preparation parameters. The growth rate, not surprisingly, increases monotonically with power in all three studies. The energy gaps monotonically increase in all three studies, which in principle could be due to increased C_H, but in fact is probably produced by increased Si incorporation. In agreement with the gap increase, the refractive index decreases monotonically. Very low powers are judged not to be good, since they correspond to low $\eta\mu\tau$ and L_0, even when E_{act} is low. There appears in all three studies to be a maximum in $\eta\mu\tau$ at intermediate powers of 30–40 W. The magnitudes of $\eta\mu\tau$ do depend on the detailed values of the parameters. Thus, for power study 2, which uses 1.50 sccm SiH_4, 40 sccm H_2 and a D-spacing of 1.0 cm, all $\eta\mu\tau$ are below 1.8×10^{-8} cm^2/V. For power study 1, which reduces SiH_4 flow to 0.6 sccm while maintaining H_2 flow at 40 sccm, and with a D-spacing of 1.0 cm, the $\eta\mu\tau$ climb to a maximum of 8×10^{-8} cm^2/V. For the third power study, which used higher H_2 dilution of 80 sccm, all $\eta\mu\tau$ except two are in the range of 10^{-7} cm^2/V, with one value (film 216) at a value of 3.1×10^{-7} cm^2/V.

By and large, looking at all of the data together, the $\eta\mu\tau$ generally increase as the activation energy decreases. However, in ranges where the E_{act} are comparable, the $\eta\mu\tau$ for the samples made with high SiH_4 flow are decidedly lower. There is no consistent behavior in the magnitudes of L_0 as a function of either activation energy or ($E_{04} - E_{act}$); they range from 350 to 700 Å for ($E_{04} - E_{act}$) between 0.6 and 0.8 eV, with some clustering in the (550–650) Å range. The variations of the different parameters for the three studies are displayed in Figures 3–5. Figure 3 also includes measurements, as a function of power, of the Urbach parameter, E_0, and the subbandgap absorption coefficient at 0.8 eV.

Table 1. Preparation Conditions and Physical Properties of 76 Films Reported in this Document. Relevant parameters: Ts, substrate temperature; D, electrode spacing; d, thickness; GR, deposition rate; E03, E04, energies at which absorption coefficients are 10^3 cm^{-1} and 10^4 cm^{-1}, respectively; No, refractive index; hmT, efficiency-mobility-lifetime product; Iph/Id ratio of photo- to dark current; So, prefactor of conductivity formula; Lo, ambipolar diffusion length; E0, Urbach energy; a0.8, absorption coefficient at 0.8 eV; x, fraction of Ge in alloy.

	Sample (#)	Study/purpose	Problems?	Ts (°C)	Power (watts)	Pressure (Torr)	H2 (sccm)	GeH4 (sccm)	SiH4 (sccm)	D (cm)	d (µm)	GR (Å/s)	E03 (eV)	E04 (eV)
1	136	Temp1		200	30.0	0.950	40.0	1.00	0.60	1.4	2.54	10.60	1.22	1.38
2	137	Temp1		225	30.0	0.950	40.0	1.00	0.60	1.4	2.42	10.10	1.21	1.37
3	138	Temp1		250	30.0	0.950	40.0	1.00	0.60	1.4	2.41	10.00	1.19	1.35
4	141	Temp1		150	30.0	0.950	40.0	1.00	0.60	1.4	1.75	9.72	1.24	1.42
5	142	Power1	y	225	15.0	0.950	40.0	1.00	0.60	1.4	1.51	4.66	1.16	1.29
6	143	Power1		225	15.0	0.950	40.0	1.00	0.60	1.4	2.47	5.15	1.12	1.27
7	144	Power1		225	40.0	0.950	40.0	1.00	0.60	1.4	2.28	10.90	1.26	1.41
8	145	Power1	y	225	50.0	0.950	40.0	1.00	0.60	1.4	2.66	12.70	1.28	1.44
9	146	Flow ratio0		225	30.0	0.950	40.0	0.50	0.30	1.4	1.62	6.43	1.25	1.41
10	160	(Rep 137)		225	30.0	0.950	40.0	1.00	1.00	1.4	2.43	10.14	1.28	1.44
11	161	D-study1		225	30.0	0.950	40.0	1.00	0.60	1.4	2.33	9.69	1.25	1.40
12	162	D-study1		225	30.0	0.950	40.0	1.00	0.60	2.4	3.03	10.51	1.22	1.38
13	163	D-study1		225	30.0	0.950	40.0	1.00	0.60	3.2	2.53	12.03	1.25	1.41
14	164	D-study1		225	30.0	0.950	40.0	1.00	0.60	1.0	2.58	8.54	1.28	1.44
15	165	D-study1		225	30.0	0.950	40.0	1.00	0.60	1.7	2.04	9.70	1.22	1.37
16	167	TEM		225	30.0	0.950	40.0	1.00	0.60	1.0				
17	168	TEM		225	30.0	0.950	40.0	1.00	0.60	3.2				
18	169	TEM		225	30.0	0.950	40.0	1.00	0.60	1.7				
19	171	Pressure1		225	30.0	0.950	40.0	1.00	0.60	1.0	4.39	8.41	1.31	1.46
20	172	Pressure1		225	30.0	1.500	40.0	1.00	0.60	1.0	3.86	9.60	1.26	1.41
21	173	Pressure1		225	30.0	1.200	40.0	1.00	0.60	1.0	2.37	9.63	1.26	1.42
22	174	Pressure1		225	30.0	0.500	40.0	1.00	0.60	1.0	2.05	4.88	1.28	1.45
23	175	Pressure1		225	30.0	2.000	40.0	1.00	0.60	1.0	2.48	10.30	1.22	1.39
24	176	TEM		225	30.0	0.950	40.0	1.00	0.60	2.4				
25	177	Flow ratio1		225	30.0	0.950	40.0	0.50	0.50	1.0	2.23	5.72	1.42	1.62
26	178	Flow ratio1		225	30.0	0.950	40.0	1.00	1.00	1.0	2.20	9.18	1.34	1.51
27	179	Flow ratio1		225	30.0	0.950	40.0	1.00	2.00	1.0	2.33	11.44	1.43	1.61
28	180	Pressure1		225	30.0	0.600	40.0	1.00	0.60	1.0	2.38	5.67	1.30	1.46
29	181	Flow ratio1		225	30.0	0.950	40.0	1.00	3.00	1.0	2.34	14.41	1.41	1.59
30	182	D-study2		225	30.0	0.950	40.0	1.00	2.00	3.2	2.53	16.89	1.39	1.57
31	183	D-study2		225	30.0	0.950	40.0	1.00	2.00	1.8	2.15	13.28	1.34	1.53
32	184	Flow ratio1		225	30.0	0.950	40.0	0.50	1.50	1.0	2.19	8.71	1.57	1.76
33	185	Flow ratio1	y	225	30.0	0.950	40.0	0.50	0.30	1.0	2.44	5.49	1.31	1.49
34	186	Flow ratio1		225	30.0	0.950	40.0	0.50	0.50	1.0	2.17	5.73	1.39	1.56
35	187	Flow ratio1		225	30.0	0.950	40.0	0.50	1.00	1.0	2.64	8.29	1.47	1.65
36	188	a-Si		225	30.0	0.950	40.0	0.00	1.00	1.0	1.37	3.79	1.96	2.18
37	189	Uniformity		225	30.0	0.950	40.0	0.50	0.50	1.0				
38	190	Uniformity		225	30.0	0.950	40.0	0.50	0.50	1.0	2.46	6.22	1.39	1.56
39	191	Dilution1		225	30.0	0.950	80.0	1.00	1.00	1.0	2.76	7.67	1.29	1.45
40	192	Dilution1		225	30.0	0.950	60.0	1.00	1.00	1.0	2.56	8.87	1.29	1.46
41	195	Power2		225	35.0	0.950	40.0	1.00	1.50	1.0	2.28	11.88	1.38	1.55
42	196	Power2		225	30.0	0.950	40.0	1.00	1.50	1.0	2.34	11.12	1.33	1.50

Table 1, continued.

	Sample (#)	Study/purpose	Problems?	Ts (°C)	Power (watts)	Pressure (Torr)	H2 (sccm)	GeH4 (sccm)	SiH4 (sccm)	D (cm)	d (µm)	GR (Å/s)	E03 (eV)	E04 (eV)
43	197	Power2		225	40.0	0.950	40.0	1.00	1.50	1.0	2.17	12.94	1.38	1.55
44	198	Power2		225	45.0	0.950	40.0	1.00	1.50	1.0	2.13	14.20	1.39	1.57
45	199	Power2		225	20.0	0.950	40.0	1.00	1.50	1.0	1.97	8.22	1.25	1.42
46	200	Dilution1		225	30.0	0.950	20.0	1.00	1.00	1.0	2.70	12.20	1.29	1.47
47	201	Norberg		225	30.0	0.950	40.0	1.00	0.60	1.0				
48	202	Norberg		225	30.0	0.950	40.0	1.00	0.60	1.0	2.13	8.07	1.25	1.42
49	203	Dilution1		225	30.0	0.950	29.7	1.00	1.00	1.0	2.07	9.84	1.32	1.51
50	213	D-study1		225	30.0	0.950	40.0	1.00	0.60	2.8	2.69	10.00	1.19	1.35
51	216	misc.		225	30.0	1.200	80.0	1.00	0.60	1.0	1.86	6.19	1.21	1.37
52	217	Power3		225	40.0	1.200	80.0	1.00	0.60	1.0	2.23	7.42	1.25	1.41
53	218	Flow ratio2		225	30.0	1.200	80.0	1.00	1.50	1.0	1.93	8.04	1.30	1.48
54	219	Power3		225	35.0	1.200	80.0	1.00	0.60	1.0	2.31	7.01	1.24	1.39
55	220	Pressure2		225	30.0	1.500	80.0	1.00	2.00	1.0	2.70	9.01	1.29	1.47
56	221	Pressure2	y	225	30.0	0.700	80.0	1.00	2.00	1.0	2.23	5.30	1.43	1.61
57	222	Pressure2	y	225	30.0	0.500	80.0	1.00	2.00	1.0	1.92	3.77	1.44	1.63
58	223	Power3		225	20.0	1.200	80.0	1.00	0.60	1.0	1.87	4.45	1.16	1.32
59	224	Dilution2	y	225	30.0	1.200	120.0	1.00	0.60	1.0	3.33	4.62	1.21	1.37
60	225	Power3		225	15.0	1.200	80.0	1.00	0.60	1.0	1.73	2.75	1.15	1.30
61	226	Power3		225	25.0	1.200	80.0	1.00	0.60	1.0	2.37	5.48	1.19	1.35
62	227	TOF (Rep216)		225	30.0	1.200	80.0	1.00	0.60	1.0	2.01	6.56	1.22	1.37
63	282	TOF (Rep216)		225	30.0	1.200	80.0	1.00	0.60	1.0	2.32	7.16	1.24	1.39
64	285	TOF (Rep216)	y	225	30.0	1.200	80.0	1.00	0.60	1.0				
65	286	TOF (Rep216)	y	225	30.0	1.200	80.0	1.00	0.60	1.0				
66	290	?		225	30.0	0.950	80.0	1.00	0.60	1.0	1.84	5.46	1.26	1.42
67	291	TOF (Rep216)	y	225	30.0	1.200	80.0	1.00	0.60	1.0				
68	292	?	y	225	30.0	1.200	120.0	1.00	0.60	1.2				
69	300	TOF (Rep216)	y	225	30.0	1.200	80.0	1.00	0.60	1.0				
70	301	TOF/D-study3		225	30.0	1.200	80.0	1.00	0.60	1.7	2.61	8.36	1.20	1.35
71	302	TOF/D-study3		225	30.0	1.200	80.0	1.00	0.60	1.4	2.60	8.01	1.22	1.37
72	303	TOF/D-study3		225	30.0	1.200	80.0	1.00	0.60	1.2	2.50	7.45	1.23	1.38
73	304	TOF	y	225	30.0	1.200	80.0	1.00	0.60	1.0				
74	305	TOF (Rep216)	y	225	30.0	1.200	80.0	1.00	0.60	1.0	2.24	7.77	1.26	1.42
75	306	TOF		225	30.0	1.500	100.0	1.00	0.60	1.2	2.50	8.16	1.24	1.39
76	309	TOF		225	30.0	1.200	80.0	1.00	0.60	1.0	2.15	7.30	1.25	1.40
77														
78	a-Ge:H	optimum a-Ge:H		200	30.0	0.950	40.0	1.00	0.00	1.4		8.19	1.10	1.24

Table 1, continued.

	Sample (#)	No	hmT (cm2/V)	iph/id	Eact (eV)	So (1/Ω cm)	stress (kbar)	Lo (Å)	E0,cpm (meV)	a0.8 (cm-1)	E0,PDS (meV)	a0.7 (cm-1)	x	AC	AD
1	136	3.91	7.40e-08	1.00e-01	0.68	6.10e+04	5.50	362	51.0						
2	137	3.99	7.90e-08	1.20e-01	0.68	3.90e+04	3.30	550	52.0	2.50					
3	138	4.10	8.40e-08	9.60e-02	0.67	4.80e+04		560							
4	141	3.86	4.20e-08	2.40e-01	0.73	5.80e+04	3.30	380							
5	142	4.26	2.70e-08	9.30e-03	0.55	3.60e+03	6.50								
6	143	4.23	1.90e-08	5.60e-03	0.66	1.10e+05	3.70	346	54.0	12.00					
7	144	3.95	7.90e-08	3.70e-01	0.72	3.40e+04	4.90	550							
8	145	3.75	2.80e-08	3.60e-01	0.73	2.70e+04	4.50	650	54.0	1.00					
9	146	3.89	5.90e-08	3.80e-01	0.71	2.20e+04	5.30								
10	160	3.88	4.30e-08	3.30e-01	0.70	1.60e+04	4.50								
11	161	4.03	5.20e-08	3.10e-01	0.75	2.90e+05	4.70	620	51.0	1.40	50.4	3.40	0.748		
12	162	4.02	5.70e-08	1.10e-01	0.69	1.60e+05	3.70	620	54.0	1.80	55.4	4.00	0.785		
13	163	3.80	7.30e-09	4.10e-02	0.71	8.00e+04	2.40	370	66.0	3.90	66.3	4.00	0.733		
14	164	3.71	6.00e-08	5.80e-01	0.73	9.20e+04	5.20	745	52.0	0.86	50.8	2.70	0.742		
15	165	4.06	7.40e-08	1.10e-01	0.68	8.20e+04	4.80	600	52.0	1.80	48.8	3.20	0.793		
16	167														
17	168														
18	169														
19	171	3.75	8.00e-08	6.30e-01	0.74	1.60e+05	6.50	627					0.718		
20	172	3.94	1.10e-07	1.40e-01	0.71	5.10e+04	5.10	553					0.749		
21	173	3.88	1.00e-07	3.90e-01	0.71	3.40e+04	5.40	564					0.747		
22	174	3.87	9.30e-08	3.10e-01	0.64	3.40e+03	6.10	699					0.776		
23	175	3.90	5.70e-08	2.10e-01	0.69	1.90e+04	4.30	506					0.717		
24	176														
25	177	3.49	2.60e-08	5.20e-01	0.73	1.90e+03	6.00						0.597		
26	178	3.78	4.00e-08	9.70e-01	0.81	1.90e+05	6.50	629					0.658		
27	179	3.69	1.60e-08	6.80e+00	0.84	5.10e+04	7.50						0.458		
28	180	3.81	7.70e-08	1.90e-01	0.75	3.70e+04		680					0.770		
29	181	3.62	8.40e-09	1.00e+00	0.80	1.40e+04	6.10						0.455		
30	182	3.58	2.90e-09	8.60e-02	0.78	2.00e+04	5.20								
31	183	3.77	9.40e-09	5.50e-02	0.72	9.30e+03	5.80								
32	184	3.48	2.00e-08	1.20e+01	0.86	8.10e+03	8.90	737					0.374		
33	185	3.63	3.50e-08	7.90e-02	0.30	3.10e-01	5.70						0.718		
34	186	3.56	2.20e-08	2.90e+00	0.74	3.90e+03	3.70								
35	187	3.50	3.40e-08	1.00e+00	0.67	1.70e+02	6.70								
36	188	3.08					4.40								
37	189		2.80e-08	5.90e-01	0.65										
38	190	3.56													
39	191	3.81	6.80e-08	5.50e-01	0.75	4.20e+04		694							
40	192	3.77	5.10e-08	8.80e-01	0.76	8.10e+04	5.70	648							
41	195	3.67	1.80e-08	1.60e+00	0.85	1.30e+05	6.50	584							
42	196	3.70	1.80e-08	8.90e-01	0.82	2.20e+05	6.30	570							

Table 1, continued.

	Sample (#)	No	hmT (cm2/V)	Iph/Id	Eact (eV)	So (1/Ω cm)	stress (kbar)	Lo (Å)	E0,cpm (meV)	a0.8 (cm-1)	E0,PDS (meV)	a0.7 (cm-1)	x	AC	AD
43	197	3.72	1.60e-08	1.90e+00	0.71	9.00e+02	6.70	604							
44	198	3.64	1.00e-08	1.00e+00	0.80	1.80e+04	5.90	636							
45	199	3.87	1.10e-08	8.80e-02	0.75	1.20e+05	6.40	422							
46	200	3.81	1.40e-08	3.90e-01	0.75	5.60e+04	5.70	519							
47	201														
48	202	3.83	8.80e-08	1.80e-01	0.75	7.80e+04	4.90								
49	203	3.73	3.30e-08	1.30e+00	0.78	6.00e+04	5.20	621							
50	213	4.00	7.80e-09	2.00e-02	0.67	4.10e+04	2.60		63.0	9.00					
51	216	3.91	3.10e-07	2.80e-01	0.62	1.10e+04	6.30	630	46.0	2.50					
52	217	3.86	1.20e-07	4.00e-01	0.63	4.90e+04		660							
53	218	3.77	4.10e-08	7.60e-01	0.74	5.10e+04		620							
54	219	3.78	1.40e-07	2.80e-01	0.70	4.20e+04		694							
55	220	3.96	1.90e-08	2.30e-01	0.75	5.80e+04	6.30	437							
56	221	3.63	3.50e-08	4.30e+00	0.77	1.40e+04		710							
57	222	3.61	5.70e-08	3.70e+00	0.64	1.80e+02		700							
58	223	4.03	9.10e-08	4.10e-02	0.55	3.50e+03	5.80	383							
59	224	4.39	2.70e-07	1.20e-01	0.38	1.20e+02		756							
60	225	4.28	3.50e-08	1.60e-02	0.63	3.10e+04		350							
61	226	3.97	1.10e-07	2.60e-02	0.65	4.50e+04		426							
62	227	3.95	1.80e-07	2.50e-02	0.76	9.40e+05		734							
63	282	3.84	2.70e-07	2.10e-01	0.55	1.40e+03		581							
64	285														
65	286														
66	290	3.88	1.10e-07	2.70e-01	0.56	3.20e+02		621							
67	291							704							
68	292														
69	300							585							
70	301	3.99	1.20e-07	7.30e-02	0.57	2.70e+03		542							
71	302	3.99	1.20e-07	9.80e-02	0.60	2.40e+03	3.00	594							
72	303	3.98	1.20e-07	1.30e-01				638							
73	304							568							
74	305	3.77	1.10e-07	3.10e-01	0.62			671							
75	306	3.96	1.60e-07	1.20e-01				667							
76	309	3.82	1.20e-07	3.30e-01	0.59	1.10e+03		675							
77															
78	a-Ge:H	4.14	2.98e-07	7.40e-02	0.54	1.27e+04	4.10	540					1.000		

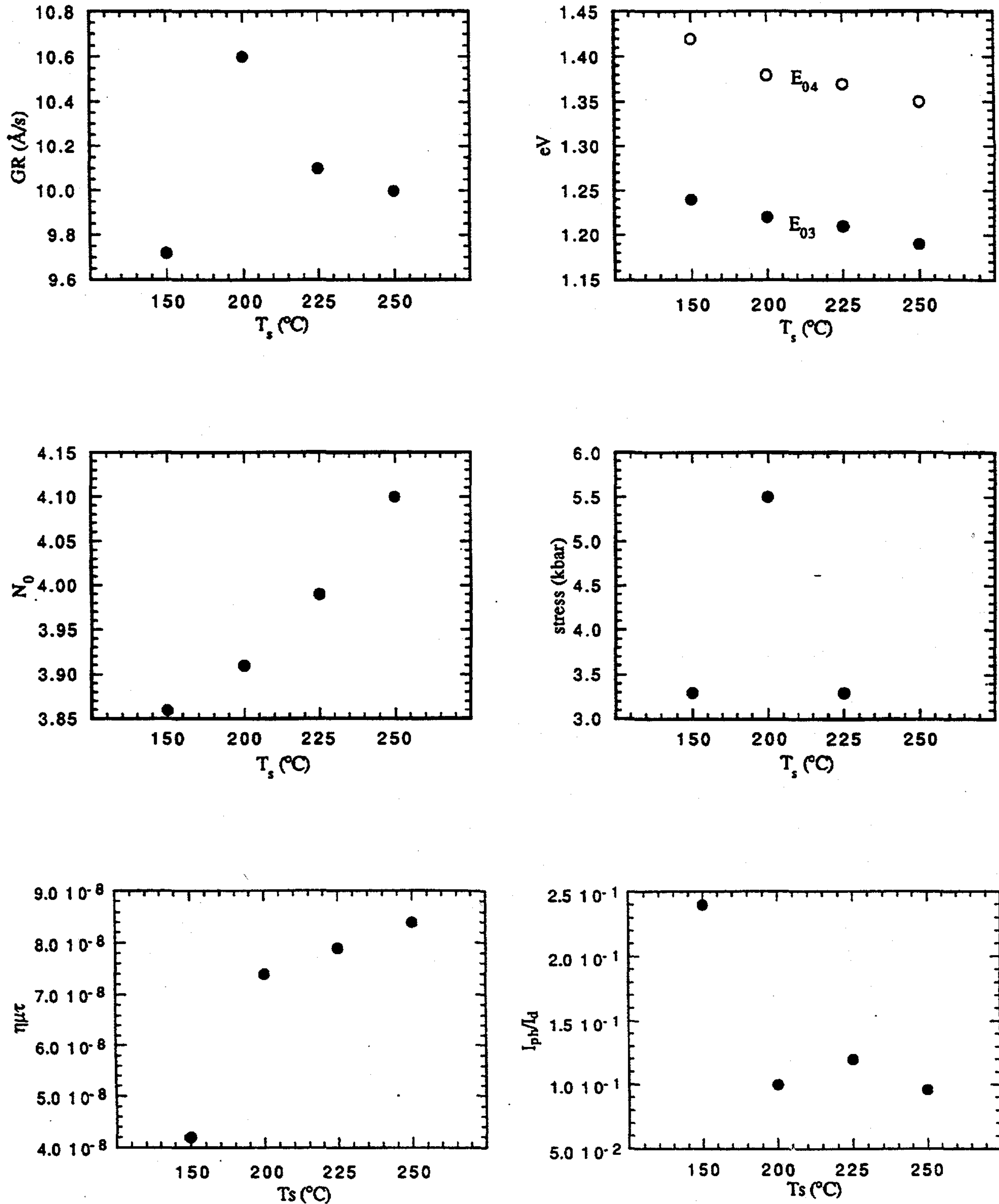

Figure 2. Variation of physical parameters of films produced at deposition temperatures T_s between 150°C and 250°C.

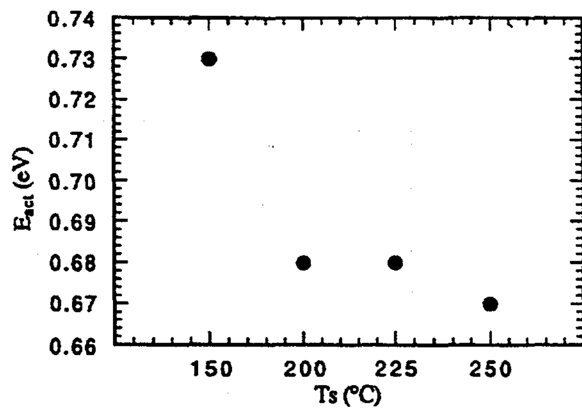

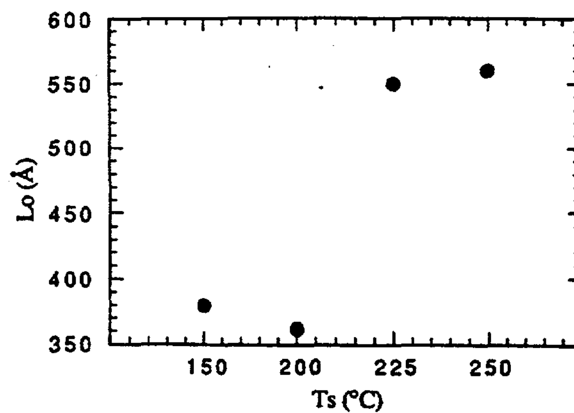

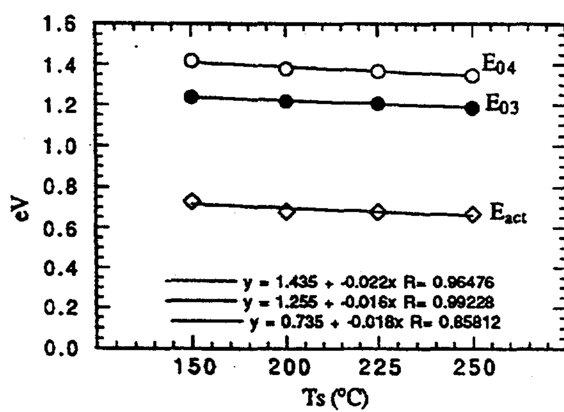

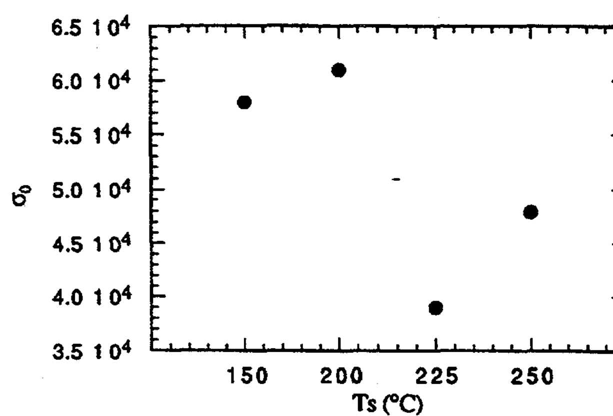

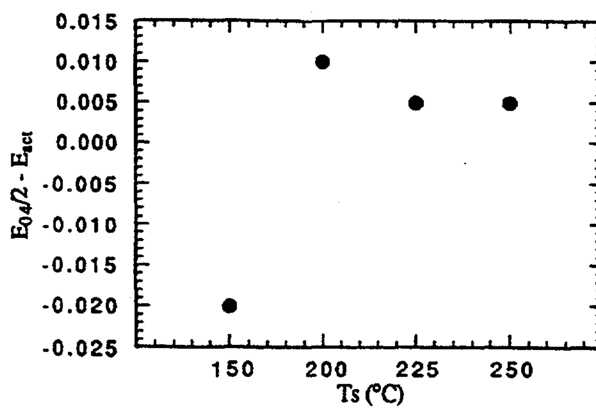

Figure 2, continued.

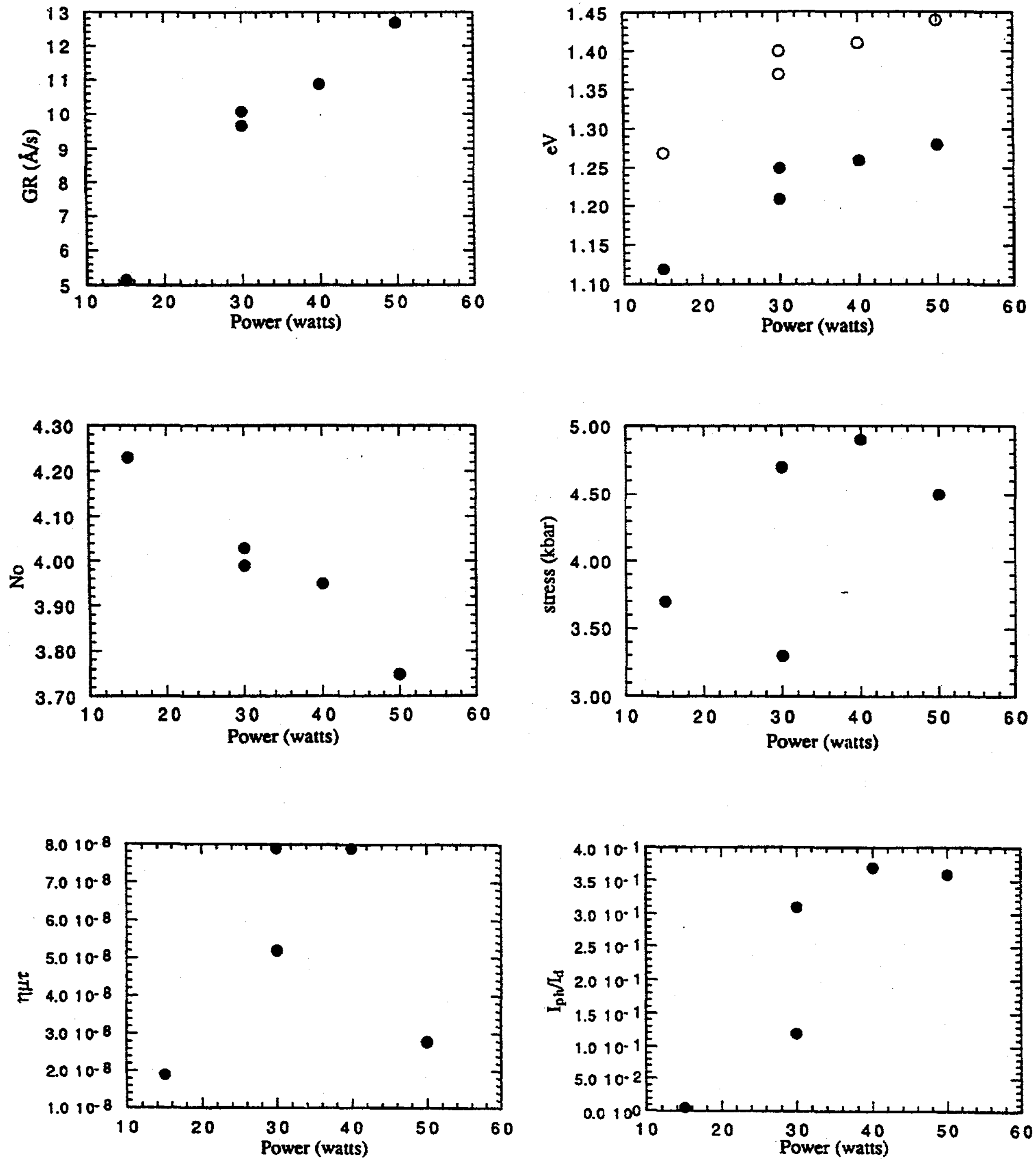

Figure 3. Variation of physical parameters of films produced at different powers, when T_s = 225°C, total pressure = 0.95 Torr, D-spacing = 1.4 cm, and the H_2:GeH_4:SiH_4 flow rates are in the ratio of *40 sccm:1.00 sccm:0.6 sccm.*

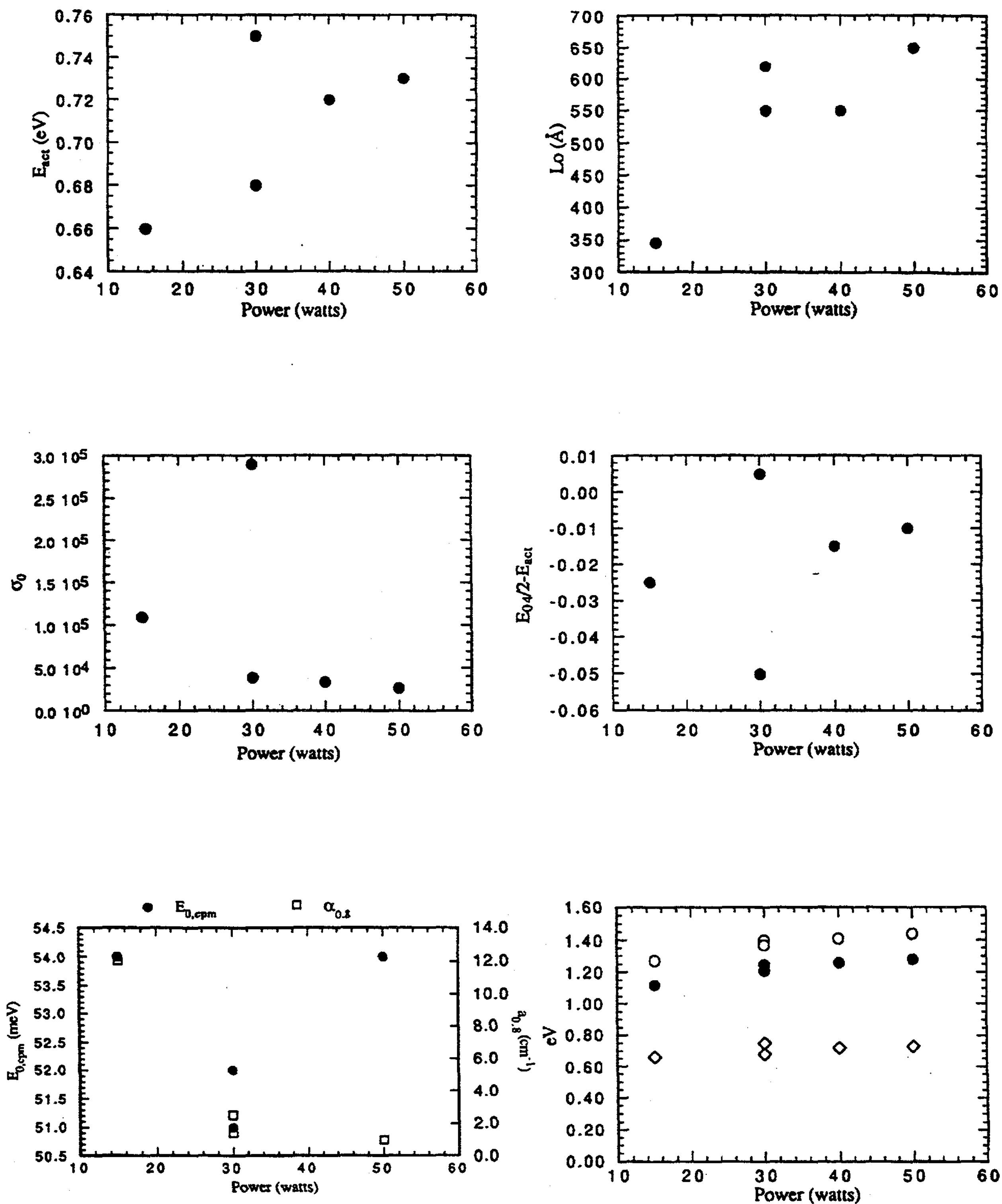

Figure 3, continued.

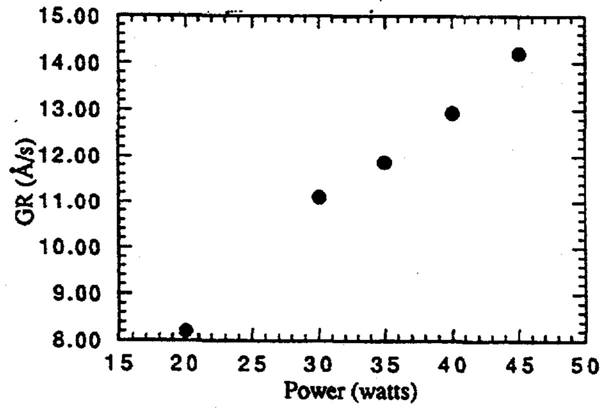

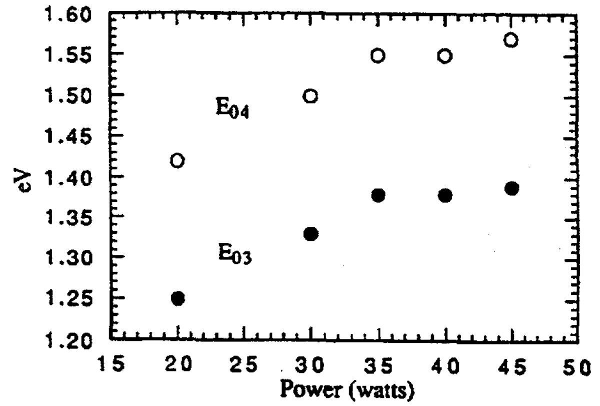

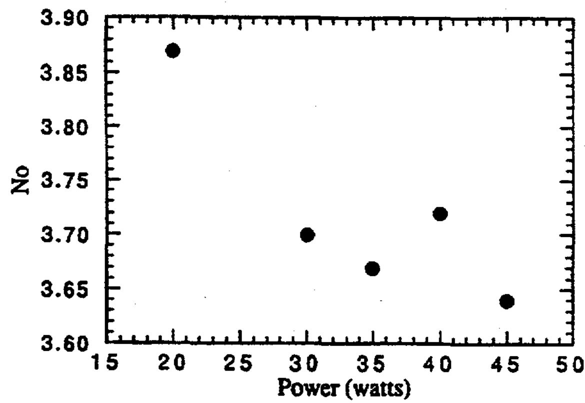

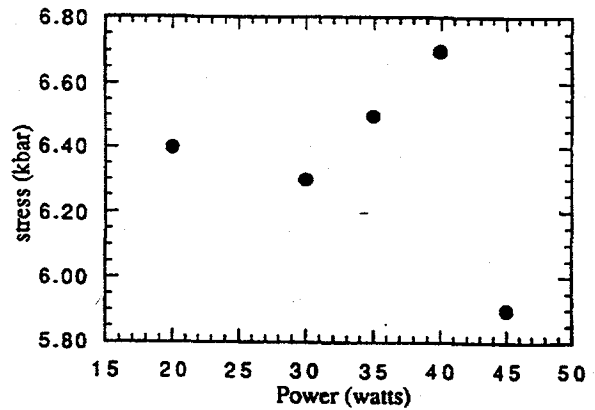

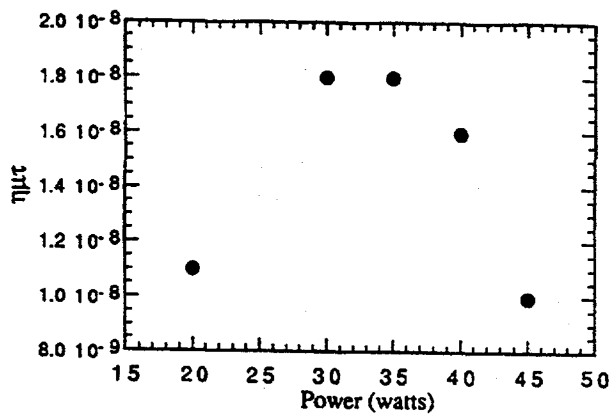

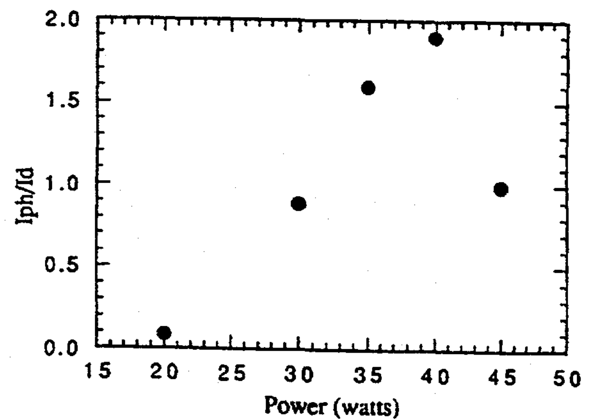

Figure 4. Variation of physical parameters of films produced at different powers, when T_s = 225°C, total pressure = 0.95 Torr, D-spacing = 1.0 cm, and the H_2:GeH_4:SiH_4 flow rates are in the ratio of 40 sccm:1.00 sccm:1.50 sccm.

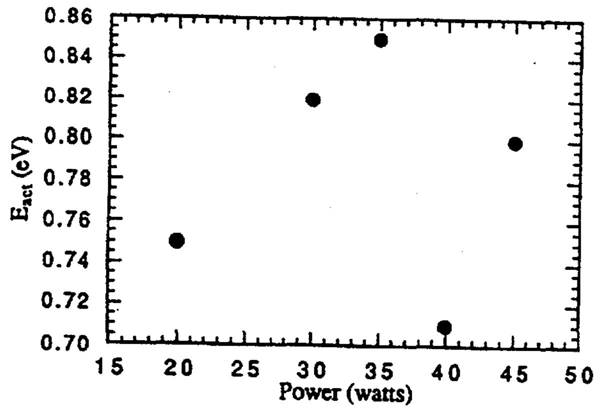

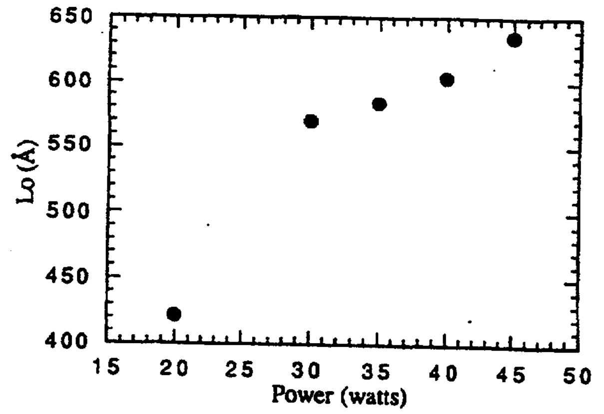

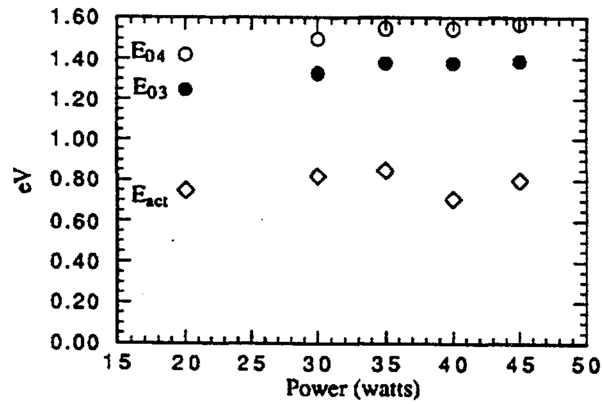

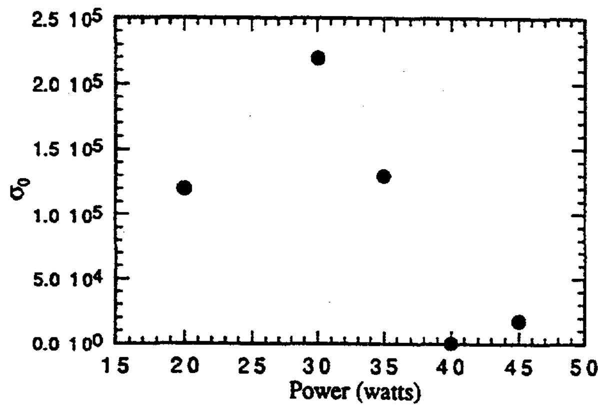

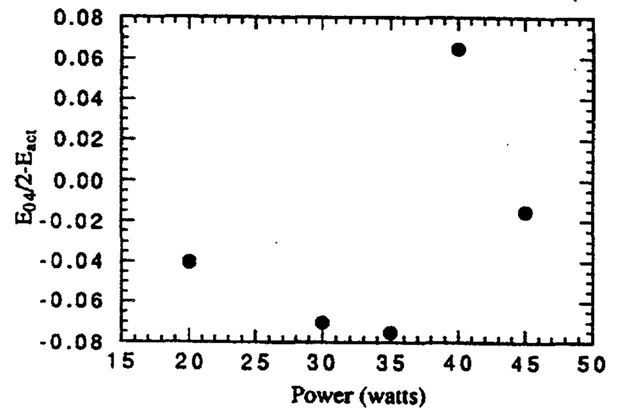

Figure 4, continued.

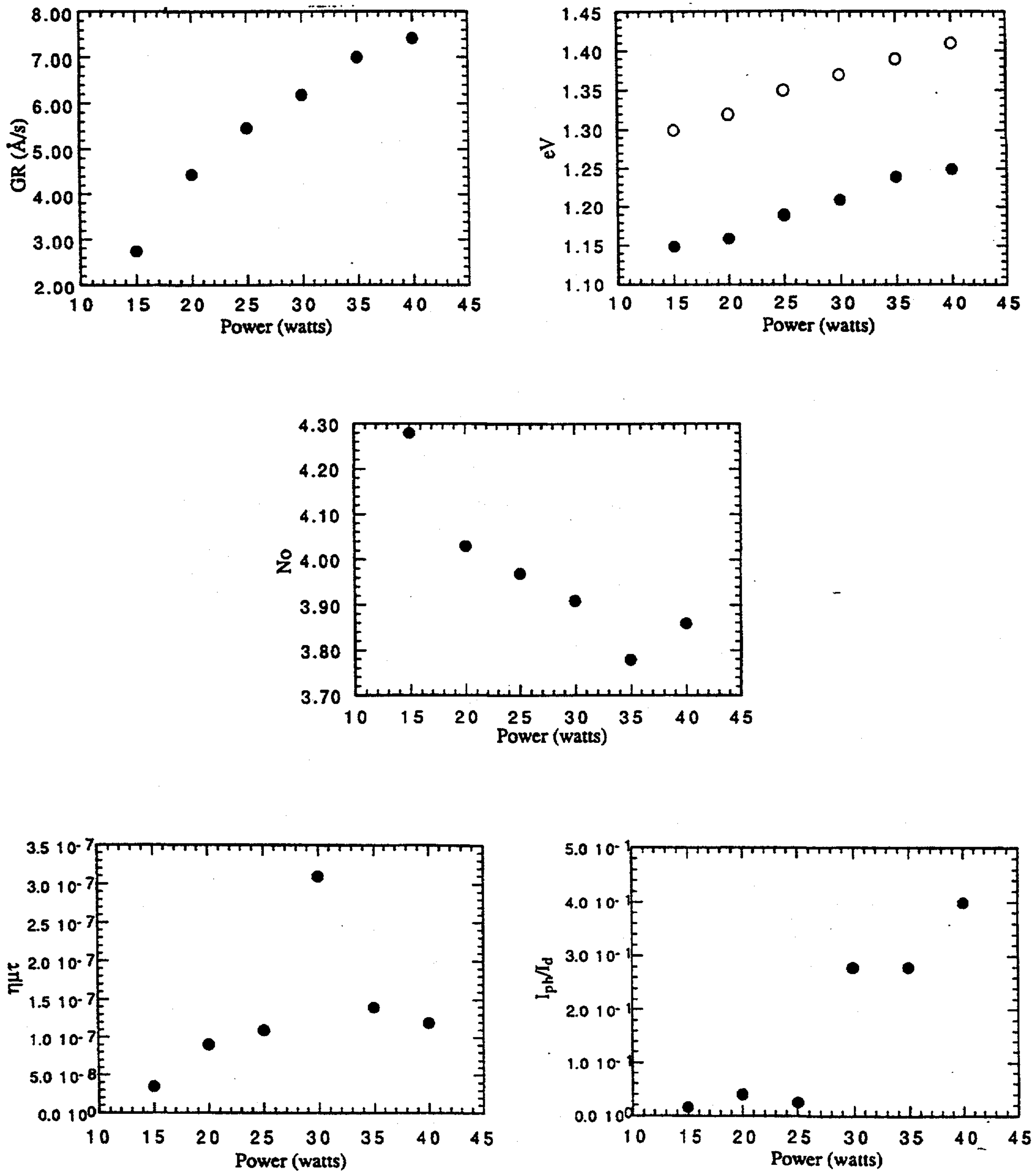

Figure 5. Variation of physical parameters of films produced at different powers, when T_s = 225°C, total pressure = 1.20 Torr, D-spacing = 1.0 cm, and the H_2:GeH_4:SiH_4 flow rates are in the ratio of 80 sccm:1.00 sccm:0.60 sccm.

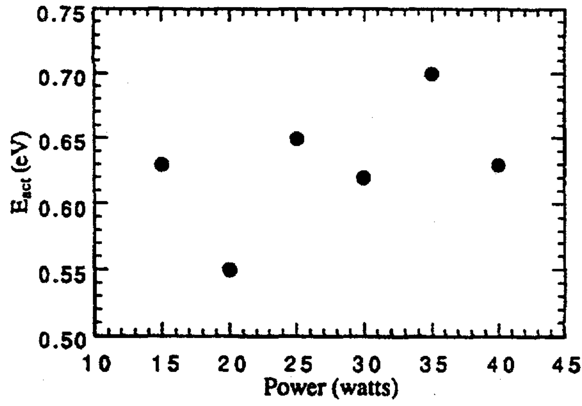

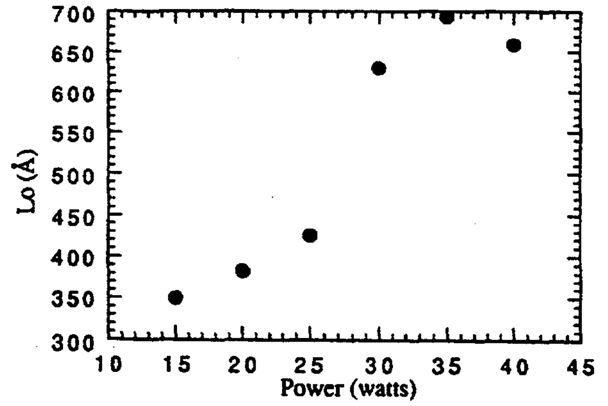

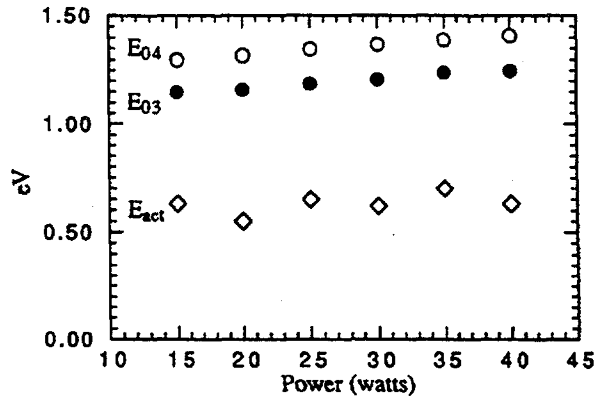

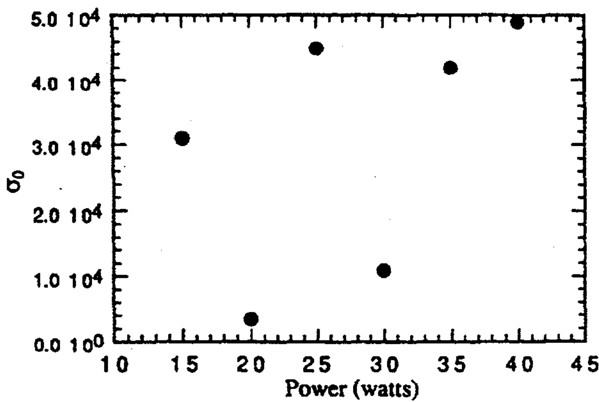

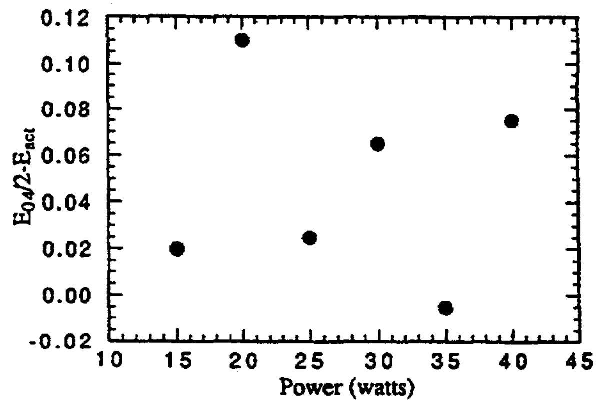

Figure 5, continued.

The effect of variation of electrode spacing D

Two studies were done as a function of D-spacing, the first with a flow of SiH_4 of 0.6 sccm, the second with a flow of 2.00 sccm. It will be recalled that *small* D-spacings appear to be optimum for pure GeH_4 decomposition and large D-spacings for pure SiH_4 decomposition. For SiH_4 flows of 0.6 sccm (161–5, 213) there is a clear deterioration in $\eta\mu\tau$ and L_0 at high values of D. The decreases in $\eta\mu\tau$ and L_0 occur even although E_{act} simultaneously decreases. For low values of D (say 1.4 cm to 2.0 cm) the $\eta\mu\tau$ are in the range of 6×10^{-8} cm^2/V, L_0 near 600 Å, N_0 near 4.03, the Fermi level near midgap, and E_{04} near 1.38 eV.

When the SiH_4 flow rate is 2.00 sccm (179, 182, 183) the behavior of the properties is generally similar. However, the deposition rate is very large, especially at large D, and the E_{04}'s are also high, presumably reflecting the greater flow of the SiH_4. All $\eta\mu\tau$ measured were below 1.6×10^{-8} cm^2/V: this value corresponds to E_{act} of 0.84 eV, but even lower values are found for *lower* E_{act}.

It appears that the low $\eta\mu\tau$ corresponding to the higher SiH_4 flow rate are not due entirely to an increase in activation energy for transport, for comparable E_{act} yield higher $\eta\mu\tau$ for the low SiH_4 flows. This corresponds to observations possible from the studies of properties with power as a variable, but with different SiH_4 flow rates. The variations of the different parameters for the two studies are displayed in Figures 6–7. Figure 6 includes the variation of the Urbach parameter, E_0, and the subbandgap optical absorption coefficient, as a function of D.

The Effect of Variation of SiH_4 Flow Rate

As might be expected, as the SiH_4 flow rate is increased, the gaps increase and N_0 decreases, monotonically, while $\eta\mu\tau$ decreases monotonically (171, 178, 179, 181).

The variations of the different parameters for two studies done are displayed in Figures 8 and 9.

The Effect of Variation of H_2 Dilution

One study was carried out (178, 191, 192, 200, 203). As the H_2 flow increased the deposition rate went down, but the gaps and the N_0 showed considerable scatter. However, $\eta\mu\tau$ and L_0 climbed monotonically as the flow of H_2 increased. The values of some parameters for the maximum flow used, 80 sccm, are of interest: GR dropped to 7.7 Å/s, E_{04} was 1.45 eV, N_0 3.81, E_{act} 0.75 eV, while $\eta\mu\tau$ was 6.8×10^{-8} cm^2/V and L_0 694 Å. There is a possibility that the decreased GR, compared to the generally larger values in the rest of this report, has led to improved material. See Figure 10.

The Effect of Variation of Total Gas Pressure

Two studies were done (171–175, 180 and 220–222). The first of these studies showed that the deposition rate climbed rapidly as the gas pressure was increased, while the gaps decreased somewhat and the N_0-variation showed scatter. The E_{act} varied more-or-less in the same way as the energy gaps, while the $\eta\mu\tau$, although high, showed scatter. The behavior of the L_0, however, was unambiguous: a decrease from a high of 700 Å at low pressure monotonically to nearly 500 Å at the top pressure. This variation, empirically at least, matched the increase in generation rate.

In the second study, the SiH_4 flow was increased to 2.0 sccm. The $\eta\mu\tau$ decreased below 1×10^{-7} cm^2/V, but, for low pressures, the L_0 remained near 700 Å. Thus, for a pressure of 0.5 Torr, a GR of 3.8 Å/s, and an E_{04} of 1.63 eV, the $\eta\mu\tau$ is 5.7×10^{-8} cm^2/V (E_{act} 0.64 eV), and the L_0 is 700 Å, with $(E_{04} - E_{act}) \sim 1$ eV.

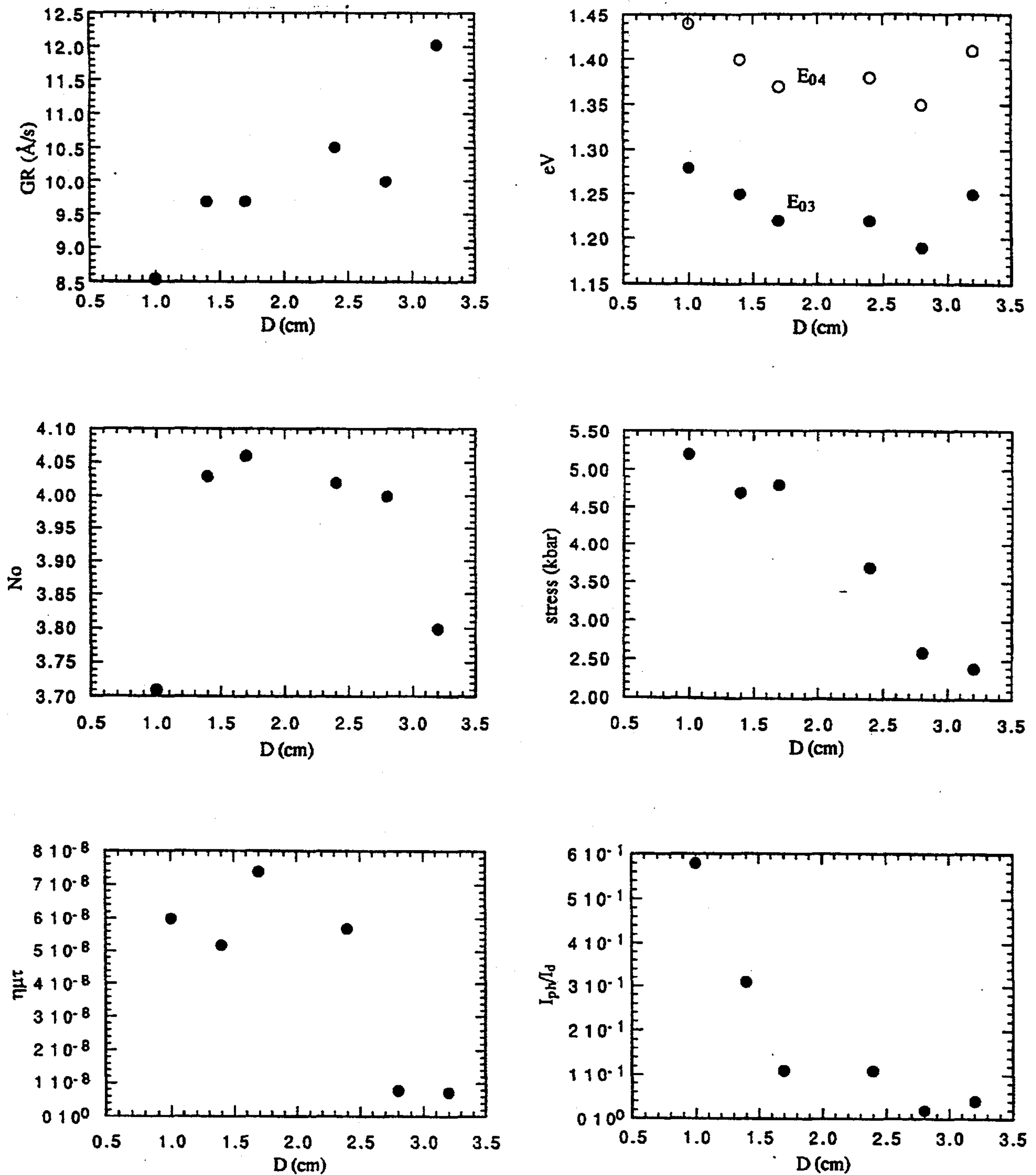

Figure 6. Variation of physical parameters of films produced at different electrode spacings, when T_s = 225°C, power = 30 W, total pressure = 0.95 Torr, and the H_2:GeH_4:SiH_4 flow rates are in the ratio of 40 sccm:1.00 sccm:0.6 sccm.

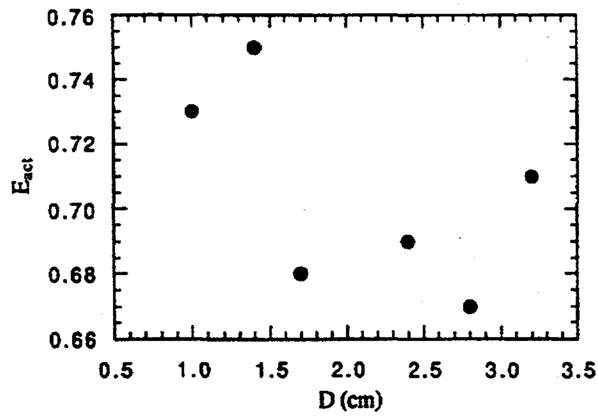

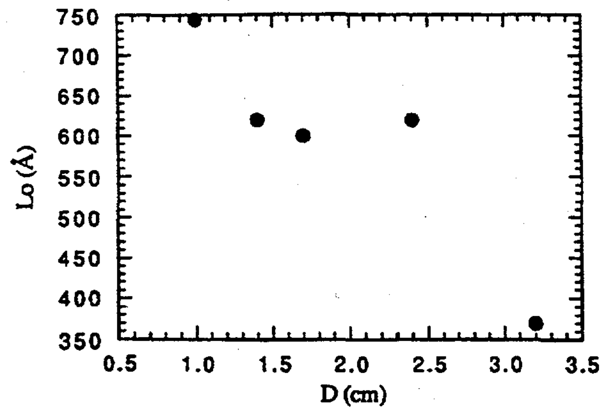

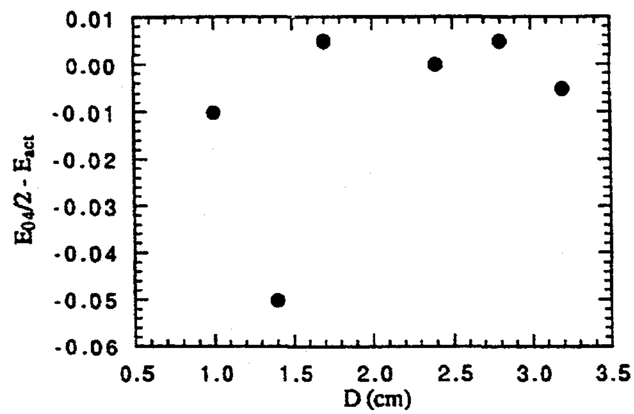

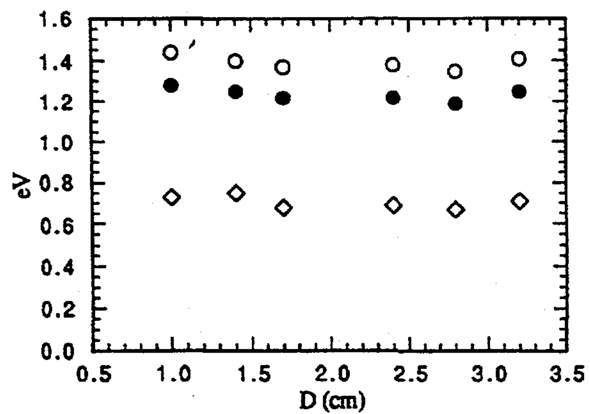

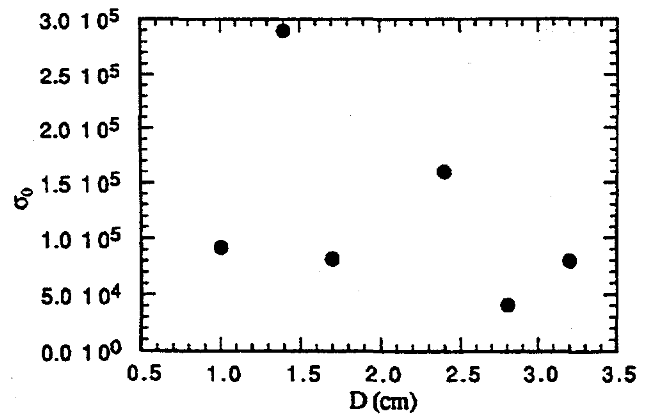

Figure 6, continued.

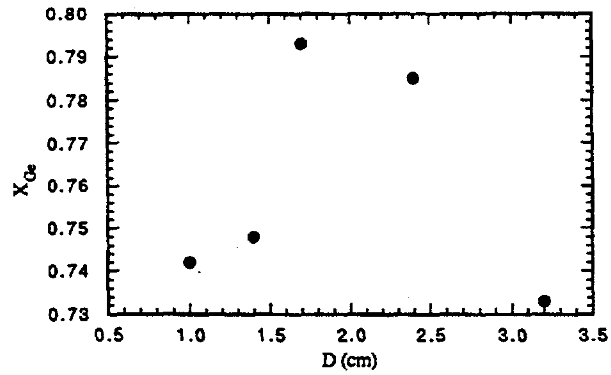

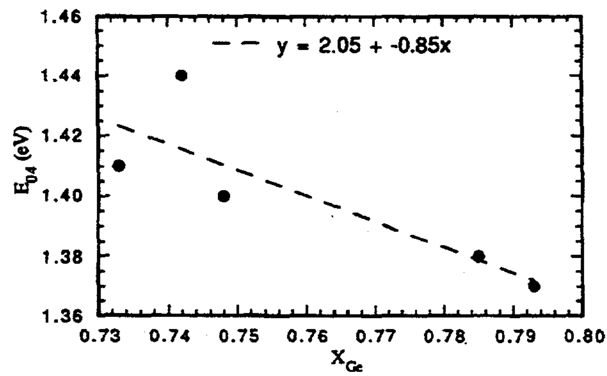

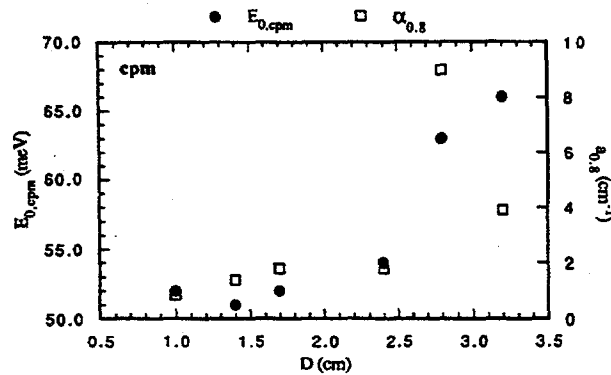

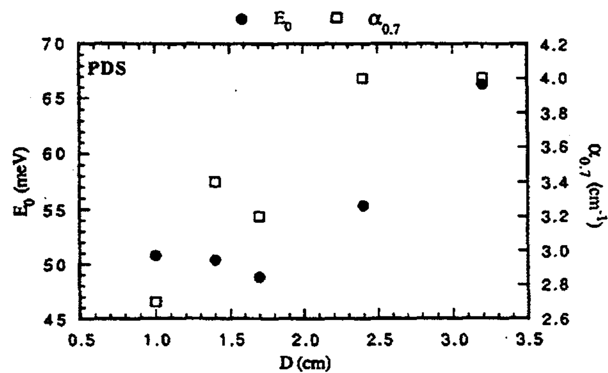

Figure 6, continued.

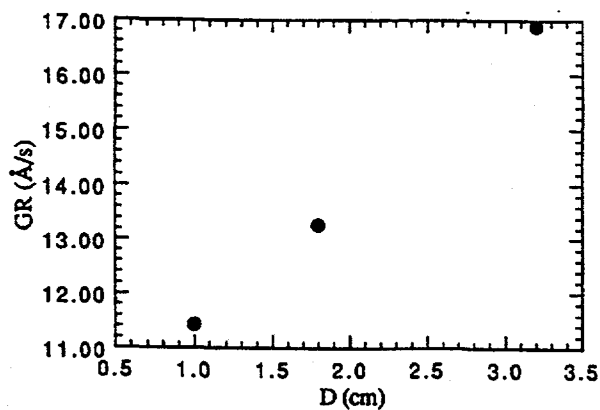

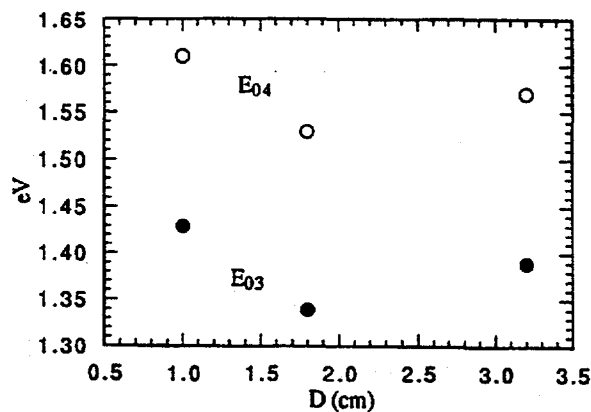

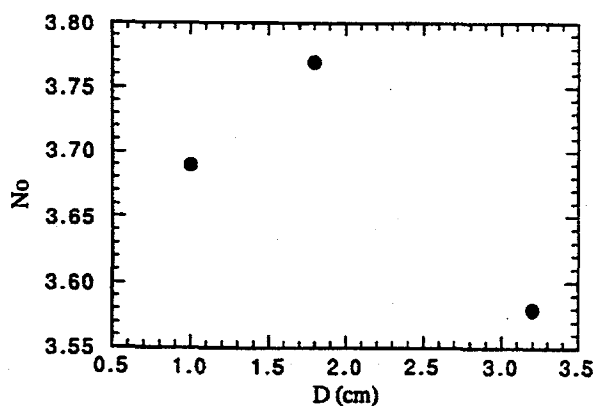

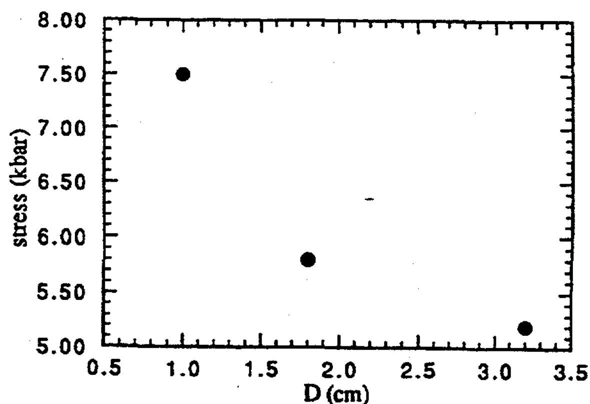

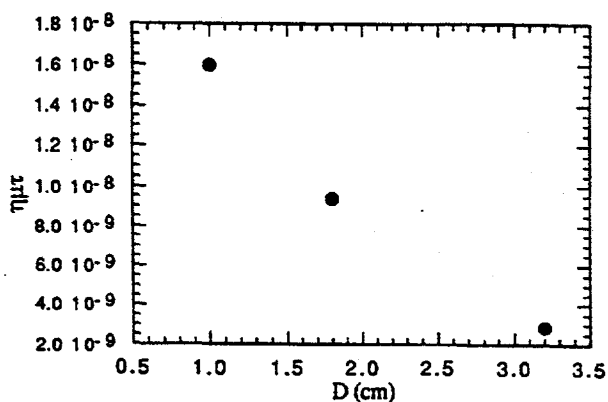

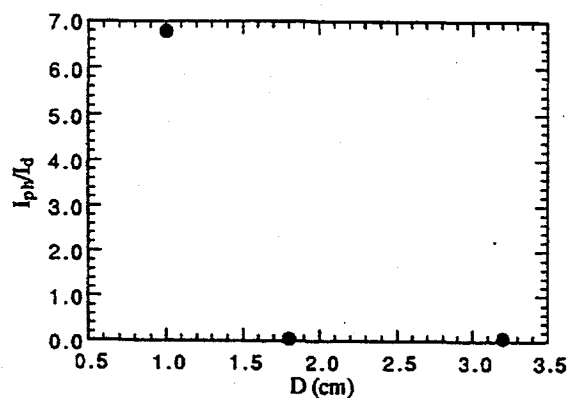

Figure 7. Variation of physical parameters of films produced at different electrode spacings, when T_s = 225°C, power = 30 W, total pressure = 0.95 Torr, and the H_2:GeH_4:SiH_4 flow rates are in the ratio of 40 sccm:1.00 sccm:2.00 sccm.

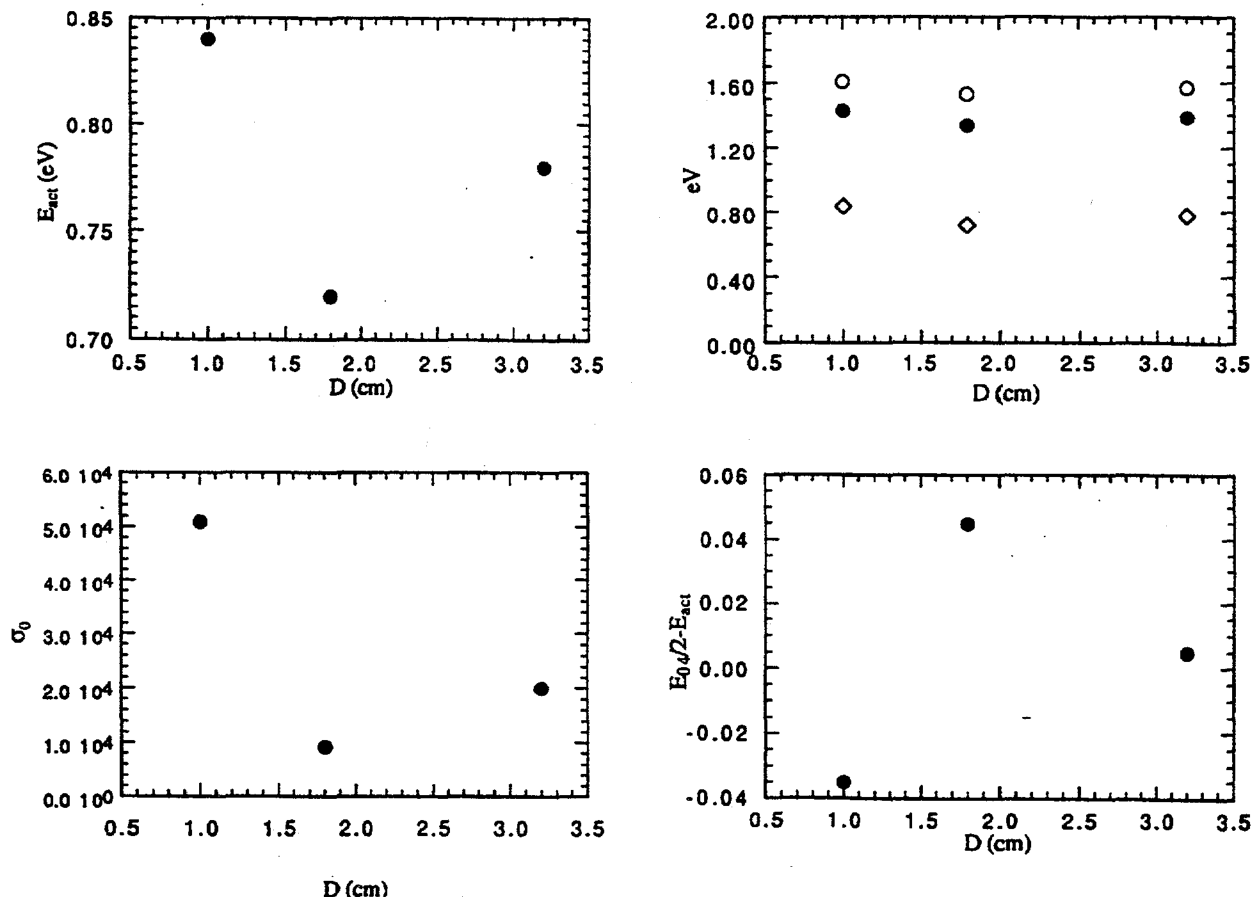

Figure 7, continued.

See Figures 11 and 12 for the details of property variation.

Discussion

It is obviously hard to discern real trends when there are so many inter-dependent deposition parameters, and it is uncertain on which property values one should focus to see correlations. Here we shall, nevertheless, attempt to draw some limited conclusions, keeping in mind the photoelectronic parameters of $\eta\mu\tau$ and L_0 for unalloyed a-Ge:H and the extrapolated $\eta\mu\tau$ and L_0 for a-$Si_{1-x}Ge_x$:H alloys of small x.

In Table 2 we select the values, or range of values, of deposition variables used to produce a-Ge:H of E_{04} gap 1.25 eV, a-$Si_{1-x}Ge_x$:H alloy of E_{04} gap 1.4 eV, and a-$Si_{1-x}Ge_x$:H alloy of E_{04} gap 1.55 eV.

In Table 3 we report several photoelectronic properties, which include $\eta\mu\tau$ and L_0. Since the film numbers are identified, their other properties, as well as the properties of similarly-produced films, are also available in Table 1.

The present studies on alloys were directed at producing E_{04} gaps of approximately 1.4 eV and 1.55 eV. The studies just described show that the gaps depend quite sensitively, not only on SiH_4 flow rate, but also on T_s, H_2 flow, power, D-spacing and pressure. Nevertheless, from Table 3, we can see that, as the Si-alloy content increases, the separation $(E_{04} - E_{03})$ increases (for E_{04} gap

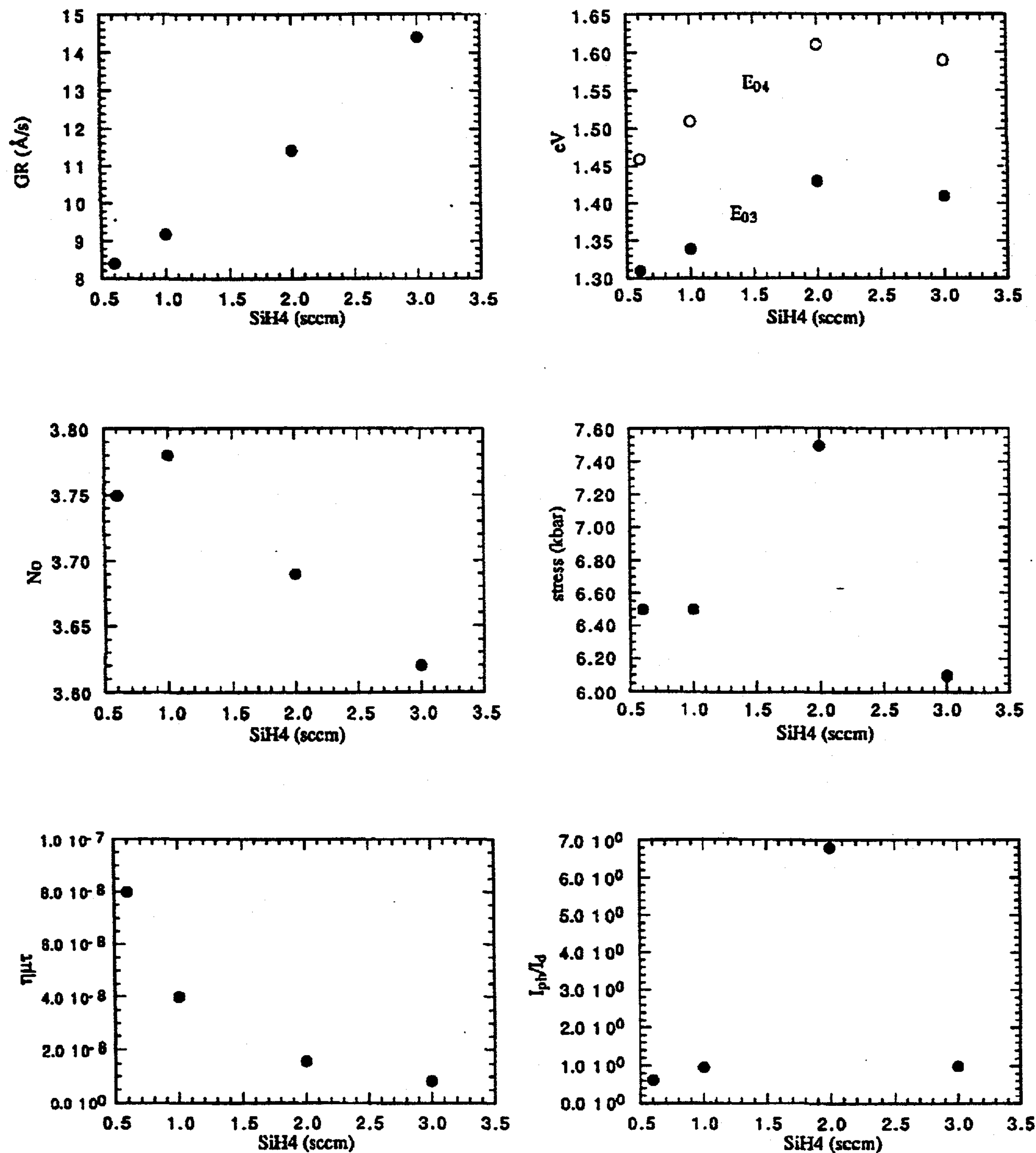

Figure 8. Variation of physical parameters of films produced at different SiH_4 flow rates, when T_s = 225°C, power = 30 W, total pressure = 0.95 Torr, D-spacing = 1.0 cm and the H_2:GeH_4 flow rates are in the ratio of 40 sccm:1.00 sccm.

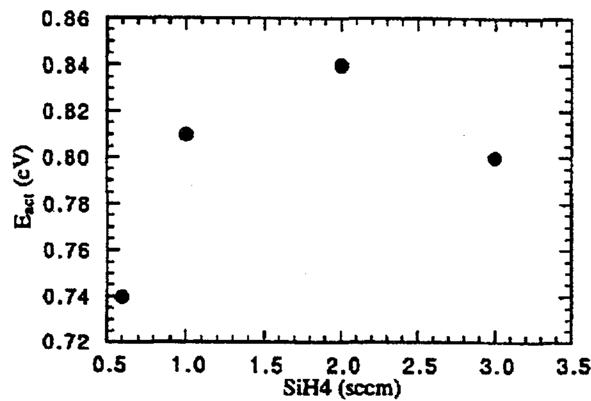

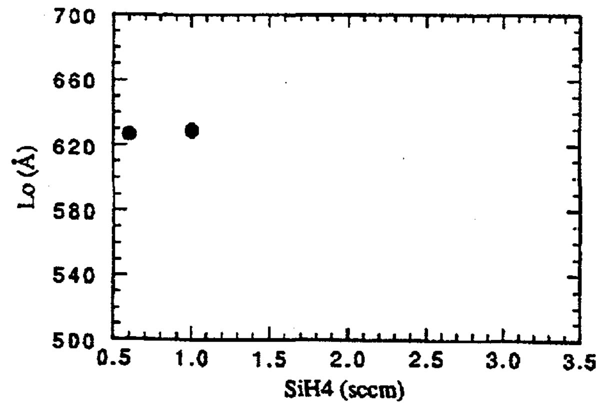

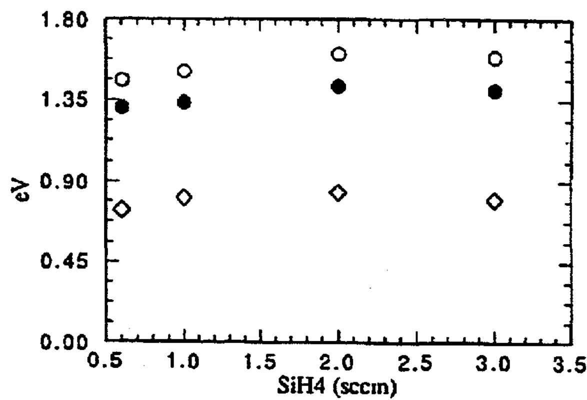

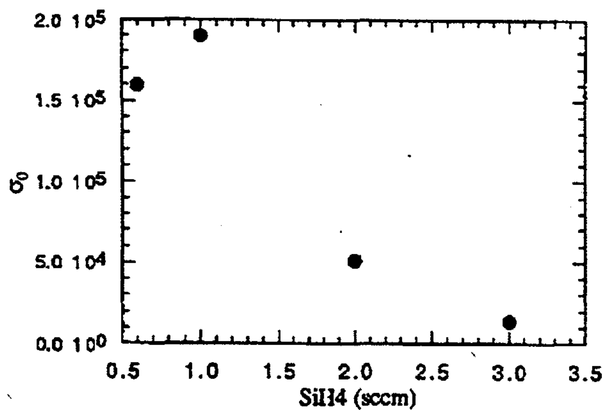

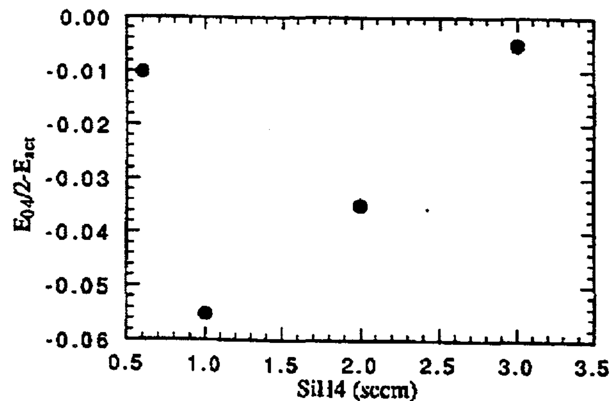

Figure 8, continued.

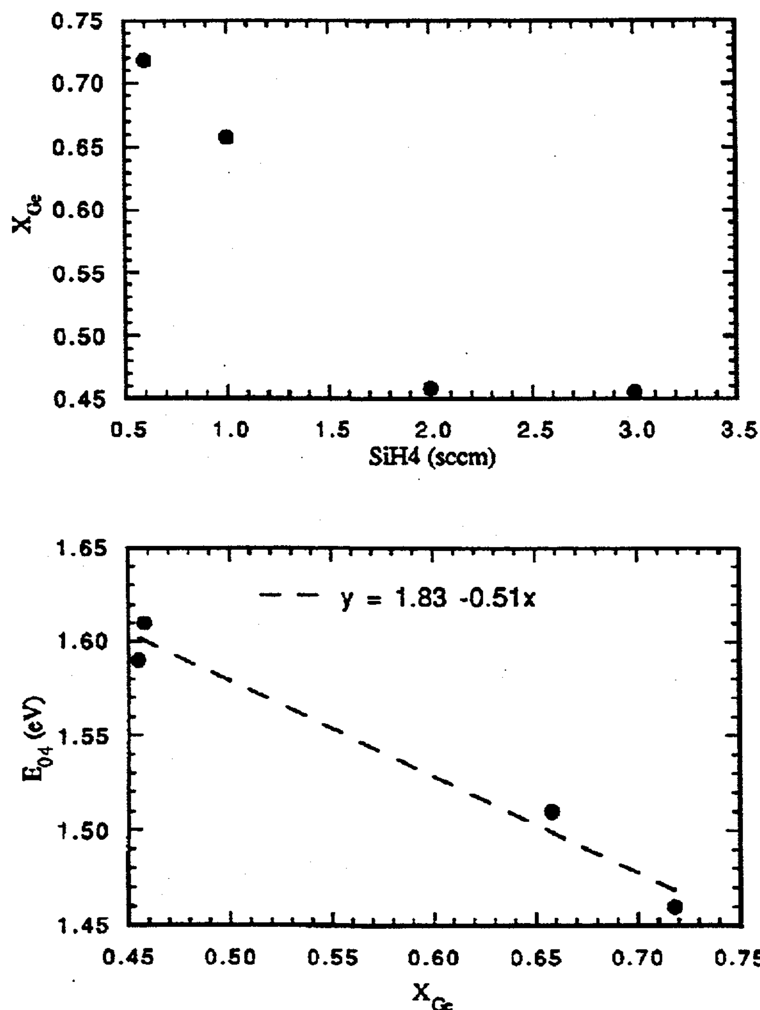

Figure 8, continued.

of 1.57 eV), which implies some broadening of the optical absorption edge. E_{act} increases, and N_0 decreases, as expected. **The most significant change seems to be that the average $\eta\mu\tau$ decreases from 3×10^{-7} cm^2V^{-1} to 7.3×10^{-8} cm^2V^{-1} to 2.7×10^{-8} cm^2V^{-1}, while there is a significant non-change in L_0, whose averages remain at 550, 619 and 615 Å.**

Although the $\eta\mu\tau$ do decrease as Si is added to Ge in the a-$Si_{1-x}Ge_x$:H alloy, the $\eta\mu\tau$ for the 1.4 eV E_{04} alloy are two orders of magnitude larger than in our earlier study where the samples were made under conditions resembling those for a-Si:H. They are also two orders of magnitude larger than those for similar bandgaps in a recently published NREL study[21] which we assume is representative of the field. We conclude that for alloys of high Ge content, the preparation conditions to start with are those optimizing a-Ge:H, which was our original postulate. The $\eta\mu\tau$ for the 1.55 eV E_{04} alloys are only slightly better than those for samples made following a-Si:H conditions. For these alloys the x-value is close to 0.5, so that this result is not unexpected. These variations in $\eta\mu\tau$ and L_0, as a function of x and E_{04}, are illustrated in Figure 13.

The order of magnitude decrease in $\eta\mu\tau$ along with the near-constancy of the ambipolar diffusion length L_0 suggests a microscopic model for the alloys. We infer that both structural and compositional disorder occur, and that the compositional disorder is significant. It is known that there

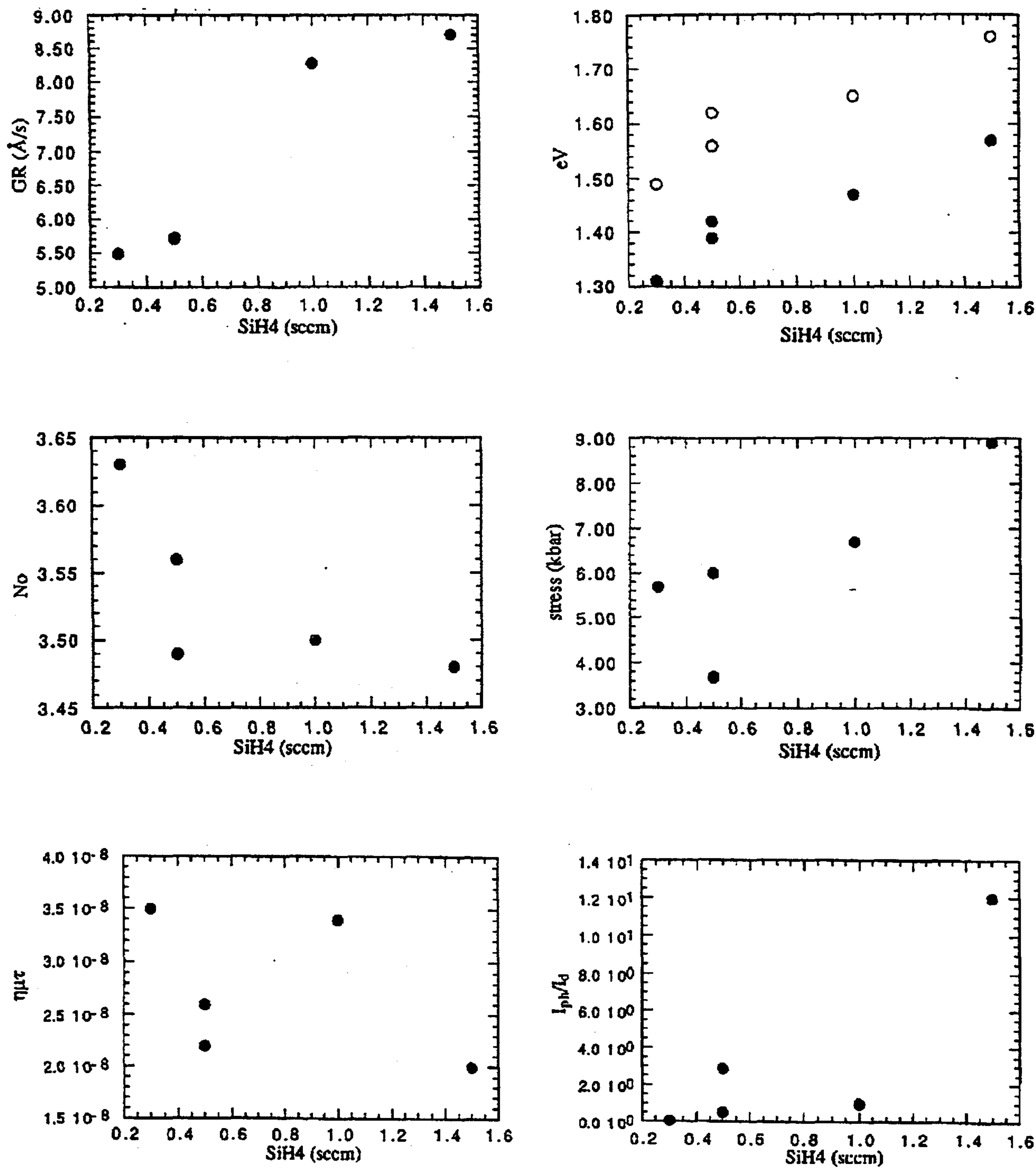

Figure 9. Variation of physical parameters of films produced at different SiH_4 flow rates, when T_s = 225°C, power = 30 W, total pressure = 0.95 Torr, D-spacing = 1.0 cm and the H_2:GeH_4 flow rates are in the ratio of 40 sccm:0.50 sccm.

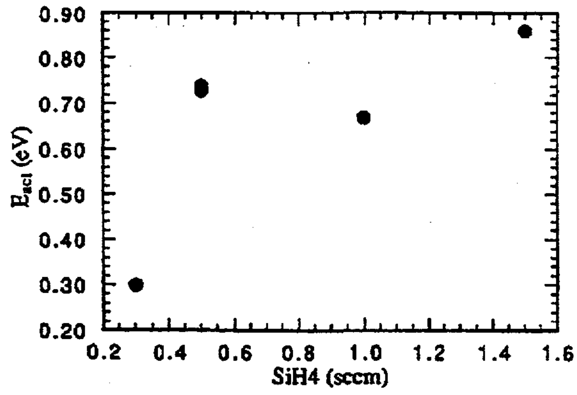

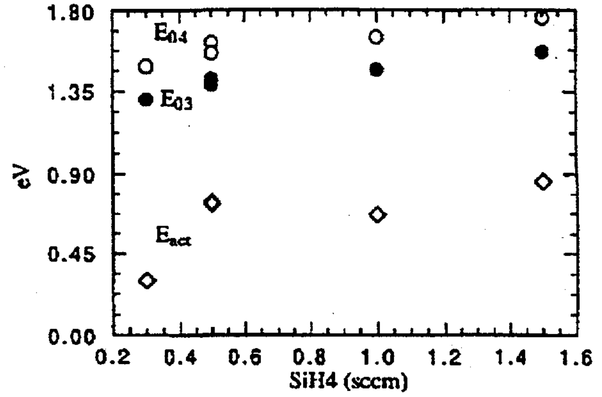

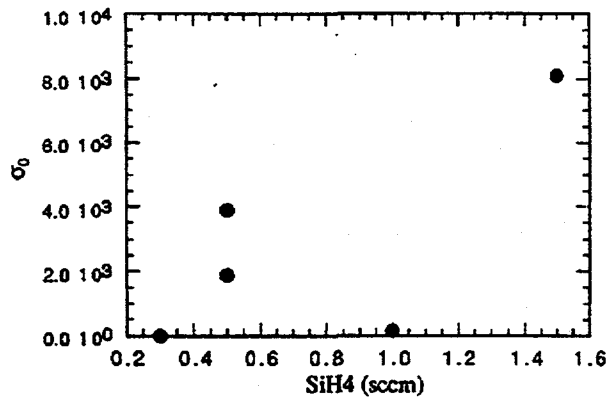

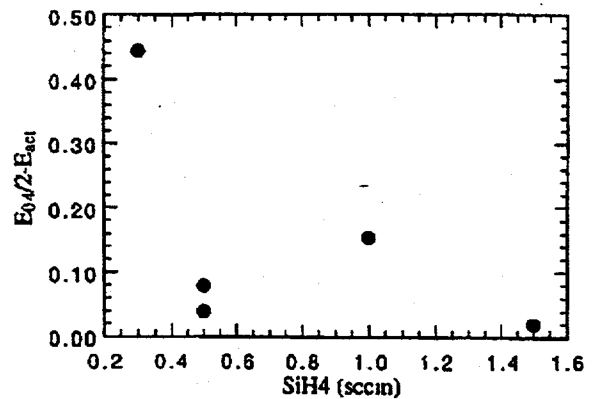

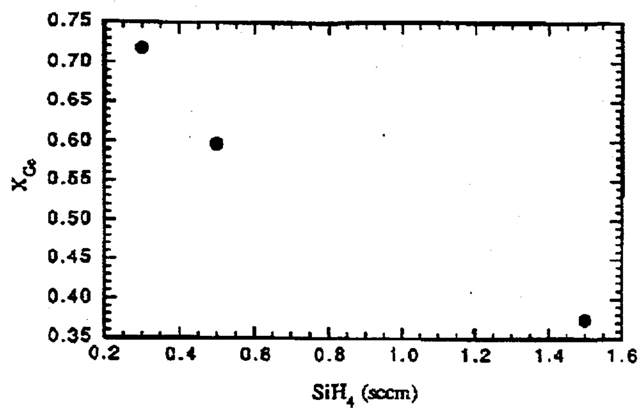

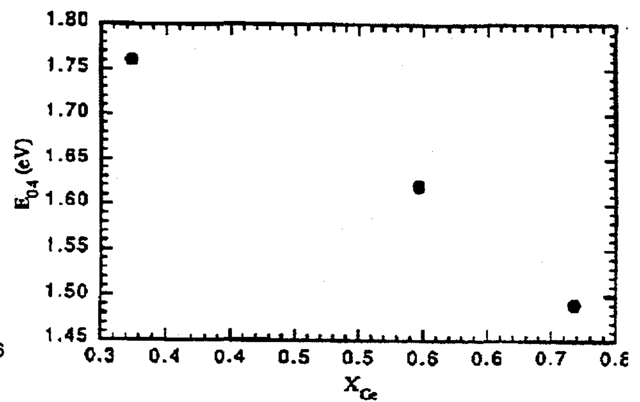

Figure 9, continued.

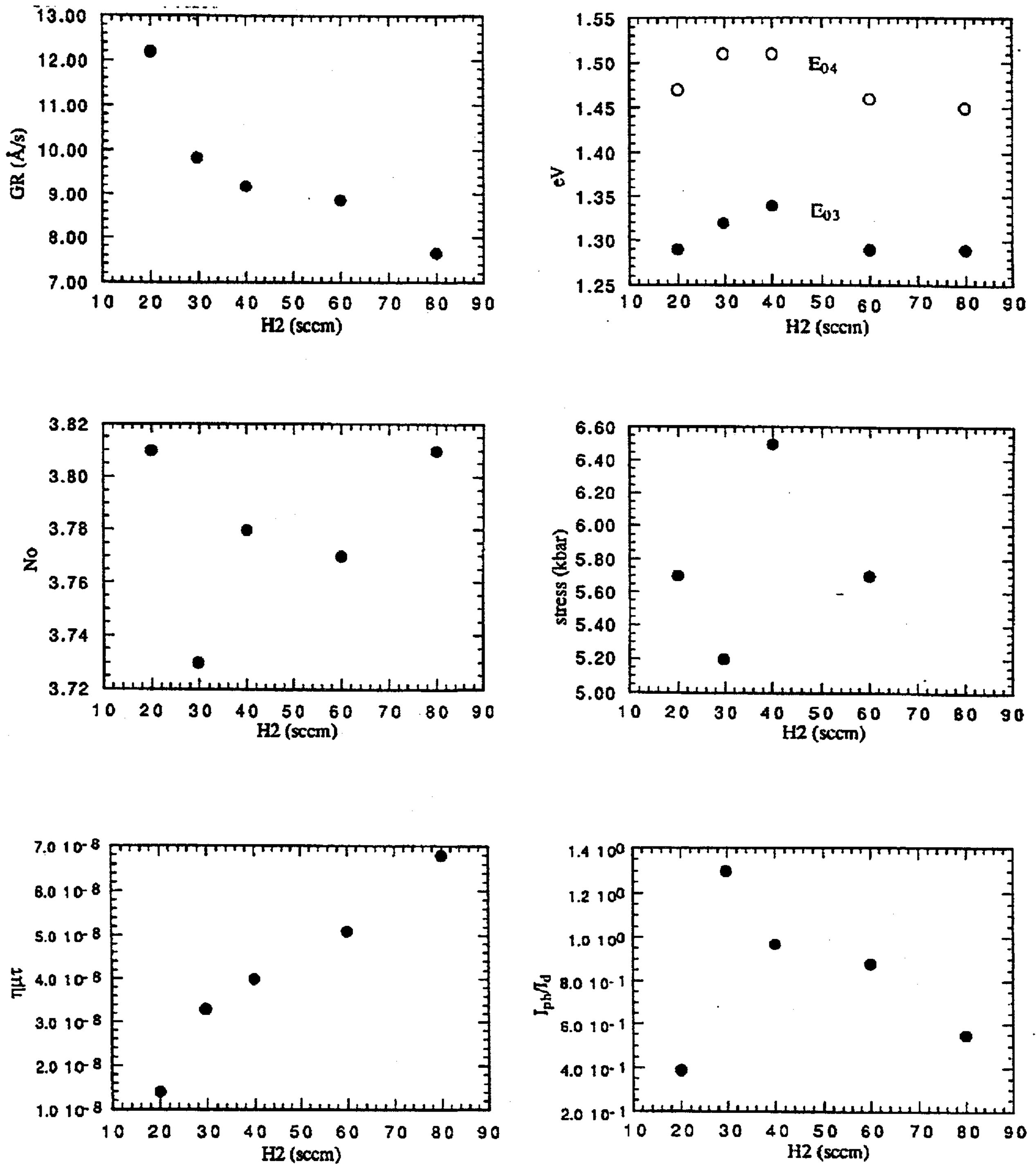

Figure 10. Variation of physical parameters of films produced at different H_2 dilution, when T_s = 225°C, power = 30 W, total pressure = 0.95 Torr, D-spacing = 1.0 cm and the GeH_4:SiH_4 flow ratio is 1.00 sccm:1.00 sccm.

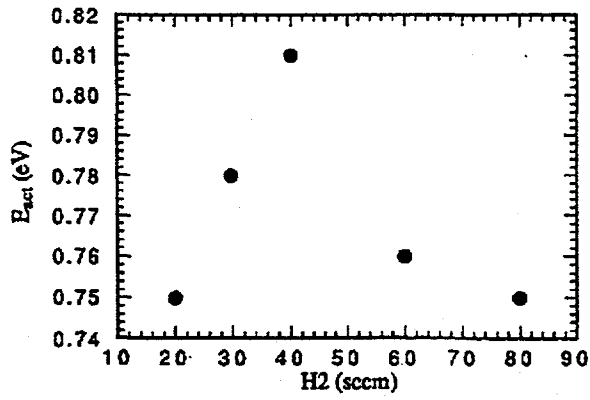

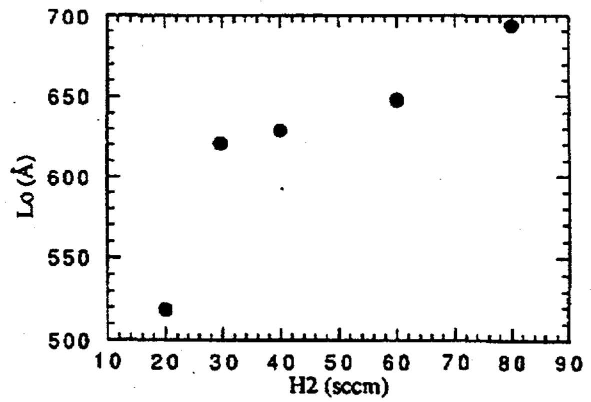

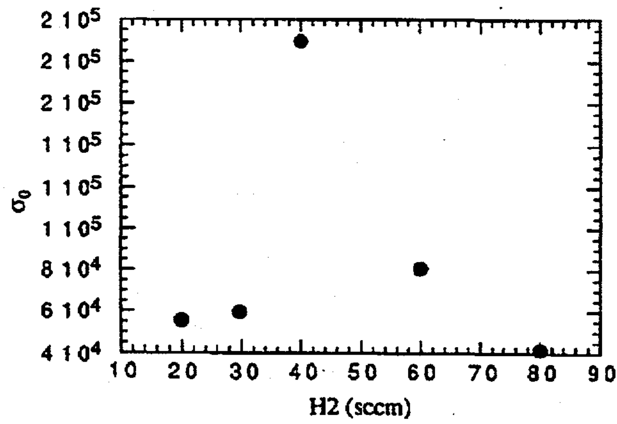

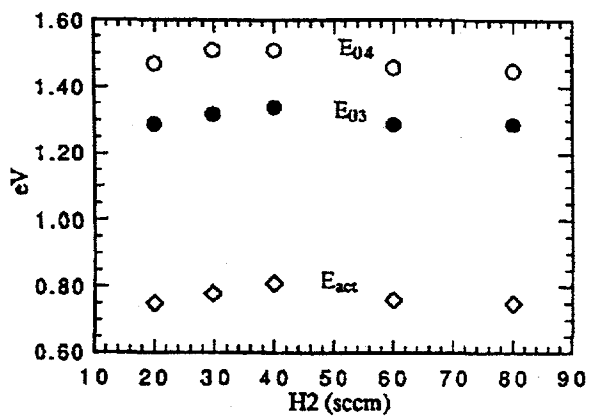

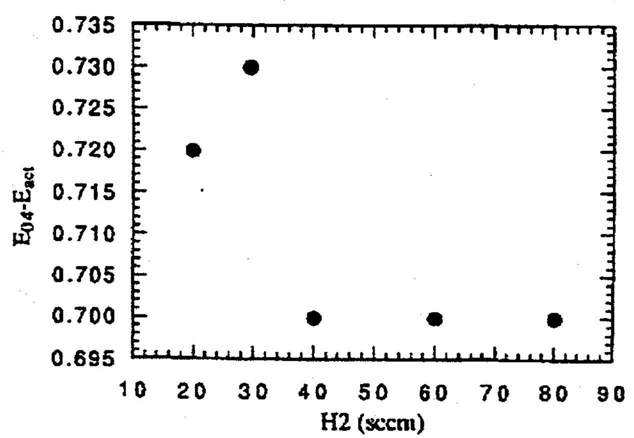

Figure 10, continued.

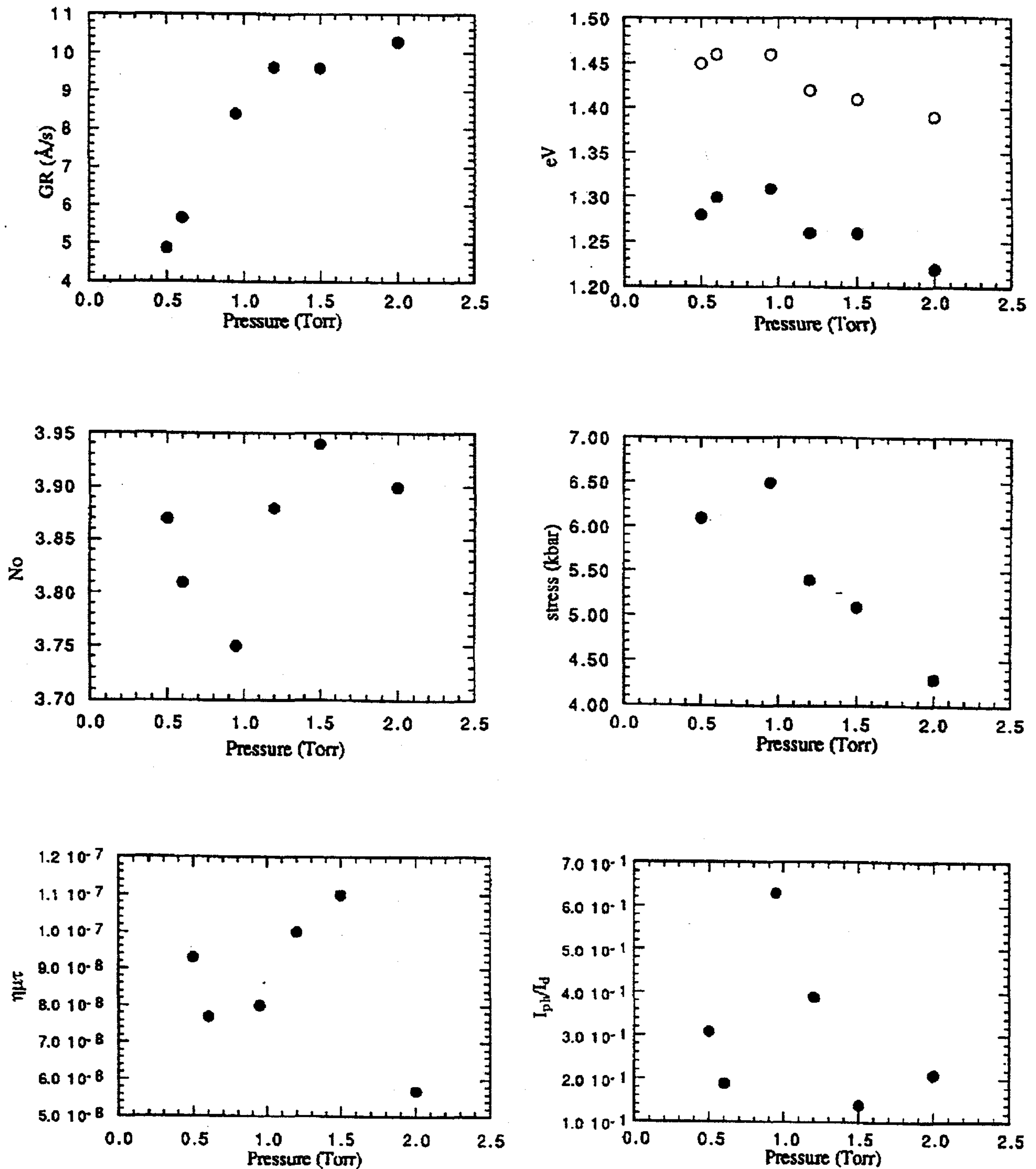

Figure 11. Variation of the physical parameters of films produced at different total pressure, when T_s = 225°C, power = 30 W, D-spacing = 1.0 cm and the H_2:GeH_4:SiH_4 flow rates are in the ratio of 40 sccm:1.00 sccm:0.60 sccm.

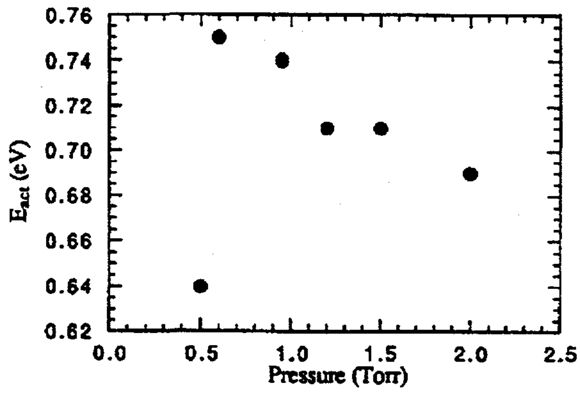

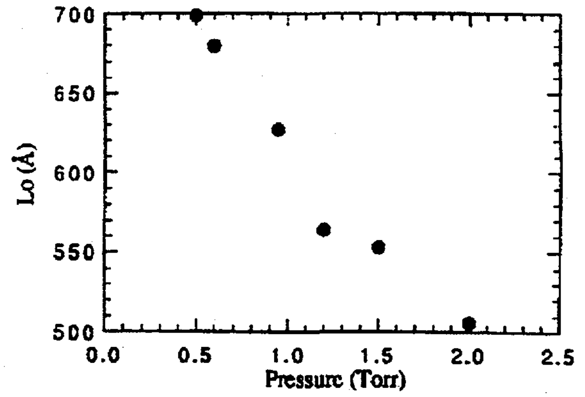

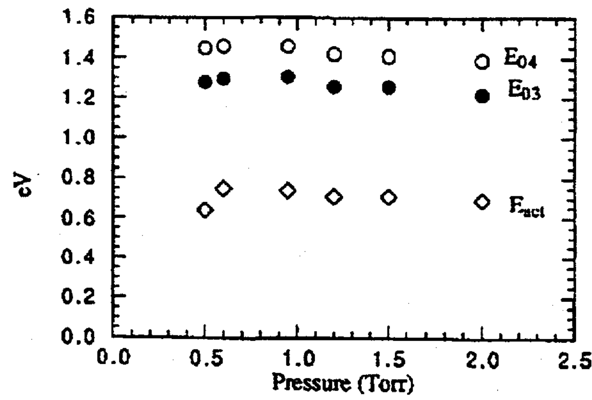

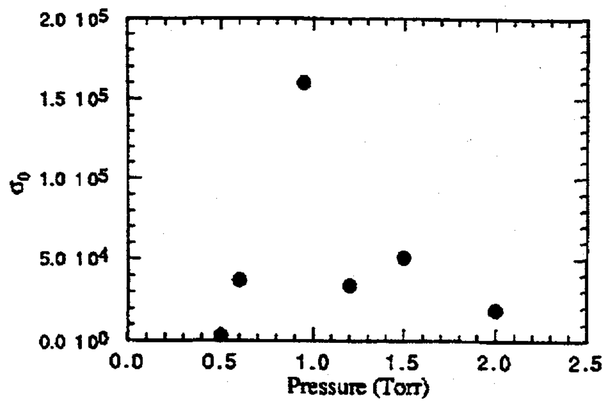

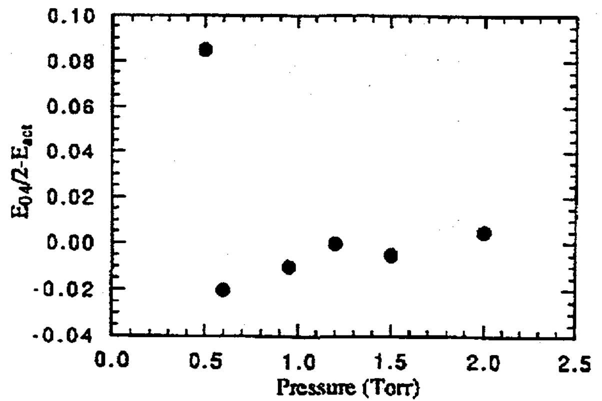

Figure 11, continued.

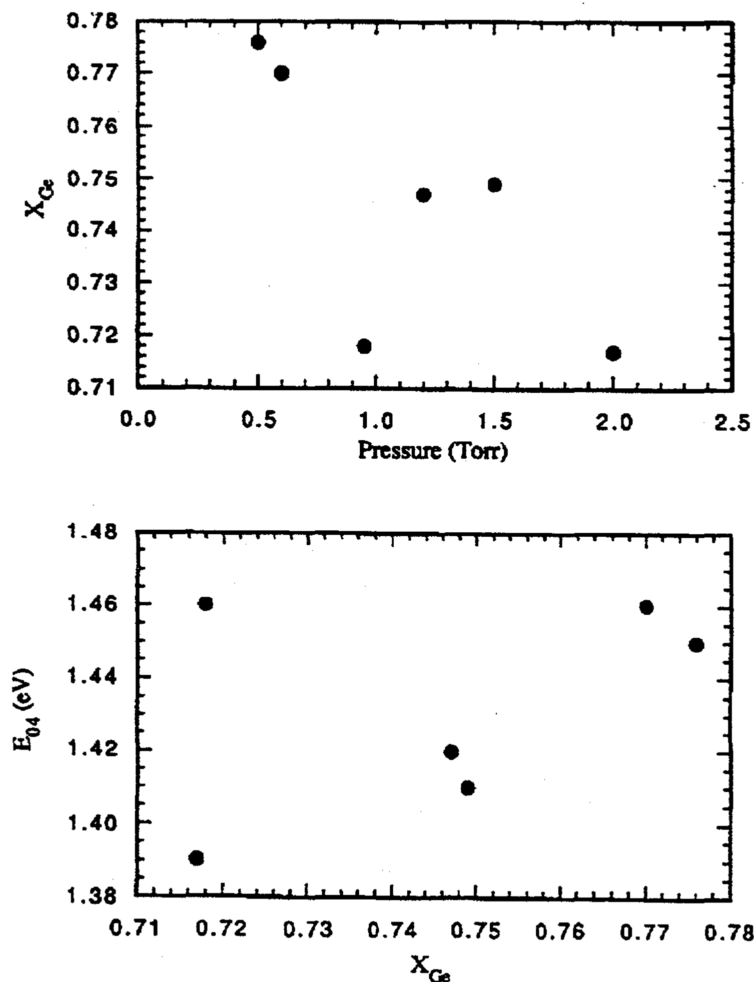

Figure 11, continued.

is very little valence band offset between a-Si:H and a-Ge:H[23] and that the bandgap difference is ascribable mostly to the edges of the conduction band. Compositional disorder will then result in a conduction band edge fluctuating in energy, a potential variation which will lead to a low, and activated, electron mobility, and reduced $\eta\mu\tau$ product. By contrast, the compositional variation does not result in a potential fluctuation at the valence band edge. Since L_0 is dominated by the minority carrier transport, it should not vary in synchronization with $\eta\mu\tau$, as is observed.

These tentative conclusions concerning compositional variations would reduce $\eta\mu\tau$ from the values for a-Si:H and a-Ge:H, as our overall studies show. The variation in L_0 between a-Si:H and our best a-Ge:H is only about a factor of two. Whether conditions can be found to eliminate compositional fluctuations, if indeed they occur as we infer, is an open question.

It is evident that our model for deterioration of $\eta\mu\tau$ and constancy of L_0 requires, if possible, direct experimental confirmation through studies of compositional variation on a 10 nm scale. To date, our attempts to demonstrate these have shown no positive results one way or the other. However, we recommend that such studies continue.

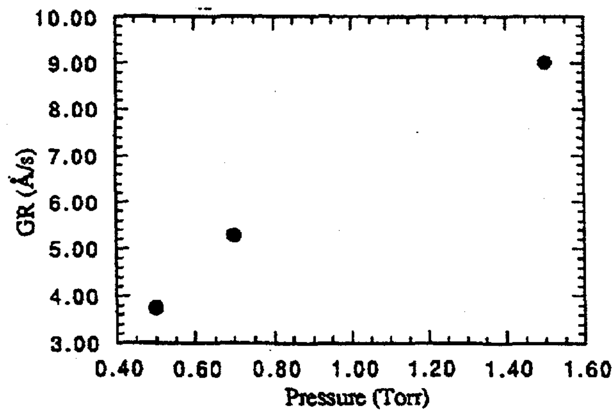

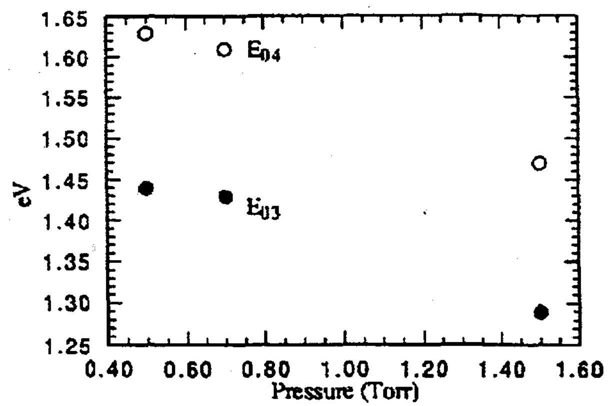

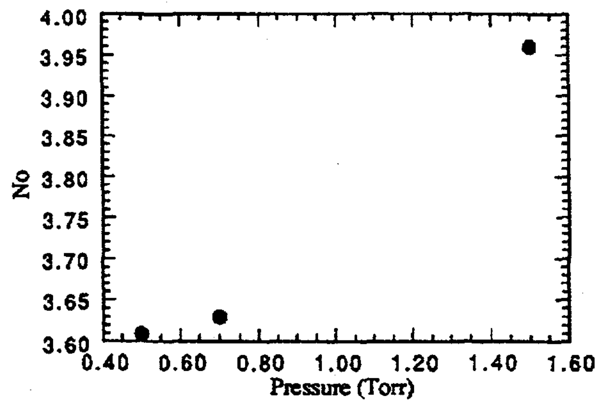

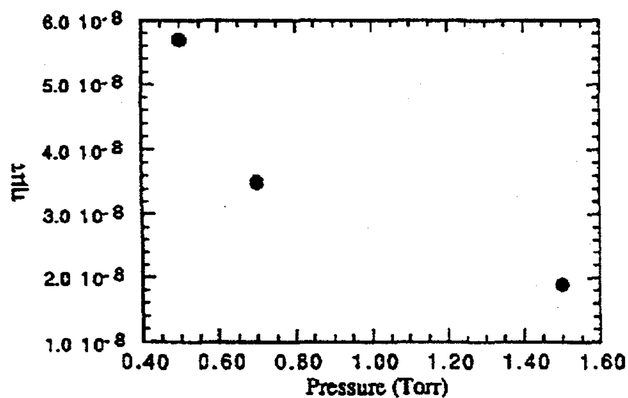

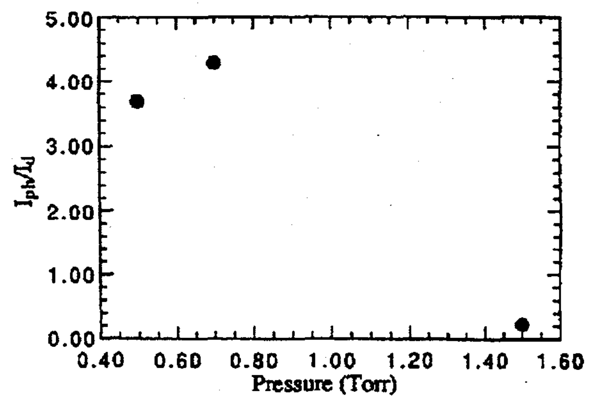

Figure 12. Variation of the physical parameters of films produced at different total pressure, when T_s = 225°C, power = 30 W, D-spacing = 1.0 cm and the H_2:GeH_4:SiH_4 flow rates are in the ratio of 80 sccm:1.00 sccm:2.00 sccm.

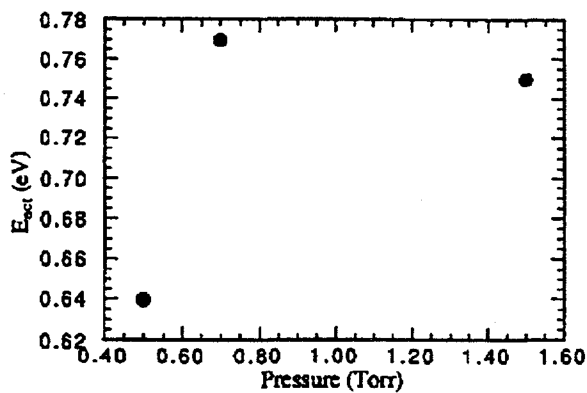

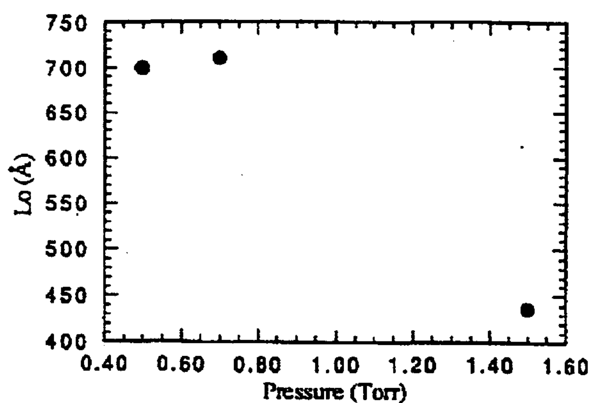

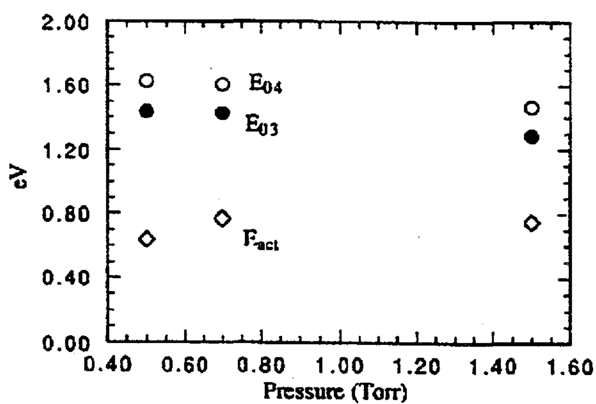

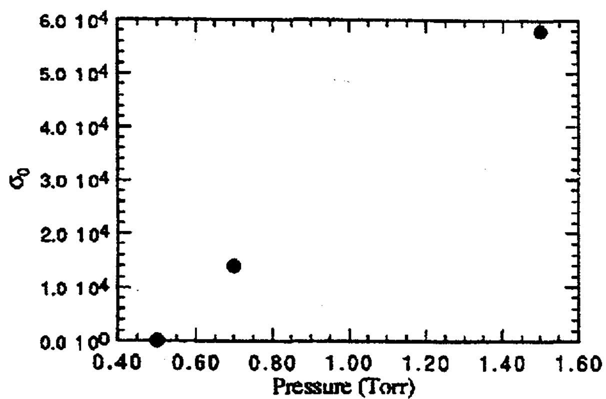

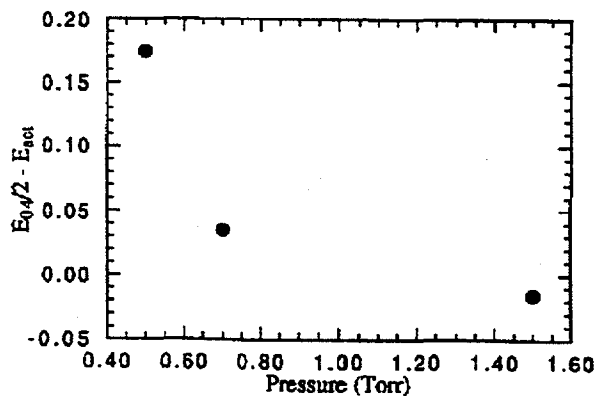

Figure 12, continued.

Table 2. Preparation Conditions for Selected Alloys of a-$Si_{1-x}Ge_x$:H of Different E_{04}.

Approximate Gap E_{04} (eV)	T_s (°C)	Power (W)	Pressure (Torr)	H_2 (sccm)	GeH_4 (sccm)	SiH_4 (sccm)	D (cm)
1.25	200–275	20–35	0.950	40–120	1.00	—	1.0–1.4
1.40	225	30	0.95	40	1.0	0.6	1.0–1.4
1.57	225	30	0.95	40	1.0	2.0	1.0–1.4
1.5	230–270	3	0.25	0	3	12	—

Line 2 refers to samples 137, 144, 161, 164, 171 and 202, while line 3 refers to samples 179, 183, 221, 222 and 220 (The conditions are not exactly those quoted, for example 183 was prepared at a slightly different D-spacing, etc.). Line 4 refers to some values taken from an earlier study at Harvard, which found $\eta\mu\tau$ values comparable with those often found in the literature.

Table 3. Photoelectronic Properties of the Films Whose Preparation Conditions are Listed in Table 2.

Sample	E_{04} (eV)	E_{03} (eV)	E_{act} (eV)	N_0	$\eta\mu\tau$ cm^2V^{-1}	L_0 (Å)
a-Ge:H	1.25	1.10	0.62	4.03	3×10^{-7}	550
137	1.37	1.21	0.68	3.99	7.9×10^{-8}	550
144	1.41	1.26	0.72	3.95	7.9	550
161	1.40	1.25	0.75	4.03	5.2	620
164	1.44	1.28	0.73	3.71	6.0	745
177	1.46	1.31	0.74	3.75	8.0	627
202	1.42	1.25	0.75	3.83	8.8	—
average	1.40	1.26	0.73	3.87	7.3	619
179	1.61	1.43	0.84	3.69	1.6×10^{-8}	—
183	1.53	1.34	0.72	3.77	0.9	—
221	1.61	1.43	0.77	3.63	3.5	710
222	1.63	1.44	0.64	3.61	5.7	700
220	1.47	1.29	0.75	3.96	1.9	437
average	1.57	1.38	0.74	3.73	2.7	615

Collaborative Research

Professor Richard Norberg, Washington University: Deuteron Magnetic Resonance Studies

Deuteron magnetic resonance (DMR) was used to resolve structures such as tightly bound D, weakly bound D, molecular HD and D_2 in microvoids and trapped on nanovoid internal surfaces in plasma-deposited a-Si:D:H and a-Ge:D:H. It has been established that the relative populations of these structures correlate with photovoltaic quality, as characterized by photoresponse $\eta\mu\tau$, in a series of deuterated a-Ge and a-Si films. This is illustrated in Figure 14. A very good correlation has also been established between the inverse rate constants for spin-lattice relaxation of magnetization and the $\eta\mu\tau$ product, as illustrated in Figure 15.

It is found that photo-illumination produces DMR-detected changes in the populations. The

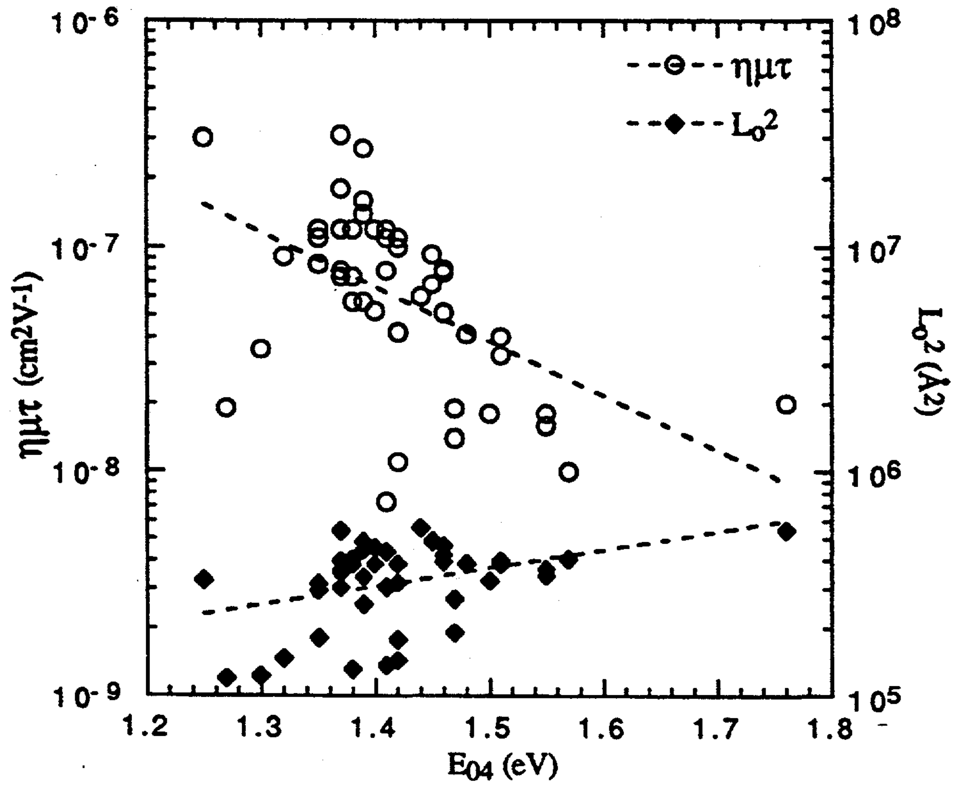

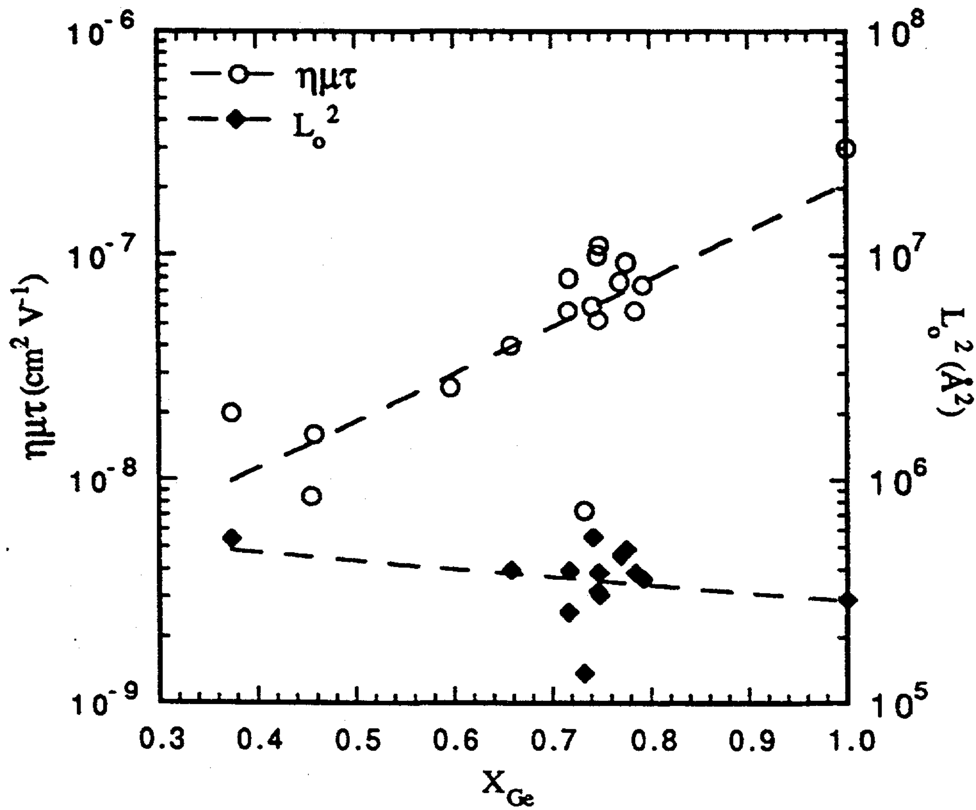

Figure 13. Variation of $\eta\mu\tau$ and L_0 with E_{04} gap and with composition x when material is prepared under conditions resembling those for optimized a-Ge:H.

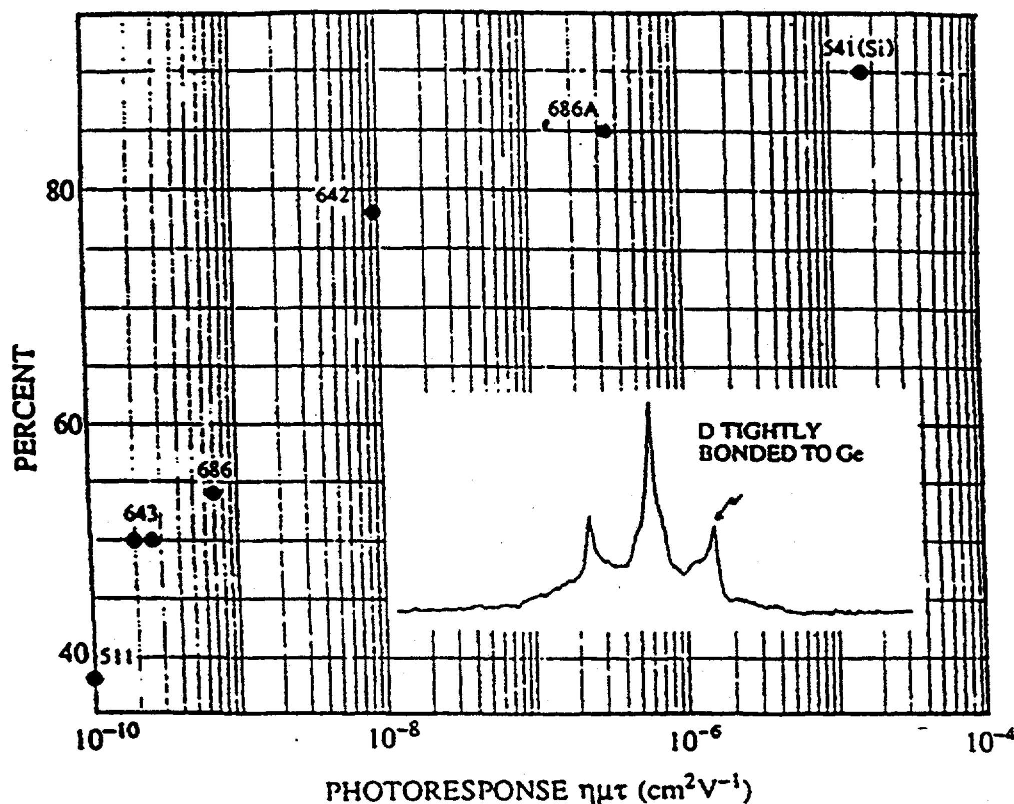

Figure 14. A comparison of the relative proportion of tightly-bonded Ge-D with $\eta\mu\tau$ products of different films of a-Ge:H:D.

changes, which are reversible upon 150°C dark anneal, include a quadrupolar 50 kHz doublet from strained-bond configurations and a paramagnetic shift from metastable electronic species. This would appear to be one of the very few basically structural measurements capable of detecting light-induced changes reflecting either hydrogen rearrangements or changes in the Si(Ge) environment. The DMR results are reported in papers 10, 11, 14, 15, 28, 33 and 35 of Section V.

Dr. M.L. Theye, Laboratoire d'Optique, Paris: Comparative Studies of Subbandgap Optical Absorption by Photothermal Deflection Spectroscopy and by Photoconductivity Using the Constant Photocarrier Method

Establishment of the subbandgap absorption spectra is considered a straightforward method to give information concerning the density-of-states distribution in the valence band tail and also in the middle of the gap. The group of Dr. Theye are expert practitioners of the PDS method, while the Harvard group provided the use of photoconductivity spectra to establish the absorption spectra. The two methods, however, do not always give the same result, and it is advisable to carry out both and to rationalize differences before conclusions regarding density of states distributions are drawn. Our earlier publications have established how differences in the deduced absorption spectrum may arise. For example, it is necessary to take account of surface absorption processes which may contribute heavily to the PDS-derived absorption spectrum, especially in very thin films, but which have no effect on photoconductivity-derived absorption spectra. Also, it is a requirement for the analysis of photoconductivity spectra (not well-recognized in the literature) that the relative contributions of electrons and holes to the photocurrent be approximately the same at all photon energies if accurate absorption spectra are to be derived. These details, as well as the large measure of agreement for Urbach edge parameters and the preparation-parameter

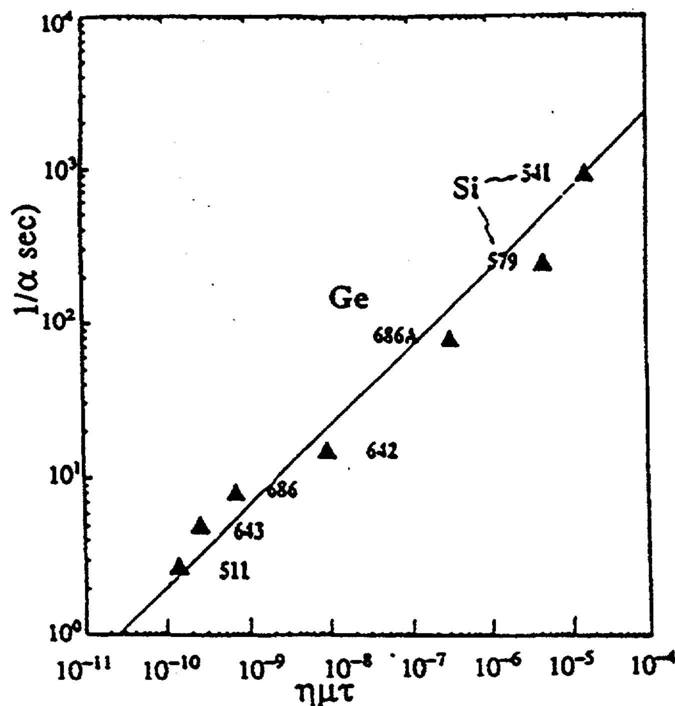

Figure 15. Demonstration that the inverse rate constants for M_z recoveries in DMR correlate with the photovoltaic quality factor $\eta\mu\tau$ in films of a-Ge:D:H and a-Si:D:H.

dependence of the absorption coefficient at the lowest energies (which can be used as a measure of the relative mid-gap state densities) have been reported already.[27]

Attention is drawn in this report to a PDS study designed to discriminate specifically between bulk, surface and interface absorption in the low photon energy range. The optical absorption spectra of our PECVD undoped a-Si:H films, deposited on silica and Corning 7059 glass substrates, were determined between 0.6 and 2 eV, using both PDS and CMP methods. All of the samples, with thicknesses ranging from 0.5 to 10 μ, had identical values of the optical gap and of the dark conductivity activation energy. The results of *conventional* PDS experiments at low modulation frequency on films with different thicknesses confirmed previously reported conclusions regarding the existence of substantial surface or interface absorption in device quality a-Si:H. By contrast, the CPM-derived absorption spectra confirmed earlier results in demonstrating very little, if any, surface or interface effect. They coincide within experimental uncertainty with the PDS-derived spectra obtained for the thickest films down to about 1.1 eV. At lower energies, the CPM-derived absorption coefficient values decrease rapidly with decreasing energy, while the PDS-derived ones remain about constant for both types of substrate. In order to explain this behavior in the low energy range, we employed PDS experiments at high modulation frequency, in which we compared the values of the phase lag of the PDS signal with respect to the exciting beam, measured on thick (7–10 μm) films for front and rear illumination, with the probe beam-sample geometry remaining unchanged. We derived from these experiments conclusive evidence that, for our films deposited either on silica or on glass substrates, the absorption measured by PDS at energies lower than 1 eV comes essentially from the free surface region. It appears that this is a new and unique contribution to the use of the PDS technique.

Professor J. Tauc, Brown University: Photomodulation Spectroscopy and Femtosecond Dynamics

As part of our investigation of improved a-Ge:H we collaborated on a comparison of the photomodulation spectra of a-Ge:H of average photoelectronic quality ($\eta\mu\tau \approx 10^{-10}$ cm^{2}V^{-1}, prepared on the "unpowered" electrode of our apparatus under conditions similar to those for preparation of a-Si:H) and of improved quality ($\eta\mu\tau \approx 3 \times 10^{-7}$ cm^{2}V^{-1}, prepared on the "powered" electrode as detailed in our earlier reports). The spectra were measured at 80 K, under both steady-state and transient conditions, between 0.06 and 1.5 eV. The spectra of the photoelectronically-poorer material was dominated by transitions between defect states in the middle of the gap and the conduction and valence bands. On the other hand, the spectra of the improved material was analyzed as requiring contributions from the states in the band tail, which indicates that the pump-beam induced quasi-Fermi levels had reached near the conduction and valence band edges. This is consistent with expectations from the reduced gap density-of-states in our improved a-Ge:H. In fact, good fits were found between the experimental spectra and those based on plausible density-of-state distributions.[6]

A number of experiments were carried out using a femtosecond pump and probe technique. In the first, 2 eV and 4 eV photons were used to study hot carriers in extended states of a-Si:H and a-Ge:H. From the measured changes in reflectivity and transmission, photoinduced changes in the real and imaginary parts of the complex dielectric constant may be deduced. It was found that the average carrier cooling rates in a-Si:H and a-Ge:H were about 2 eV/ps and 1 eV/ps respectively. In these experiments photoinduced bleaching associated with the filling of band states (removal of absorptive transactions) was found to dominate over intraband contributions to the absorptions, at least at energies significantly larger than the bandgap.[28]

IV. Theses Completed

Abstract of thesis of Dr. S.M. Lee: Structural and Optical Properties of Variable Bandgap Crystalline and Amorphous Semiconductors of Tetrahedral Coordination

A two part study of the structural and optical properties of variable bandgap crystalline and amorphous group IV semiconductors is presented here. The first covers an extensive set of experiments on the novel semiconducting material $Ge_{1-x}Sn_x$. Successful production of single phase alloys was accomplished with ion implantation and r.f. sputtering. The former technique produced amorphous submicron thick films embedded in single crystal wafers of Ge. Free-standing amorphous membranes were then prepared by anodic etching and characterized by transmission electron microscopy. The alloys were subsequently crystallized by heating with the electron beam of the microscope. This produced crystalline alloys, some with the same composition as the as-deposited material.

The r.f. sputtering technique was used to produce $Ge_{1-x}Sn_x$ with $0 \leq x \leq 0.38$ and thicknesses ranging from 500 Å–10 μm. These materials were studied with the aid of differential scanning calorimetry (DSC), transmission electron microscopy (TEM), and x-ray diffraction. The thin materials (500–1000 Å) were deposited in an amorphous state. Crystallization to the diamond cubic form and subsequent Sn precipitation were observed upon annealing. The deposition conditions for these thin films were optimized to produce single phase crystallized alloys. The thick films, 4–8 μm, were deposited in crystalline form with no precipitated Sn present. A grain growth exotherm was observed in both the DSC and isothermal calorimetry spectra. The absorption edge of these films was measured and absorption coefficients were calculated. The energies at which these coefficients occurred were found to vary approximately linearly with Sn concentration.

The second part of this thesis examines the structural properties of the tetrahedralloy coordinated semiconductors, a-Si_xGe_{1-x}:H(:F)(:D), for $x = 1.0$, 0.43, and 0.0, made under different deposition

conditions by r.f. glow discharge. The structures of these samples were examined by DSC, TEM, and x-ray measurements. In addition, an attempt was made to correlate the observed structural changes in the a-Si:H samples with their measured optoelectronic properties. We showed that in this system of materials, very different amorphous microstructures could produce nearly identical photoelectronic properties.

Abstract of thesis of Dr. Y.-M. Li: Optical and Phototransport Properties of Hydrogenated Amorphous Semiconductors

A study of the optical and phototransport properties of hydrogenated, tetrahedrally bonded amorphous semiconductor films produced by the radio frequency glow discharge technique is presented. The first part of this thesis reports an extensive investigation of hydrogenated and hydrogenated-fluorinated amorphous Si-Ge alloys a-$Si_{1-x}Ge_x$:H and a-$Si_{1-x}Ge_x$:H:F. The optical and vibrational properties of the two sets of alloys are described and compared. The photoconductivity of these materials is discussed with focus on the following two questions: 1) the drastic deterioration of the photoconductivity of a-$Si_{1-x}Ge_x$:H with increasing x; 2) the improved photoconductive response $\eta\mu\tau$ (quantum efficiency-mobility-lifetime product) in the fluoride $\{SiF_4 + GeF_4 + H_2\}$ derived alloys over that of the hydride $\{SiH_4 + GeH_4\}$ derived alloys of roughly 50 *at.*% Ge, or with a bandgap near 1.4 eV. The phototransport properties of a-$Si_{1-x}Ge_x$:H and a-$Si_{1-x}Ge_x$:H:F are analyzed in light of information provided by various types of electronic and structural characterization. Some specific models for the electronic band structure, charge transport, and recombination are probed. It is concluded that a *uniform* increase in the gap density of states can only partially account for the severe quality degradation of a-$Si_{1-x}Ge_x$:H(:F) relative to a-Si:H. The inferior photosensitivity of a-$Si_{1-x}Ge_x$:H(:F) is caused, in part, by an increase in *structural heterogeneity.* Possible enhancement of recombination of excess carriers in the alloys due to clustered and/or charged defects, tunneling recombination, and reduced bandgap is assessed. The efficacy of hydrogen and fluorine in determining the properties of a-SiGe alloys is evaluated. It is found that the *replacement* of hydrogen by fluorine *in* a-SiGe can not be responsible for the observed improvement of $\eta\mu\tau$ in the fluoride-derived of a-$Si_{0.5}Ge_{0.5}$:H:F over the hydride-derived of a-$Si_{0.5}Ge_{0.5}$:H. The improved photoresponse in a-$Si_{0.5}Ge_{0.5}$:H:F over a-$Si_{0.5}Ge_{0.5}$:H is attributable to an improved film microstructure of the former.

The second part of this thesis covers several related topics on photoconduction and sub-bandgap optical absorption in amorphous semiconductors. Various photoconductivity techniques for deriving the *s*ub-bandgap *o*ptical *a*bsorption (SOA) spectrum $\alpha(h\nu)$, such as the constant photocurrent method (CPM) and the normalization methods, are examined and compared. These methods have been found capable of obtaining the SOA $\alpha(h\nu)$ associated with optical transitions generating the dominant photocarriers (electrons). It is argued that these methods are essentially equivalent because of their common requirement that the $\eta\mu\tau$ be *spectrally* independent of photon energy, $h\nu$. Photocurrent decay experiments have established the spectral dependence of photoconductivity response time which is a measure of the lifetime averaged over all free and trapped excess carriers. There are indications that for near-midgap excitation, $\eta\mu\tau$ varies somewhat with $h\nu$. Thus, the photocurrent-derived $\alpha(h\nu)$ at very low energies should be viewed only as an estimate of the optical absorption. Through a comparative study of the SOA spectra found by the CPM and the PDS (photothermal deflection spectroscopy), supplemented by dark and photo-transport measurements, it is shown that the surface/interface effects can be dominant in the optoelectronic measurements in undoped device-quality a-Si:H films of thickness less than 3 microns. Such an effect is not as marked in the phosphorus-doped a-Si (a-Si:H:P) films. It is argued that the total density of defects can not be deduced *quantitatively* from the SOA $\alpha(h\nu)$ alone. Further, the density of gap states can not be determined by deconvoluting the SOA $\alpha(h\nu)$ without a number of unwarranted assumptions, assessed in detail, such as a constant dipole matrix element and a parabolic density of states in the conduction band. Finally, explanations are proposed for the commonly observed large difference between $(\mu\tau)_{TOF}$ from the time-of-flight transient photoconductivity and $(\eta\mu\tau)_{SSPC}$ from the steady state photoconductivity experiments. This is done by examining the nature and dis-

tribution of deep traps/recombination centers in the gap, and the difference in the interaction of excess carriers with gap states between the two types of non-equilibrium transport processes.

Abstract of thesis of Dr. W.A. Turner: An Optimization of the Photoelectronic Properties of Glow Discharge Prepared a-Ge:H

Samples of amorphous hydrogenated germanium were prepared using the r.f. glow discharge method under the systematic variation of the substrate temperature, level of applied power, externally applied d.c. bias, and dilution of the germane gas plasma by different amounts of H_2, He, Ar, and GeF_4. The samples were subjected to a battery of optical, electrical, and structural measurements and the results of these characterizations were evaluated to determine the set of conditions under which the best material was prepared. The highest quality samples deposited in this investigation were prepared on the electrically driven electrode of a capacitively coupled, diode configuration under conditions of moderate substrate temperature, low levels of applied power, and high dilution of the germane gas plasma by H_2.

The optical and electrical properties of this optimized material are all consistent with material containing a low density of defect related states in the energy gap. In particular we note an $\eta\mu\tau = 3.2 \times 10^{-7}$ cm^2/V and ratio of photocurrent to dark current of 1.3×10^{-1} measured using photoconductivity, at $\mu\tau = 4 \times 10^{-8}$ cm^2/V measured using time of flight, an Urbach energy of 47 meV and α at 0.7 eV of 2.6 cm^{-1} measured using the constant photocurrent method, a dangling bond spin density of 5×10^{16} cm^{-3} measured using electron spin resonance, photoluminescence with a peak energy position of 0.81 eV and full width at half maximum of 0.19 eV, an activation energy of 0.52 eV and $\sigma_0 = 6.1 \times 10^3$ (Ω-cm)$^{-1}$ measured using dark conductivity, and an E_{04} band-gap of 1.24 eV measured by optical absorption.

Structural measurements indicate a homogeneous material lacking any island/tissue and columnar structure when investigated using transmission and scanning electron microscopy, respectively. Hydrogen concentrations calculated from infrared and gas evolution measurements can only be reconciled by postulating a large quantity of unbonded hydrogen whose presence is confirmed using deuteron magnetic resonance. Differential scanning calorimetry measurements show crystallization occurring at 421°C and the presence of large compressive stresses has been confirmed using a bending-beam method.

Samples prepared on the unpowered electrode are electrically and structurally inferior to samples prepared on the electrically driven electrode. They are often low density, open-porosity material which suffers from severe, post-deposition, atmospheric contamination. When prepared under conditions which minimize these problems and improve the structure, the material has insufficient bonded hydrogen to compensate defect related states in the energy gap and, as a result, poor photoelectronic properties.

We believe that the vast differences in the properties of samples prepared on the two electrodes is a result of a substantial increase in bombardment of the growing surface by charged particles accelerated across the self bias between the plasma and the electrode at the electrically driven electrode.

Abstract of thesis of Dr. S.J. Jones: Structural Studies of a-Ge:H and a-$Si_{1-x}Ge_x$:H Alloys

The structural properties of hydrogenated amorphous germanium and silicon germanium alloys, prepared using the r.f. glow discharge method, were studied using transmission and scanning electron microscopy, gas evolution, differential scanning calorimetry and infrared absorption spectroscopy techniques. In particular, the presence or absence of a two phase microstructure was monitored as a variety of deposition parameters was systematically varied. For each set of deposition conditions, samples were made for both structural and opto-electronic analysis in order that

variations in the film microstructure could be correlated with possible changes in the material's photoelectronic properties.

Amorphous germanium films deposited on the unpowered electrode at substrate temperatures less than 250°C displayed a two phase microstructure as shown by the 1) island/tissue microstructures visible in transmission electron micrographs of planar views of 500 Å thick films, 2) columnar microstructures visible in scanning electron micrographs of the cross sectional views of micron thick films, 3) large amounts of low temperature gas evolution, 4) two crystallization peaks in the differential scanning calorimetry spectra for films deposited on Al substrates and 5) the appearance of oxygen related peaks in the infrared spectroscopy spectra as the films were exposed to the atmosphere. These signatures of the two phase microstructure were not observed, as low bonded hydrogen contents and significant dangling bond densities were, when films deposited at substrate temperatures greater than 300°C were measured. Fixing the substrate temperature at 250°C, the two phase microstructure remained in the films as the following deposition conditions were varied: the applied power, the d.c. substrate bias, the amount of H_2 dilution and the type of diluent gas (H_2, He, Ar and GeF_4). For all of the films deposited on the unpowered electrode, the photoelectronic properties were judged to be poor with $\eta\mu\tau < 10^{-8}$ cm^{2}V^{-1} for the as-deposited films.

The structural measurements indicated that the two phase microstructure was absent from the hydrogenated amorphous germanium and silicon germanium alloy films deposited on the powered electrode under conditions of moderate applied powers and small electrode separations. They also showed that, in contrast to those prepared on the unpowered electrode, these films contained significant amounts of unbonded hydrogen. The photoelectronic properties for these films were far superior to those for films having the two phase microstructure with $\eta\mu\tau \sim 1.3 \times 10^{-7}$ cm^{2}V^{-1}.

Abstract of thesis of Dr. P. Wickboldt: Deposition and Examination of Glow Discharge Produced a-Ge:H

This thesis presents the results of extensive studies of the deposition and examination of amorphous hydrogenated germanium (a-Ge:H) thin films deposited from an rf glow discharge of GeH_4 and H_2 gases. For the purpose of these studies, a diode type capacitively coupled glow discharge system was constructed.

Results are presented of the measurements of film stress for a large number of a-Ge:H films. The stress is found to vary from high tensile (+6.6 kbar) to high compressive (-7.8 kbar), and correlates with total hydrogen content, microstructure and photoconductivity. The origin of these stresses is considered and discussed in the context of other measurements. The effects of air exposure and annealing are demonstrated. Two examples are given of the effects of varying a deposition parameter on the film properties; the effects of varying the electrode gap and the power. By piecing together extensive measurements of optical, electronic and structural properties, the electrode gap study is used to demonstrate the link between structure and electronic transport, and to clarify an earlier model of a-Ge:H film structure. The results suggest a strategy for further optimization of a-Ge:H optoelectronic properties by adjusting growth conditions to reduce the formation of columnar-type microstructure. Finally, a basic examination of the GeH_4 + H_2 glow discharge is presented. Using measurements of the DC and rf cathode potentials, it is determined that the discharges used to deposit a-Ge:H are in the so called γ mode in which the discharge characteristics are dominated by ion-induced electron emission (γ electrons) from the cathode. Then, using a residual gas analyzer (RGA), an examination is made of discharge chemistry which centers around a comparison to SiH_4 + H_2 chemistry. The RGA measurements for the SiH_4 + H_2 discharge is found to follow what is expected from a basic model of SiH_4 chemistry, while the measurements of the GeH_4 + H_2 chemistry demonstrate a very different behavior, preventing any assumptions that GeH_4 and SiH_4 have parallel chemistry. A review of the literature reveals at least one possible and significant explanation for this difference. Measurements were then made to determine the changes which occur in the glow discharge when the electrode gap and power are varied, and how these

changes result in differences in the film properties. The results of the electrode gap study suggest that beneficial discharge chemistry is promoted by a higher kinetic energy of the electrons in the discharge.

V. Publication List 1988-92

1. Eggert, J.R.; Paul, W. (1988). "Recombination in Disordered Semiconductors: The NAN Distribution." Phys. Rev. (B37); p. 4051.

2. Mackenzie, K.D.; Burnett, J.H.; Eggert, J.R.; Li, Y.M.; Paul, W. (1988). "Comparison of the Structural, Electrical and Optical Properties of Amorphous Silicon-Germanium Alloys Produced from Hydrides and Fluorides." Phys. Rev. (B38); pp. 6120–6136 (1988).

3. W. Paul (1989). "Heterogeneities in a-SiGe:H Alloys," in *Amorphous Silicon and Related Materials, Advances in Silicon and Related Materials, Advances in Disordered Semiconductors, Vol. 1*, edited by H. Fritzsche, pp. 63–79. Singapore: World Scientific Publishing.

4. Lee, S.M.; Jones, S.J.; Li, Y.M.; Turner, W.A.; Paul, W. (1989). "Comparison of the Structural Properties of a-Si:H Prepared from SiH_4 and $SiH_4 + H_2$ Plasmas, and Correlation of the Structure with the Photoelectronic Properties." Phil. Mag. (B60:4); p. 547.

5. Li, Y.M.; Turner, W.A.; Lee, C.; Paul, W. 1989. "Substrate Temperature Dependence of the Optical and Electronic Properties of Glow Discharge Produced at a-Ge:H," in *Proc. Materials Research Society* Spring Meeting, San Diego, Vol. 149, pp. 187–192. Pittsburgh, PA: Materials Research Society.

6. Turner, W.A.; Jones, S.J.; Lee, C.; Lee, S.M.; Li, Y.M.; Paul, W. (1989). "The Effect of Hydrogen Dilution of the Gas Plasma on Glow Discharge a-Ge:H," in *Proc. Materials Research Society* Spring Meeting, San Diego, Vol. 149, pp. 69–74. Pittsburgh, PA: Materials Research Society.

7. Jones, S.J.; Lee, S.M.; Turner, W.A.; Paul, W. (1989). "Substrate Temperature Dependence of the Structural Properties of Glow Discharge Produced a-Ge:H," in *Proc. Materials Research Society* Spring Meeting, San Diego, Vol. 149, pp. 45–50. Pittsburgh, PA: Materials Research Society.

8. Sharma, D.K.; Narasimhan, K.L.; Kumar, S.; Arora, B.M.; Paul, W.; Turner, W.A. (1989). "Current Transport in a-Si:Ge Alloy Schottky Barriers." J. Appl. Phys. (65); pp. 1996–1999.

9. Jones, S.J.; Turner, W.A.; Paul, W. (1989). "The Effect of Sample Substrate on the Structural Properties of Co-deposited a-Ge:H Films." J. Non-Cryst. Solids (114); p. 525.

10. Volz, M.P.; Fedders, P.A.; Norberg, R.E.; Turner, W.A.; Paul, W. (1989). "Deuteron Magnetic Resonance in Amorphous Germanium." J. Non-Cryst. Solids (114); p. 546

11. Santos-Filho, P.; Volz, M.P.; Corey, R.L.; Kim, Y.W.; Fedders, P.A.; Norberg, R.E.; Turner, W.A.; Paul, W. (1989). "Molecular HD and D_2 in Amorphous Semiconductors." J. Non-Cryst. Solids (114); p. 235.

12. Zallen, R.; Holtz, M.; Geissberger, A.E.; Sadler, R.A.; Paul, W.; Theye, M.L. (1989). "Raman Scattering Studies of Implantation-Amorphized GaAs: Comparison to Sputtered and Evaporated a-GaAs Films." J. Non-Cryst. Solids (114); p. 795.

13. Fournier, D.; Roger, J.P.; Boccara, A.C.; Theye, M.L.; Chahed, L.; Turner, W.A.; Paul, W. (1990). "Subgap Amorphous Silicon Photothermal Deflection Spectroscopy; Spatial Absorption Localization Studies," in *Photoacoustic and Photothermal Phenomena II*, Vol. 62, editors J.C. Murphy,

J.W. Maclachlan-Spicer, L. Aamodt, and B.S.H. Royce, pp. 156–159. Springer Series in Optical Sciences.

14. Volz, M.P.; Santos-Filho, P.; Conradi, M.S.; Fedders, P.A.; Norberg, R.E.; Turner, W.A.; Paul, W. (1989). "Unique Deuteron Spin Echoes from HD and Ortho-D_2 in Large Crystal Fields." Phys. Rev. Letters (63); p. 2582.

15. Turner, W.A.; Jones, S.J.; Pang, D.; Bateman, B.F.; Chen, J.H.Li, Y.M.; Marques, F.C.; Wetsel, A.E.; Wickboldt, P.; Paul, W.; Bodart, J.; Norberg, R.E.; El Zawawi, I.; Theye, M.L. (1990). "Structural, Optical and Electrical Characterization of Improved Amorphous Hydrogenated Germanium." J. Appl. Phys. (67); p. 7430–7438.

16. Turner, W.A.; Pang, D.; Wetsel, A.E.; Jones, S.J.; Chen, J.H.; Paul, W. (1990). "Optimization of the Properties of Undoped a-Ge:H." Proc. of the Materials Research Society (192); pp. 493–498.

17. Jones, S.J.; Turner, W.A.; Pang, D.; Paul, W. (1990). "The Effect of Sample Substrate on the Structural Properties of Co-deposited Films of a-Ge:H." Proc. of the Materials Research Society (192); pp. 553–557.

18. Wetsel, A.E.; Jones, S.J.; Turner, W.A.; Pang, D.; Paul, W.; El Zawawi, I.; Bouizem, Y.; Chahed, L.; Theye, M.L.; Marques, F.C.; Chambouleyron, I. (1990). "Comparison of the Properties of Sputtered and Glow Discharge a-Ge:H Films." Proc. of the Materials Research Society (192); pp. 547–552.

19. Wraback, M.; Tauc, J.; Pang, D.; Paul, W.; Vardeny, Z. (1990). "Femtosecond Dynamics of Photo-Generated Carriers in Amorphous Hydrogenated Germanium," in *Ultrafast Phenomena VII*, editors C.B. Harris, E.P. Ippen, G.A. Mourou and A.H. Zewail, pp. 306–308. Berlin: Springer.

20. Paul, W.; Jones, S.J.; Turner, W.A. (1991). "Studies on the Structure of a-Ge:H using DSC, GE and TEM Techniques." Phil. Mag. (B63); pp. 247–268.

21. Wraback, M.; Tauc, J.; Pang, D.; Paul, W.; Lee, J.-K.; Schiff, E.A. (1991). "Femtosecond Studies of Photoinduced Bleaching and Surface Effects in a-Si:H and a-Ge:H." J. Non-Cryst. Solids (137&138); pp. 531–534.

22. Chahed, L; Theye, M.L.; Fournier, D.; Roger, J.P.; Boccara, A.C.; Li, Y.M.; Turner, W.A.; Paul, W. (1991). "Surface Effects in Hydrogenated Amorphous Silicon Studied by Photothermal Deflection Experiments." Phys. Rev. (B43); pp. 14488–14497.

23. Jones, S.J.; Turner, W.A.; Pang, D.; Paul, W. (1991). "An Electron Microscopy Study of the Effects of Deposition Conditions for Growth of Glow Discharge Prepared a-Ge:H Films," in Materials Research Society Symposium Proceedings *Evolution of Thin Film and Surface Microstructure*, Vol. 202, editors C.V. Thompson, J.Y. Tsao and D.J. Srolovitz, p. 43.

24. Turner, W.A.; Jones, S.J.; Li, Y.M.; Pang, D.; Wetsel, A.E.; Paul, W. (1991). "Structural, Optical, and Electrical Studies of Amorphous Hydrogenated Germanium." Solar Cells (30) pp. 245–254.

25. Chen, L.; Tauc, J.; Pang, D.; Turner, W.A.; Paul, W. (1991). "States in the Gap of Improved a-Ge:H Studied by Photomodulation Spectroscopy," in *Proc. Materials Research Society* Spring Meeting, Anaheim, Vol. 219, pp. 575–580. Pittsburgh, PA: Materials Research Society.

26. Li, Y.M.; Paul, W. (1991). "Comments on the Determination of Defect Density in a-Si:H Alloys by Subbandgap Optical Absorption," in *Proc. Materials Research Society* Spring Meeting, Anaheim, Vol. 219, pp. 587–591. Pittsburgh, PA: Materials Research Society.

27. Paul, W. (1991). "Influence of Deposition Conditions on the Optical and Electronic Properties of a-Ge:H," in *Proc. Materials Research Society* Spring Meeting, Anaheim, Vol. 219, pp. 211–222. Pittsburgh, PA: Materials Research Society.

28. Norberg, R.E.; Fedders, P.A.; Bodart, J.; Corey, R.; Kim, Y.W.; Paul, W.; Turner, W.A. (1991). "Correlation of Structure and Structural Changes with Photovoltaic Quality of a-Si:D,H and a-Ge:D,H Films," in *Proc. Materials Research Society* Spring Meeting, Anaheim, Vol. 219, pp. 223–228. Pittsburgh, PA: Materials Research Society.

29. Paul, W.; Jones, S.J.; Turner, W.A.; Wickboldt, P. (1992). "Structural Properties of Amorphous Hydrogenated Germanium." J. Non-Cryst. Solids (141); pp. 271–286.

30. Wickboldt, P.; Jones, S.J.; Marques, F.; Pang, D.; Turner, W.A.; Wetsel, A.E.; Paul, W.; Chen, J.H. (1991). "A Study of the Properties of a-Ge:H Produced by RF Glow-Discharge as the Electrode Gap is Varied: The Link Between Microstructure and Optoelectronic Properties." Phil. Mag. (64); pp. 655–674.

31. Paul, W. (1991). "Structural, Optical and Photoelectronic Properties of Improved PECVD a-Ge:H," in Proceedings of the 14th ICAS, Garmisch, Germany. J. Non-Cryst. Solids (137&138); pp. 803–808.

32. Wickboldt, P.; Marques, F.; Jones, S.J.; Pang, D.; Turner, W.A.; Paul, W. (1991). "Stress Measurement of Glow-Discharge Produced a-Ge:H Thin Films and its Relation to Electronic and Structural Properties." J. Non-Cryst. Solids (137&138); pp. 83–86.

33. Norberg, R.E., Fedders, P.A.; Bodart, J.; Corey, R. (1991) "Connections Between Photovoltaic Quality and the Structure of Deuterated Amorphous Si and Ge Films." J. Non-Cryst. Solids (137&138); pp. 71–74.

34. Lee, C.; Turner, W.A.; Paul, W. (1991). "True Position of Dangling Bonds in the Gap of Undoped Hydrogenated Amorphous Silicon." J. Non-Cryst. Solids (137&138); pp. 367–370.

35. Norberg, R.E.; Bodart, J.; Corey, R.; Fedders, P.; Paul, W.; Turner, W.A.; Jones, S.J. (1992). "Deuteron Magnetic Resonance Studies of Structure and Photo-induced Metastable Rearrangements in Deuterated Amorphous Si, Ge and SiGe Films." in *Proc. Materials Research Society* Spring Meeting, San Francisco, Vol. 258, pp. 377–382. Pittsburgh, PA: Materials Research Society.

36. Liu, E.Z.; Pang, D.; Paul, W.; Chen, J.H. (1992). "Time-of-Flight Measurement on a-Ge:H and a-SiGe:H Alloys." in *Proc. Materials Research Society* Spring Meeting, San Francisco, Vol. 258, pp. 529–534. Pittsburgh, PA: Materials Research Society.

37. Hong, S.J.; Lee, C.C.; Paul, W. (1992). "Direct Evidence of Geminate Recombination in Hydrogenated Amorphous Silicon at Low Temperature." Solid State Commun. (82); pp. 131–134.

38. Chen, J.H.; Wickboldt, P.; Pang, D.; Wetsel, A.E.; Paul, W. (1992). "Effects of Gas Dilution on the Growth and Properties of Glow Discharge a-Ge:H." in *Proc. Materials Research Society* Spring Meeting, San Francisco, Vol. 258, pp. 547–552. Pittsburgh, PA: Materials Research Society.

39. Paul, W.; Street, R.A.; Wagner, W. (1992). "Hydrogenated Amorphous Semiconductors." J. Elect. Mat. (29); pp. 39–48.

VI. Abstracts of Papers Published Since 1991

(The reference numbers given refer to the Publication list of Section V)

20. Studies on the Structure of a-Ge:H using Differential Scanning Calorimetry, Gas Evolution on Heating and Transmission Electron Microscopy

This paper contains a review of our recent studies on the medium-range order in glow-discharge-produced a-Ge:H using a combination of differential scanning calorimetry, isothermal calorimetry, gas evolution, and transmission and scanning electron microscopy. Taken together with evidence from Raman and infrared spectroscopy and X-ray diffraction, and evidence of changes in the structural parameters with carefully chosen annealing procedures, these data suggest correlations between deposition, structural and photoelectronic parameters and properties. The data show conclusively that the best material for fundamental and device studies has a high atomic density and a homogeneous structure with minimal admixture of low-density tissue to high-density islands. In material prepared under less than optimum conditions, there occurs, to a greater or lesser degree, heterogeneity revealed directly by electron microscopy, and indirectly by structural relaxation at relatively low temperatures and even two stages of crystallization in the two-phase island-and-tissue network. These effects also occur in unhydrogenated Ge and in unhydrogenanted and hydrogenated amorphous Si and Si-Ge alloys. Increased heterogeneity in the structure can be correlated unambiguously with a deterioration in the photoelectronic properties.

21. Femtosecond Studies of Photoinduced Bleaching and Hot Carrier Dynamics in a-Si:H and a-Ge:H

The femtosecond pump and probe technique with 2eV and 4eV photons was applied to the study of hot photocarriers with considerable excess energy in extended states of a-Si:H and a-Ge:H. Photoinduced charges in the complex dielectric constant $\epsilon_1 + i\epsilon_2$ were calculated from the measured changes in reflectivity ΔR and transmission ΔT. This technique enables us to estimate that the average carrier cooling rates in our a-Si:H and a-Ge:H samples are about 2eV/psec and 1eV/psec, respectively. Photoinduced bleaching associated with the filling of band states dominates over intraband contributions to $\Delta\epsilon_1$ and $\Delta\epsilon_2$ for photon energies significantly exceeding the bandgap.

22. Studies of Surface Effects in Hydrogenated Amorphous Silicon by Photothermal Deflection Experiments

The optical absorption spectra of glow-discharge undoped a-Si:H films deposited on silica and Corning 7059 glass substrates have been determined between 0.6 and 2eV, using both the photothermal deflection spectroscopy (PDS) and constant photocurrent (CPM) methods. All the samples, with thicknesses ranging from 0.5 to 10 μm, had identical values of the optical gap and of the dark conductivity activation energy (with the minor exception of the thinnest film for the latter). The results of conventional PDS experiments at low modulation frequency on films with different thicknesses confirm previously reported conclusions regarding the existence of substantial surface or interface absorption in device-quality undoped a-Si:H films. In contrast, the CPM-derived absorption spectra show very little, if any, surface or interface effect. They coincide with experimental uncertainties with the PDS-derived spectra obtained for the thickest films, down to about 1.1 eV. At lower energies, the CPM-derived absorption coefficient values decrease rapidly with decreasing energy, while the PDS-derived ones remain roughly constant for both types of substrates. In order to discriminate between bulk, surface and interface absorption in this low energy range, we used PDS experiments at high modulation frequency, in which we compared the values of the phase lag of the PDS signal with respect to the exciting beam, measured on thick (7–10 μm) films for front and rear illumination, the probe beam-sample geometry remaining identical in both cases. We derive conclusive evidence that, for our films deposited either on silica or on glass substrates, the absorption measured by PDS at energies lower than 1 eV comes essentially from the free surface

region.

23. An Electron Microscopy Study of the Effects of Deposition Conditions on the Growth of Glow Discharge Prepared a-Ge:H Films.

Electron microscopy techniques have been used to study the effect of deposition conditions on island growth and coalescence in r.f. glow discharge prepared a-Ge:H. Planar views of 500 Å thick films were obtained using transmission electron microscopy (TEM) while scanning electron microscopy (SEM) was used to investigate the cross-sectional microstructure of thicker films. Films were prepared on both electrodes of a capacitively-coupled, diode deposition system. The substrate temperature, level of applied power, externally applied d.c. substrate bias, and the germane to diluent gas ratio were systematically varied. For films prepared on the unpowered electrode, island coalescence was dramatically enhanced with increasing substrate temperature while columnar structure, found for samples prepared at lower substrate temperatures, vanished. Both effects are attributed to the elimination of a coalescence barrier with increased temperature. Increasing negative substrate bias slightly increased island coalescence while increasing the level of applied power had no visible effect on film microstructure. The island size decreased with increasing dilution of the gas plasma by H_2. The addition of GeF_4 to the gas plasma leads to a low density, porous film. This observation is attributed to either a difference in the plasma chemistry or increased film etching due to the presence of F in the gas plasma. High quality films prepared on the powered electrode were found to be more structurally homogeneous and environmentally stable than films prepared on the unpowered electrode at the same substrate temperature. Enhanced bombardment and/or a different plasma chemistry near the powered electrode are two-factors which may contribute to the observed difference in microstructure.

24. Structural, Optical, and Electrical Studies of Amorphous Hydrogenated Germanium

High-density, non-porous, highly photoconductive films of amorphous hydrogenated Germanium (a-Ge:H) showing minimal microstructure were prepared using the r.f. glow discharge method out of a glas plasma of GeH_4 and H_2. These films, deposited onto substrates mounted on the powered electrode of a diode reactor, showed remarkable improvement over codeposited material taken from the unpowered electrode. Films were also prepared under the systematic variation of substrate temperature, discharge power, and dilution of the plasma by H_2. For the reactor geometry used, dilution of the plasma is found to be essential to the preparation of high-quality a-Ge:H. The conditions for the preparation of optimized a-Ge:H material were quite different from those found to produce optimized a-Si:H in this reactor. We assert this to be the principle cause of the finding of inferior properties for a-SiGe:H alloys when compared with a-Si:H.

25. States in the Gap of Improved a-Ge:H Studied by Photomodulation Spectroscopy

The photomodulation spectra of a-Ge:H of average photoelectronic quality ($\eta\mu\tau = 1\times10^{-10}$ cm^2/V) and of improved quality ($\eta\mu\tau \approx 3 \times 10^{-7}$ cm^2/V), produced under different plasma conditions in an r.f. diode reactor by glow discharge, were measured at 80K and are analyzed in analogy with earlier studies of a-Si:H. The spectra of the poorer material are dominated by transitions between dangling bond states and the conduction and valence bands. By contrast, the spectra of the better material require contributions of transitions from the band tail states, indicating that the reduced defect density has resulted in pump-beam induced quasi-Fermi levels reaching near the conduction and valence band edges. A very acceptable fit between plausible density-of-states distributions and the experimental spectra has been found.

26. Comments on the Determination of Defect Density in a-Si:H Alloys by Integrating the Subbandgap Optical Absorption Coefficient

The validity of determining the defect density in a-Si:H and its alloys by integrating the subbandgap optical absorption coefficient is examined. It is shown that a formula derived for estimating Si-H bond density has been *incorrectly* applied to defect related absorption. In addition, the complex defect absorption processes have been oversimplified, by assumption, to the case of a single type of transition. Further, in practice, the defect absorption spectrum can not be unambiguously obtained at energies near and above the low end of the optical absorption edge. It is concluded that the integration method for quantitative defect density determination should be viewed as best as an *empirical* practice with considerable arbitrariness.

27. Influence of Deposition Conditions on the Optical and Electronic Properties of a-Ge:H

We have measured the optical absorption edge spectra for absorption coefficients between 1 and 10^5 cm^{-1}, the photoluminescence spectra at 77K, the conductivity-temperature relations, and the photoconductivity magnitude and spectral dependence for a series of r.f. glow discharge films of a-Ge:H. The films were deposited at the powered cathode and unpowered anode of a diode capacitive reactor having very different electric fields and plasma conditions, while substrate temperature, H_2 dilution of GeH_4 plasma and applied r.f. power were varied. The structure of the films are radically different, with the anode-deposited films displaying a microstructure of low density material (voids) and the cathode-deposited films displaying homogeneity similar to that of device-quality a-Si:H. A self consistent explanation of the differences in measured optical and electronic properties is given, taking full account of the structural observations. From this analysis the conditions required for the production of a-Ge:H of good photoelectronic quality may be inferred. Preliminary structural, optical and photoelectronic data for a-$Si_{1-x}Ge_x$:H of large x, prepared under conditions extrapolated from the a-Ge study, indicate significant improvements from current data in the literature.

28. Correlation of Structure and Structural Changes with Photovoltaic Quality of a-Si:D,H and a-Ge:D,H Films

Deuteron magnetic resonance (DMR) resolves structures such as tightly bound D, weakly bound D, molecular HD and D_2 in microvoids and trapped on nanovoid internal surfaces in plasma-deposited a-Si:D,H and a-Ge:D,H. The relative populations of these structures correlate with photovoltaic quality as characterized by photo response function $\eta\mu\tau$ in a series of deuterated a-Ge and a-Si films. It is found that photo-illumination produces DMR-detected changes in these populations. The changes, which are reversible upon a 150°C dark anneal, include a quadrupolar doublet from strained-bond configurations and a shift from metastable electronic species. The spin-lattice relaxation of most of the components follows an error-function behavior characteristic of magnetization transport under extreme inhomogeneity.

29. Structural Properties of Amorphous Hydrogenated Germanium

The medium-range order on a scale of 100 Å is an important determinant of the properties of amorphous semiconductor films such as a-Ge:H: if the material has a high-density, closed structure, it is likely to have good phototransport properties and to be environmentally stable; if, on the other hand, it has an open network structure, with many voids and wide grain boundaries, it is very likely to be a poor photoelectronic material and to have properties changing with time because of atmospheric contamination. Two types of film with these extreme, contrasting structural attributes, prepared under different conditions in an r.f. PECVD reactor with parallel-plate electrodes of different area, have been compared. The measurements reported are primarily structural: infrared vibrational absorption, gas evolution versus temperature, transmission and scanning electron microscopy, differential scanning calorimetry, deuteron magnetic resonance and forward recoil

spectroscopy. An encompassing, self-consistent explanation of the results of these measurements in terms of the different constitution of the films is proposed. Several specific problems are addressed: the identification of the features in the infrared spectra, the influence of O on the spectra and on gas evolution, and the presence of H_2 molecules in the material.

30. A Study of the Properties of Hydrogenated Amorphous Germanium Produced by r.f. Glow-Discharge as the Electrode Gap is Varied: The Link Between Microstructure and Optoelectronic Properties

Hydrogenated amorphous germanium films were deposited by r.f. glow discharge on the powered electrode of a diode-type deposition system. By varying the electrode gap D and keeping all other deposition parameters constant, a continuous monotonic change in both the optoelectronic and the structural properties of the films was observed. As D was decreased from 3.2 to 1.2 cm the product $\eta\mu\tau$ of the quantum efficiency η, mobility μ and lifetime τ increased from 2.1×10^{-9} to 1.7×10^{-7} cm^2V^{-1}, and the photoluminescence intensity increased. Other measurements taken indicate that changes in the electronic density of states cannot account for the observed improvement in the phototransport. Rather, we implicitly link this improvement to the observed changes in film structure. As D was decreased, the structure varied continuously from being heterogeneous of the order of 200 Å and porous, to being homogeneous and non-porous. This change in structure was inferred from measurements of film stress, transmission electron microscopy, infrared transmission spectroscopy, gas evolution during controlled annealing and differential scanning calorimetry. The heterogeneous structure is interpreted in terms of a two-phase "island-tissue" model that accounts for the observed changes in all the structural measurements as well as the deterioration in the optoelectronic properties. Such an island-tissue structure is probably caused by low surface mobility of adatoms arriving at the growing surface. Mechanisms involved in determining the surface mobility, and how they may change with D, are discussed. It is suggested that the ion bombardment plays a crucial role in eliminating the heterogeneities when considered with other deposition mechanisms. Measurements taken of the electrode bias voltages suggest that ion bombardment decreases with decreasing D.

31. Structural, Optical and Photoelectronic Properties of Improved PECVD a-Ge:H

The preparation conditions by PECVD for a-Ge:H with photoelectronic properties approaching those of a-Si:H are described. Emphasis is placed on the identification by TEM, SEM, NMR and other techniques of structural defects on a scale of 1 nm and larger, and their elimination by adjustment of deposition parameters. Evidence concerning the valence and conduction band densities of states is reviewed, and preliminary information on the extension of this approach to improvement of a-$Si_{1-x}Ge_x$:H alloys examined.

32. Stress Measurement of Glow-Discharge Produced a-Ge:H Thin Films and its Relation to Electronic and Structural Properties

Stress measurements are reported for thin films of a-Ge:H deposited under a large variety of conditions using glow discharge CVD. The stress is nonuniform with thickness, and, for films exhibiting high tensile stress, changes reversibly due to atmospheric contamination. Strong correlations are observed for stress with hydrogen content, structure, and photoresponse. In particular, higher photoresponse is observed for films with a higher compressive stress.

33. Connections Between Photovoltaic Quality and the Structure of Deuterated Amorphous Si and Ge Films

Hydrogen arrangements and rearrangements have been examined in a series of photoillumination and 150°C dark anneal sequences. Deuteron nuclear magnetic resonance (DMR) distinguishes

among a variety of hydrogen configurations in a series of plasma-deposited a-Si:D,H and a-Ge:D,H films. These populations and their spin-lattice relaxation correlate with the photovoltaic quality in a series of differently-prepared films. Films with a higher fraction of tightly bound H (or D) are of better photovoltaic quality. We have detected reversible light-induced DMR changes including a resonance shift and changes in a quadrupolar doublet resonance line shape. We hope to determine whether the light-induced changes reflect hydrogen rearrangements or changes in the Si (Ge) environment.

34. True Position of Dangling Bonds in the Gap of Undoped Hydrogenated Amorphous Silicon

We have studied the shift in Fermi Energy E_F after prolonged light soaking in undoped hydrogenated amorphous silicon in order to find the position of negatively charged dangling bonds D^- in the gap. The results show that D^- should lie lower than $0.75 \sim 0.80$ eV below the conduction band edge which is in agreement with photothermal deflection spectroscopy (PDS) and other results but contrary to those of photomodulation spectroscopy and others.

35. Deuteron Magnetic Resonance Studies of Structure and Photo-Induced Metastable Rearrangements in Deuterated Amorphous Si, Ge and SiGe Films

The spin dynamics of deuteron magnetic resonance (DMR) components have been studied in deuterated plasma-deposited thin films of a-Si, Ge and SiGe. Transient recoveries of perturbed deuteron magnetization components evolve via magnetization transport in the limit of large inhomogeneity. The evolution is well-described by an error function expression whose parameters correlate with the film photovoltaic quality as measured by the photoresponse $\eta\mu\tau$ and the photosensitivity, $\Delta I/I_d$. These relaxation results are correlated with our continuing DMR measurements of reversible metastable photo-induced rearrangements in high-quality a-Si:D,H films. These studies indicate that about 0.5% of the hydrogens interact with a light-induced defect.

36. Time-of-Flight Measurement on a-Ge:H and a-SiGe:H Alloys

We report TOF measurements on high quality intrinsic a-Ge:H and a-SiGe:H films of $E_{04} = 1.4$eV in temperature ranges of 200 to 280 and 230 to 300K, respectively. Complete charge collection is achieved in all measurements. For a-Ge:H films, the $(\mu\tau)_e$ product obtained from the Hecht plot is $(5 \pm 3) \times 10^{-8}$ cm^2/V above 240K and decreases at lower temperatures. The electron transit signal is dispersive at all temperatures. The α obtained from $t_t \propto V^{-1/\alpha}$ is 0.23 at 200K and approaches 1.0 at 260K. The electron drift mobility μ_d shows activated behavior, with an energy of 0.37 ± 0.05eV, and has an extrapolated room temperature value of 0.03 cm^2/Vs. Compared to a-Ge:H, μ_d of a-SiGe:H alloy samples is lower by one order of magnitude but has a similar activation energy. These results are consistent with a band tail hopping transport model.

37. Direct Evidence of Geminate Recombination in Hydrogenated Amorphous Silicon at Low Temperature

The time-of-flight experiment for hydrogenated amorphous silicon at low temperatures between 5.7 and 25.5K was done with varying electric field applied. Sudden increase of the charge collection was observed at the biasing electric field of $\sim 1.8 \times 10^5$ Vcm^{-1}, and this feature as well as magnitude of the charge collection did not significantly change with varying temperature in this range of temperatures. We tentatively attribute these phenomena to the breaking of the photo-generated geminate electron-hole pairs. Field enhanced tunneling through the barrier of the mutual Coulomb attraction between the geminate pair is proposed as a possible model for the mechanism of the breaking.

38. Effects of Gas Dilution on the Growth and Properties of Glow Discharge a-Ge:H

We compare films of a-Ge:H deposited by plasma enhanced chemical vapor deposition (PECVD) using GeH_4 diluted with H_2, He and Ar. The nominal deposition conditions used were those which have produced high quality a-Ge:H with H_2 dilution. Using H_2 and He as diluents, three studies were done in which the parameters of substrate temperature, diluent gas flow and electrode gap spacing were independently varied. The photoelectronic properties of the films made with He dilution were quite good, although never better than those made with H_2 dilution. The overall results indicated that for our nominal conditions hydrogen plays an important and crucial role in producing high quality films, and we believe that this role is mainly to reduce the probability of germane radical incorporation. In contrast to He and H_2 dilution, dilution with Ar produced films with much poorer microstructure and a photoresponse two orders of magnitude lower. We attribute this to polymerization of the germane radicals which led to observed dust particles and a reduction in ion bombardment of the growing film.

39. Hydrogenated Amorphous Semiconductors

Solar cells based on hydrogenated amorphous silicon are now made from a variety of materials including alloys and microcrystalline films. Research aimed at improving cell efficiency should emphasize the studies of alloys and metastable defects. We discuss several research topics related to the growth, structure, and electronic properties of these materials, which should lead to improved photovoltaic devices.

VII. References

1. Paul, W.; Jones, S.J.; Turner, W.A. (1991). "Studies on the Structure of a-Ge:H using DSC, GE and TEM Techniques." Phil. Mag. (B63); pp. 247–268.

2. Wraback, M.; Tauc, J.; Pang, D.; Paul, W.; Lee, J.-K.; Schiff, E.A. (1991). "Femtosecond Studies of Photoinduced Bleaching and Surface Effects in a-Si:H and a-Ge:H." J. Non-Cryst. Solids (137&138); pp. 531–534.

3. Chahed, L; Theye, M.L.; Fournier, D.; Roger, J.P.; Boccara, A.C.; Li, Y.M.; Turner, W.A.; Paul, W. (1991). "Surface Effects in Hydrogenated Amorphous Silicon Studied by Photothermal Deflection Experiments." Phys. Rev. (B43); pp. 14488–14497.

4. Jones, S.J.; Turner, W.A.; Pang, D.; Paul, W. (1991). "An Electron Microscopy Study of the Effects of Deposition Conditions on the Growth of Glow Discharge Prepared a-Ge:H Films," in Materials Research Society Symposium Proceedings *Evolution of Thin Film and Surface Microstructure*, Vol. 202, editors C.V. Thompson, J.Y. Tsao and D.J. Srolovitz, p. 43.

5. Turner, W.A.; Jones, S.J.; Li, Y.M.; Pang, D.; Wetsel, A.E.; Paul, W. (1991). "Structural, Optical, and Electrical Studies of Amorphous Hydrogenated Germanium." Solar Cells (30) pp. 245–254.

6. Chen, L.; Tauc, J.; Pang, D.; Turner, W.A.; Paul, W. (1991). "States in the Gap of Improved a-Ge:H Studied by Photomodulation Spectroscopy," in *Proc. Materials Research Society* Spring Meeting, Anaheim, Vol. 219, pp. 575–580. Pittsburgh, PA: Materials Research Society.

7. Li, Y.M.; Paul, W. (1991). "Comments on the Determination of Defect Density in a-Si:H Alloys by Subbandgap Optical Absorption," in *Proc. Materials Research Society* Spring Meeting, Anaheim, Vol. 219, pp. 587–591. Pittsburgh, PA: Materials Research Society.

8. Paul, W. (1991). "Influence of Deposition Conditions on the Optical and Electronic Properties of a-Ge:H," in *Proc. Materials Research Society* Spring Meeting, Anaheim, Vol. 219, pp. 211–222. Pittsburgh, PA: Materials Research Society.

9. Norberg, R.E.; Fedders, P.A.; Bodart, J.; Corey, R.; Kim, Y.W.; Paul, W.; Turner, W.A. (1991). "Correlation of Structure and Structural Changes with Photovoltaic Quality of a-Si:D,H and a-Ge:D,H Films," in *Proc. Materials Research Society* Spring Meeting, Anaheim, Vol. 219, pp. 223–228. Pittsburgh, PA: Materials Research Society.

10. Paul, W.; Jones, S.J.; Turner, W.A.; Wickboldt, P. (1992). "Structural Properties of Amorphous Hydrogenated Germanium." J. Non-Cryst. Solids (141); pp. 271–286.

11. Wickboldt, P.; Jones, S.J.; Marques, F.; Pang, D.; Turner, W.A.; Wetsel, A.E.; Paul, W.; Chen, J.H. (1991). "A Study of the Properties of a-Ge:H Produced by RF Glow-Discharge as the Electrode Gap is Varied: The Link Between Microstructure and Optoelectronic Properties." Phil. Mag. (64); pp. 655–674.

12. Paul, W. (1991). "Structural, Optical and Photoelectronic Properties of Improved PECVD a-Ge:H," in Proceedings of the 14th ICAS, Garmisch, Germany. J. Non-Cryst. Solids (137&138); pp. 803–808.

13. Wickboldt, P.; Marques, F.; Jones, S.J.; Pang, D.; Turner, W.A.; Paul, W. (1991). "Stress Measurement of Glow-Discharge Produced a-Ge:H Thin Films and its Relation to Electronic and Structural Properties." J. Non-Cryst. Solids (137&138); pp. 83–86.

14. Norberg, R.E., Fedders, P.A.; Bodart, J.; Corey, R. (1991) "Connections Between Photovoltaic Quality and the Structure of Deuterated Amorphous Si and Ge Films." J. Non-Cryst. Solids (137&138); pp. 71–74.

15. Lee, C.; Turner, W.A.; Paul, W. (1991). "True Position of Dangling Bonds in the Gap of Undoped Hydrogenated Amorphous Silicon." J. Non-Cryst. Solids (137&138); pp. 367–370.

16. Norberg, R.E.; Bodart, J.; Corey, R.; Fedders, P.; Paul, W.; Turner, W.A.; Jones, S.J. (1992). "Deuteron Magnetic Resonance Studies of Structure and Photo-induced Metastable Rearrangements in Deuterated Amorphous Si, Ge and SiGe Films." in *Proc. Materials Research Society* Spring Meeting, San Francisco, Vol. 258, pp. 377–382. Pittsburgh, PA: Materials Research Society.

17. Liu, E.Z.; Pang, D.; Paul, W.; Chen, J.H. (1992). "Time-of-Flight Measurement on a-Ge:H and a-SiGe:H Alloys." in *Proc. Materials Research Society* Spring Meeting, San Francisco, Vol. 258, pp. 529–534. Pittsburgh, PA: Materials Research Society.

18. Hong, S.J.; Lee, C.C.; Paul, W. (1992). "Direct Evidence of Geminate Recombination in Hydrogenated Amorphous Silicon at Low Temperature." Solid State Commun. (82); pp. 131–134.

19. Chen, J.H.; Wickboldt, P.; Pang, D.; Wetsel, A.E.; Paul, W. (1992). "Effects of Gas Dilution on the Growth and Properties of Glow Discharge a-Ge:H." in *Proc. Materials Research Society* Spring Meeting, San Francisco, Vol. 258, pp. 547–552. Pittsburgh, PA: Materials Research Society.

20. Paul, W.; Street, R.A.; Wagner, W. (1992). "Hydrogenated Amorphous Semiconductors." J. Elect. Mat. (29); pp. 39–48.

21. Tsao, Y.S.; Xu, Y.; Ramsey, E.A.; Crandall, R.S.; Salamon, S.J.; Balberg, I.; Nelson, B.P.; Xiao, Y.; Chen, Y. (1991). Materials Research Society Symposium Proceedings, Vo. 219, p. 769.

22. Mackenzie, K.D.; Burnett, J.H.; Eggert, J.R.; Li, Y.-M.; Paul, W. (1988). Phys. Rev. (B38); p. 6120.

23. Evangelisti, F. (1985). J. Non-Cryst. Solids (77/78); p. 969.

24. Report to the SERI for the period up to December 1990, issued December 1991.

25. See, for example, papers 15, 16, 24, 25, 27 and 31 in the Publication List of Section V.

26. See papers 15 and 18 in the Publication List of Section V.

27. See papers 15 and 18 in the Publication List of Section V.

28. To be published.

Document Control Page	1. NREL Report No.	2. NTIS Accession No.	3. Recipient's Accession No.
	NREL/TP-411-5457	DE93010021	

4. Title and Subtitle	5. Publication Date
Structural and Electronic Studies of a-SiGe:H Alloys	April 1993
	6.
7. Author(s) W. Paul	8. Performing Organization Rept. No.
9. Performing Organization Name and Address Harvard University Cambridge, Massachusetts 02138	10. Project/Task/Work Unit No. PV341101
	11. Contract (C) or Grant (G) No. (C) XX-8-18131-1 (G)
12. Sponsoring Organization Name and Address National Renewable Energy Laboratory 1617 Cole Blvd. Golden, CO 80401-3393	13. Type of Report & Period Covered Technical Report 1 January 1991 - 28 February 1993
	14.

15. Supplementary Notes
NREL technical monitor: B. Stafford

16. Abstract (Limit: 200 words)

This report describes work to produce alloys of a-$Si_{1-x}Ge_x$:H of improved photoelectronic quality by plasma-enhanced chemical vapor deposition (PECVD). The goal was to discover optimum preparation conditions for the end-component, a-Ge:H, to establish whether modification of the usual practice of starting from a-Si:H preparation conditions was advisable. Such modification, found to be necessary, gave films of a-Ge:H with efficiency-mobility-lifetime products ($\eta\mu\tau$) 10^2 to 10^3 higher than were earlier available, in homogeneous environmentally stable material. Both a-Ge:H and a-$Si_{1-x}Ge_x$:H of large x were studied in detail. Alloy material was shown to have $\eta\mu\tau$ 10^2 larger than found earlier. However, just as the $\eta\mu\tau$ of a-Si:H decreases when Ge is added, so also the $\eta\mu\tau$ of these alloys decreases with Si addition. By contrast, the ambipolar diffusion lengths, L_o, which are governed by the hole mobility, vary by only a factor of two over the whole alloy series. Using the experimental finding of a small valence band offset between a-Si:H and a-Ge:H, compositional fluctuations on a 10-nm scale are suggested to explain the behavior of $\eta\mu\tau$ and L_o. The implications for eventual improvement of the alloys are profound, but require direct experimental tests of the postulated compositional fluctuations.

17. Document Analysis

a. Descriptors
electronic ; amorphous silicon ; alloys ; photovoltaics ; solar cells

b. Identifiers/Open-Ended Terms

c. UC Categories
271

18. Availability Statement	19. No. of Pages
National Technical Information Service U.S. Department of Commerce 5285 Port Royal Road Springfield, VA 22161	64
	20. Price A04

Form No. 0069E (6-30-87)